THE CRYSTAL STRUCTURE OF COMPOUNDS DERIVED FROM THE REACTION OF METAL CARBONYLS AND DIPHOSPHINES

by

L.R. NASSIMBENI, B.Sc. (Hons.) M.Sc. (Rhodes)

A thesis submitted in fulfilment of the requirements for the Degree of Doctor of Philosophy of the University of Cape Town.

Department of Chemistry,
University of Cape Town,
Cape Town.

October 1969

A C K N O W L E D G E M E N T S

The author wishes to thank Professor E.G. Prout, M.Sc., Ph.D., (Natal), of the University of Cape Town, for his guidance and interest throughout the project.

The author is also indebted to Mr. M.H. Linck, Dr. G. Gafner, Dr. D.A. Thornton, Dr. H. Eales and Mr. J.H.W. Ward for their assistance, and to the South African Council for Scientific and Industrial Research for research grants.

CONTENTS

1. INTRODUCTION

1.1 SUBSTITUTED METAL CARBONYL COMPLEXES.

A characteristic feature of the d-group transition metals is their ability to form complexes with a variety of neutral molecules such as carbon monoxide, isocyanides, substituted phosphines, arsines, sulphides and other ligands. The complexes formed are diverse, ranging from molecular compounds such as $[Cr(CO)_6]$, through mixed species such as $[Co(CO)_3(NO)]$ to complex ions such as $[Mn(CNR)_6]^+$. In many of these complexes the metal atoms carry either small positive, zero or small negative charge and the ligands can stabilise low oxidation states because the donor atoms of the ligands possess vacant orbitals in addition to lone pairs of electrons. The stoichiometry of most of the complexes formed can be predicted in terms of the "inert-gas rule", which can be used to design new compounds.

The most important π-bonding ligand is carbon monoxide. The interest in metal carbonyls over the last twenty years has arisen as a result of many novel organometallic compounds in which a metal carbonyl system forms an integral part of the structure. Several recent publications illustrate their remarkable variety[1].

In general deductions about molecular structure may be made by various methods. The most important methods yielding indirect evidence of molecular structure are spectroscopic: infar red, nuclear magnetic resonance and electron spin resonance spectroscopy are the most commonly used. Other methods depend on the physical properties of substances,

such as refractive index and dielectric constant. In particular, studies of electric polarization yield values for dipole moments. The most powerful tool for the study of the structure of compounds, however, is X-ray crystallography.

Using the latter method, a large number of structures of inorganic coordination compounds have been elucidated. For example X-ray diffraction has enabled the study of closed metal carbonyl clusters[2] leading to a study of metal-metal bonds of varying bond order. The structures of many substituted metal carbonyl compounds such as the tricyclic complex $[SFe(CO)_3]_2$[3] and the Hieber-Gruber[4] compounds $X_2Fe_3(CO)_9$ (X = S, Se) have recently been published[5]. In fact the interest in inorganic complex compounds and their structural elucidation by X-ray methods has mushroomed in the last five years[6].

Little was known about dinuclear transition metal complexes having carbon, sulphur or halogens as bridging atoms until the development of facile preparations of tetra-alkyl- and tetra-aryldiphosphines. The subject has been summarised by Hayter[7] who also described a series of diphenylphosphido-bridged compounds of palladium. Chatt and Thornton[8] described the reactions of a number of diphosphines [R_2P-PR_2 ; R = Me, Et or Ph] and some analogous diarsines with the carbonyls of zerovalent iron, chromium, molybdenum and tungsten. These reactions yield a variety of phosphorus- and arsenic-bridged dinuclear carbonyls of two types, designated type A and type B which can be formulated on the basis of the inert gas rule: Type A as phosphido- and arsenido-bridged carbonyls. Type B as diphosphine- and diarsine-bridged carbonyls.

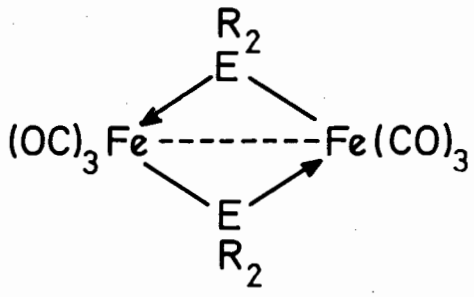

I

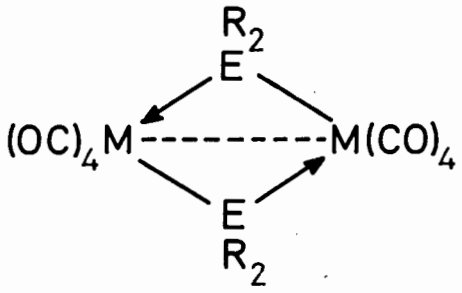

II

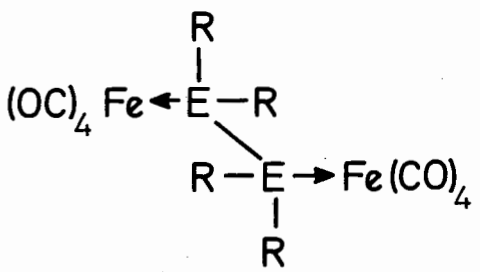

III

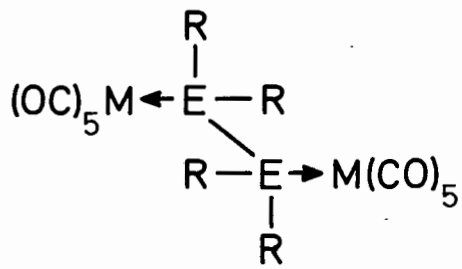

IV

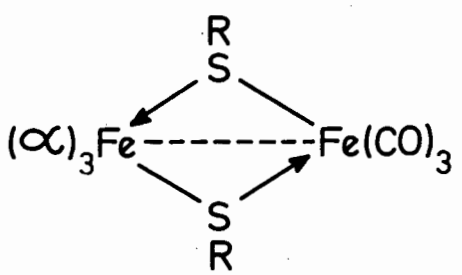

V

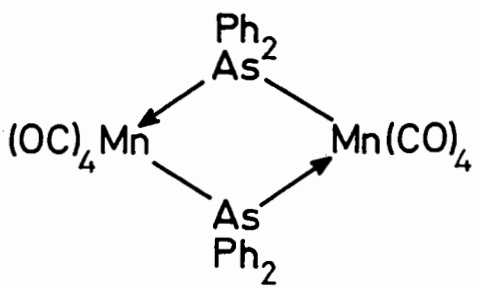

VI

E = P or As; M = Cr, Mo, or W.

Fig.1

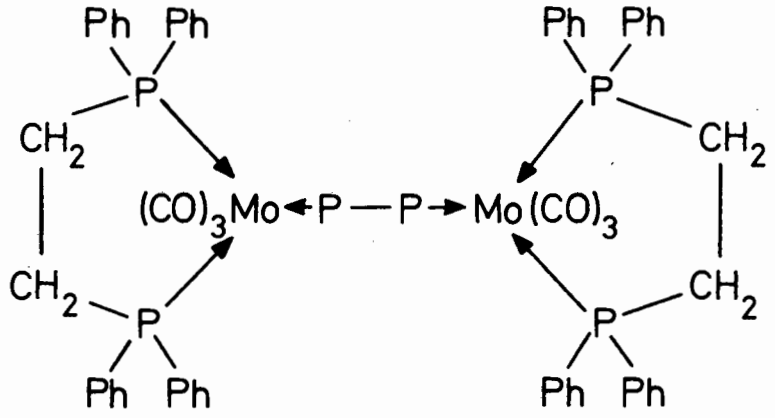

VII

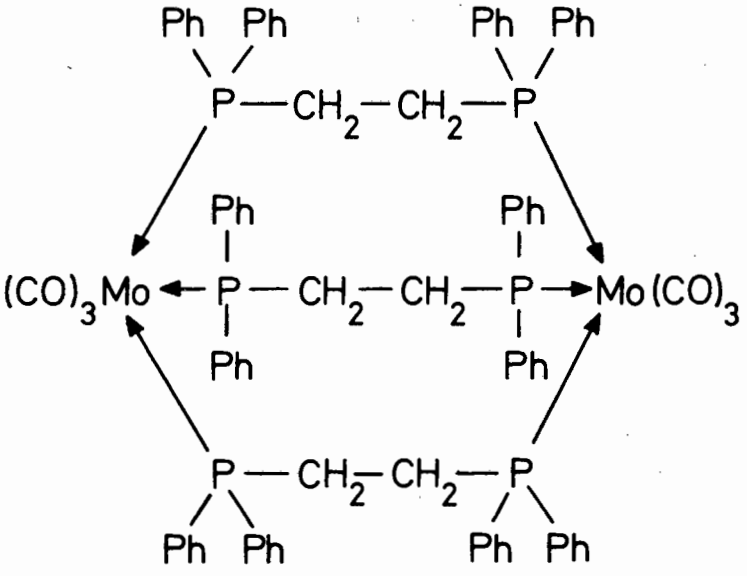

VIII

Fig.2

does not give rise to

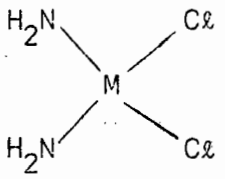

but produces the polymer:[13]

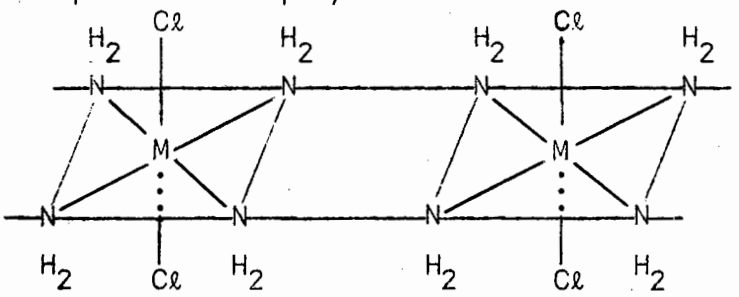

Therefore although no direct evidence was available, structure IV was considered to be an appropriate formulation for the diphosphine-bridged carbonyl (M = Cr, Mo or W). The structure was also reasonable in terms of vibrational spectra which are discussed.

Chatt and Thomson[14] extended the work of Chatt and Thornton[8] in preparing dinuclear phosphorus- and arsenic-bridged carbonyl compounds by synthesizing many of the compounds excluded from the earlier study. They showed moreover that type B compounds may be converted to type A by thermal decomposition. This suggests that type B compounds may be intermediates in the formation of type A complexes. Thomson[15] carried out very interesting photochemical experiments with compounds of type A which led to the proposal of tentative structures. Irradiation of a benzene solution of

bis(μ-dimethylphosphido)bis(tetracarbonylmolybdenum)

and triphenyl phosphine with visible light produced the insoluble compound IX (Fig. 3). Even in the presence of large excess of triphenylphosphine, compound IX was the only product and there was

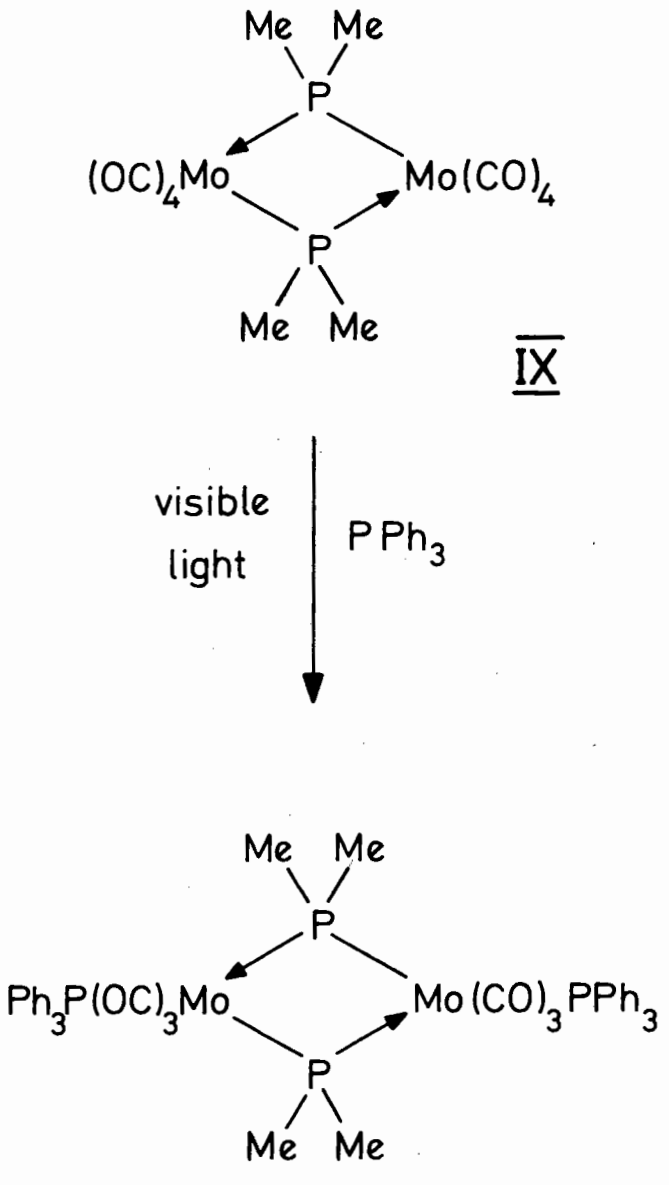
Me Me
P
(OC)4Mo
Mo(CO)4
P
Me Me
IX
visible
light
P Ph3
Me Me
P
Ph3P(OC)3Mo
Mo(CO)3PPh3
P
Me Me

Fig.3

no evidence of further substitution. The experiment was also carried out with triethylphosphine, with formation of the analogous ethyl compound. Since the starting complex in the reaction is diamagnetic it was considered to have a metal-to-metal (M-M) bond. Furthermore Thomson showed that, after irradiation, the (M-M) bond remained intact. The structures predicted by Thomson for the compounds of type A are shown in Figs. 4 and 5. These will now be discussed.

Structure X in which the (M-M) bond is bent and occupies the vacant octahedral positions of the iron atoms was proposed by Hayter[16]. This structure is based on that established by X-ray crystallography by Dahl and Wei[17] for the similar compound $[Fe_2(CO)_6(SEt)_2]$.

In structure X there are two carbonyl groups situated *trans*- to the (M-M) bond and four *trans*- to the phosphine groups. Thomson's photochemical experiments indicated that two carbonyl groups are replaced by phosphine much more readily than the remaining four. He thus proposed that the two carbonyl groups *trans*- to the (M-M) bond were the uniquely replaceable groups and that under the influence of visible light no other groups were replaced. The other possibility put forward was that the two carbonyls *trans*- to the phosphines were replaced and that the product was deactivated towards further attack by the presence of the additional phosphines. This possibility was subsequently discounted by Thomson[15] on the basis of further experimental evidence.

As shown in Fig. 3, in the case of the molybdenum compound the photochemical experiments also show the probability of one carbonyl group occupying a unique position. This is not expected from structure XI but

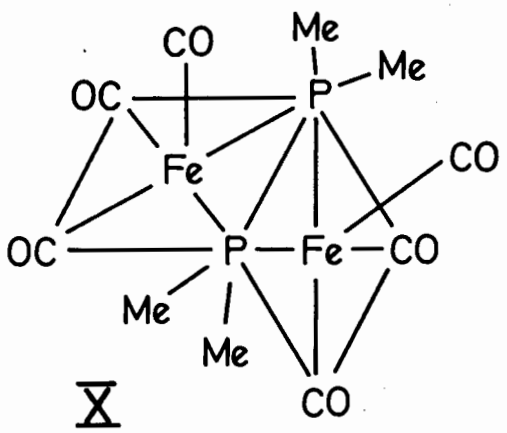
CO
Me
Me
OC
P
Fe
CO
OC
P
Fe
CO
Me
Me
CO

X

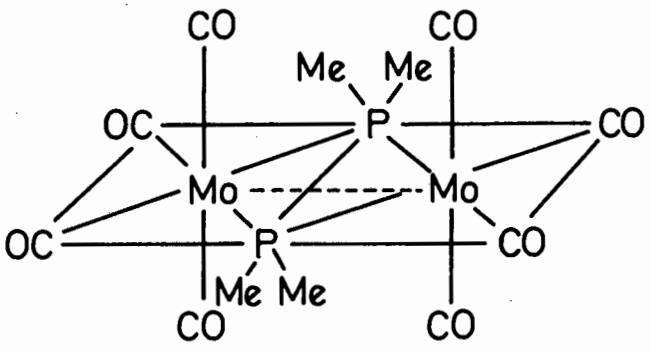
CO
CO
Me
Me
OC
P
CO
Mo
Mo
OC
P
CO
Me
Me
CO
CO

XI

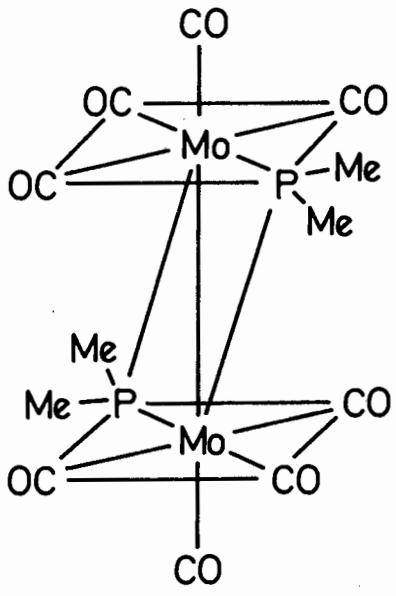
CO
OC
CO
Mo
OC
P
Me
Me
Me
P
CO
Mo
OC
CO
CO

XII

Fig. 4

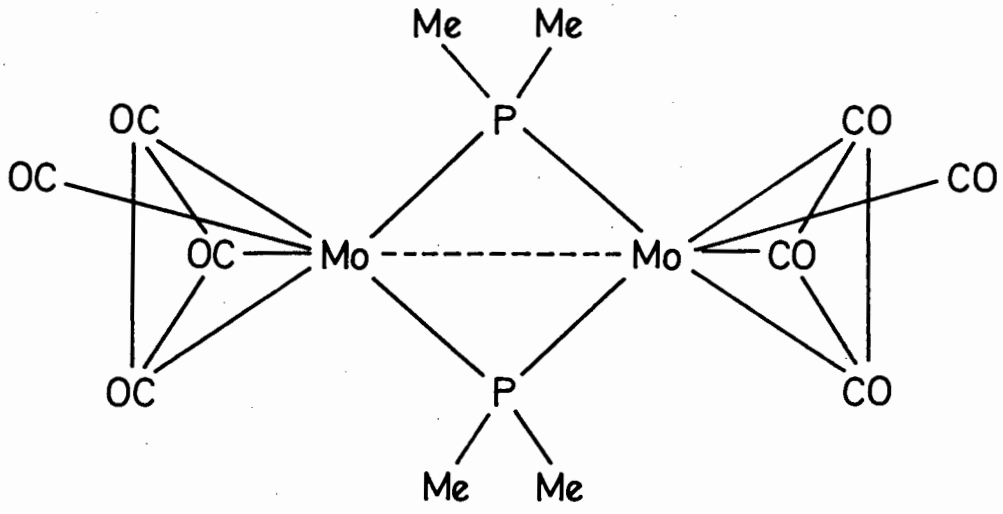

XIII

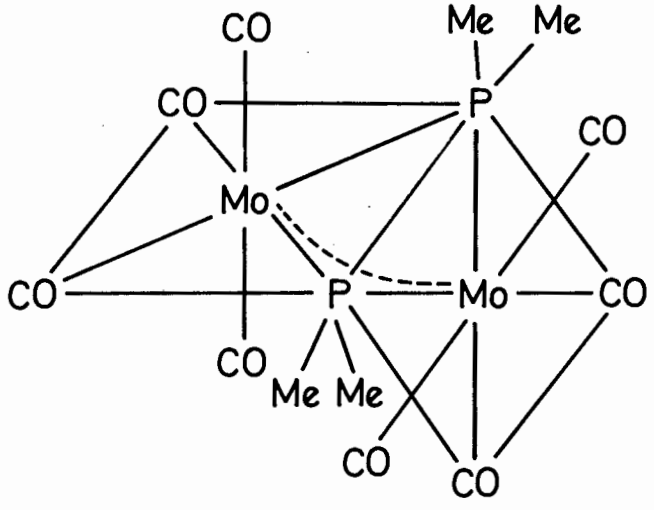

XIV

Fig.5

there now arise the possibilities of structures XII, XIII and XIV. Structure XII is analogous with that proposed by Nigam, Nyholm and Stiddard[18] for $[Mo\ (diarsine)\ (CO)_3I_2]$. Both structures XII and XIII are similar to structure X in their possession of unique carbonyl groups *trans-* to the (M-M) bond. Structure XIV, the typical 'folded textbook' structure, also fulfils this condition and is not centro-symmetric, which would explain the dipole measurements, a discussion of which is deferred to the following section.

1.2 STRUCTURAL EVIDENCE FROM INFRA RED SPECTRA, PROTON MAGNETIC RESONANCE SPECTRA, AND DIPOLE MOMENTS.

1.2 (a) Infra-Red Spectra.

The carbonyl stretching frequencies (ν_{CO}) in chloroform for various compounds corresponding to structures I and IV are listed in Table 1. These show that the carbonyl groups are in terminal positions. The carbonyl absorption patterns of the compounds containing Group VI metals are similar to those normally observed for compounds of the type *cis-* $[M\ (CO)_4\ L_2]$[19] (type A) and $[M\ (CO)_5\ L]$[20] (type B) (L = monodentate phosphine) which are in accordance with the suggested structures.

The carbonyl stretching frequencies of the iron compounds $[Fe_2\ (CO)_6L_2]$ yielded a different pattern from that usually exhibited by the tricarbonyl iron group, showing the possibility of coupling between the two $Fe\ (CO)_3$ groups. This suggests that there is a difference between structures I and II, which will be discussed in more detail later.

TABLE 1

Infrared carbonyl stretching frequencies (cm^{-1}) in chloroform and dipole moments in benzene (25°C) in μ(D) of compounds of general formula $[M_2(CO)_nL]$

Type	Structure	Formula	ν_{CO}				μD
A	II	$[Cr_2(CO)_8(PMe_2)_2]$	2011s	1952vs,b			1.4
A	II	$[Cr_2(CO)_8(PEt_2)_2]$	2003s	1942vs,b			0.9
A	II	$[Mo_2(CO)_8(PEt_2)_2]$	2019s	1948vs,b			0.6
A	II	$[W_2(CO)_8(PEt_2)_2]$	2024s	1946vs,b			0.9
A	II	$[Mo_2(CO)_8(AsMe_2)_2]$	2026s	1960vs,b			1.1
A	II	$[W_2(CO)_8(AsMe_2)_2]$	2018s	1946vs,b			1.1
A	II	$[Mo(CO)_8(PPh_2)_2]$	2035s	1969vs,b			-
A	II	$[W_2(CO)_8(PPh_2)_2]$	2034s	1961vs,b			-
A	II	$[Mo_2(CO)_8(AsPh_2)_2]$	2033s	1965vs,b			-
A	I	$[Fe_2(CO)_6(PMe_2)_2]$	2047s	2009vs	1976s	1963s	3.6
A	I	$[Fe_2(CO)_6(PEt_2)_2]$	2045s	2007vs	1972s	1962s	3.8
A	I	$[Fe_2(CO)_6(AsMe_2)_2]$	2037s	2024vw	1998vs	1965s	4.2
B	III	$[Fe_2(CO)_8(PMe_2)_2]$	2059sh	2049s	1982w-m	1947vs,b	
B	IV	$[Mo_2(CO)_{10}(PMe_2)_2]$	2079w,sh	2069m	1990w	1954vs,b	3.7
B	IV	$[W_2(CO)_{10}(PMe_2)_2]$	2079w,sh	2068m	1981w	1946vs,b	3.9
B	IV	$[Mo_2(CO)_{10}(PEt_2)_2]$	2076w,sh	2068m	1988w	1950vs,b	3.7
B	IV	$[W_2(CO)_{10}(PEt_2)_2]$	2075w,sh	2067m	1980w	1944vs,b	3.6
B	IV	$[Mo_2(CO)_{10}(AsMe_2)_2]$	2077w,sh	2069m	1992w	1954vs,b	3.9
B	IV	$[W_2(CO)_{10}(AsMe_2)_2]$	2079w,sh	2070m	1985w	1947vs,b	3.1

s, strong. m, medium. w, weak. b, broad, sh, shoulder.

The spectra of the complexes containing the $(PMe_2)_2$ bridging group are sufficiently simple to allow them to be divided, on infrared evidence alone, into the two types A and B (Table 2). The spectra of type B are simpler. In them the symmetric deformation of the methyl groups appears as a sharp doublet, whereas the Cr (type A) compound yields two bands of unequal intensity and the tricarbonyl Fe compound (type A) shows three bands. Also the type B compounds show $P-CH_3$ stretching bands $\nu_{P-C(as)}$ and $\nu_{P-C(s)}$ of equal intensities at nearly identical frequencies whereas in type A compounds these bands are close together, broader and of differing intensities. Finally, the methyl rocking frequencies ρ_{Me} found near 940 cm^{-1} and 890 cm^{-1} show a slight splitting in type A compounds but no splitting in the type B compounds. These features indicate some dissymetry in the structure of the chromium and tricarbonyl iron compounds which is also apparent from their dipole moments.

1.2 (b) Proton Magnetic Resonance Spectra.

Chatt and Thomson[21] obtained proton magnetic resonance spectra for the type A compounds:

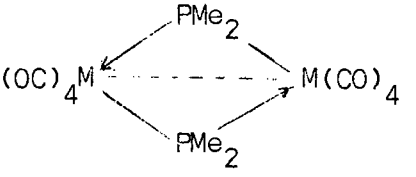

(Structure II)

and for the type B compounds:

$(OC)_5M \leftarrow PMe_2 - PMe_2 \rightarrow M(CO)_5$ (Structure IV)

M = Cr, Mo, W.

Their results are shown in Table 3.

TABLE 2

Phosphorus-methyl stretching frequencies (cm^{-1}) in chloroform of compounds containing $(PMe_2)_2$-bridging group.

Type	Structure	Formula	$\nu_{P-C(as)}$	$\nu_{P-C(s)}$
A	I	$[Fe_2(CO)_6(PMe_2)_2]$	722s	705s
A	II	$[Cr_2(CO)_8(PMe_2)_2]$	731m	712vs
B	III	$[Fe_2(CO)_8(PMe_2)_2]$	745m	693m
B	II	$[Mo_2(CO)_8(PMe_2)_2]$	735m	684m
B	II	$[W_2(CO)_8(PMe_2)_2]$	736m	684m

s, strong. m, medium. w, weak. b, broad. sh, shoulder.

TABLE 3.

Chemical shifts (τ) and phosphorus-hydrogen coupling constants [J(PH)] for $CDCl_3$ solutions of dinuclear phosphorus-bridged carbonyl complexes.

Compound	τ	Multiplicity	J(PH) (c/sec)
type A M = Cr	7.68	Doublet	10.6
type A M = Mo	7.68	Doublet	9.4
type A M = W	7.56	Doublet	9.8
type B M = Cr	8.28	Triplet	4.2
type B M = Mo	8.31	Triplet	5.3
type B M = W	8.15	Triplet	4.3

Deutereochloroform solutions of the type B complexes gave rise to a triplet in which the central band is a weak one with sharper peaks on either side of it. Type A compounds gave rise to a sharp doublet, the splitting being ca 10c/sec at both 60 and 100 Mc/sec. Chatt and Thomson's interpretation of these spectra was that the splitting patterns were dependent on the environment of the diethylphosphido-groups. The doublets obtained from the type A compounds were attributed to the spin-spin coupling of six identical hydrogen nuclei with their adjacent phosphorus nucleus. The spectra from the type B compounds may arise from a balance between proton-phosphorus coupling and a simple proton resonance.

1.2 (c) Dipole moments - (Table 1).

The Group VI metal compounds can be classified into two categories - type A, with dipole moments of about 1D and type B with dipole moments of about 4D. The iron compounds show the opposite pattern, type A having dipole moments of approximately 4D and type B (only one compound is listed) with dipole moment of 2.5D.

With the exception of the latter moment, the other values can be explained on the basis of the structures I → IV.

As discussed above we may expect the type A compounds with Cr, Mo or W (structure II), to have the configuration shown in structures XI, XII, XIII and XIV.

Structures XI and XIII are flat, which would imply a zero dipole moment.

Structure XIV has folding about the P-P line, and since the phosphorus atoms must carry a positive charge relative to the rest of the molecule, this would give rise to a dipole moment. The magnitude of the dipole moment would depend on the degree of folding. This folding would also bring the metal atoms closer, facilitating the formation of a metal-metal bond, but would be counteracted by the steric effect of the carbonyl groups perpendicular to the plane containing the phosphorus atoms. The low values of the dipole moments would indicate a compromise between the folding and the steric hindrance forces.

In the iron compounds of type A there is no steric hindrance (structure X) to hinder folding about the P-P line, so that the molecule can fold until each iron atom fills approximately the sixth coordination position of the other, cf $[Rh_2 Cl_2 (CO)_4]^{22}$. This would account for the high dipole moment.

Type B compounds, with proposed structures III, IV, have free rotation about the P-P bond and the observed dipole moments of the Cr, Mo, W compounds are consistent with this. The moment of the corresponding Fe compound 2.5D is lower than expected but the difference is probably not significant.

2. OBJECT OF RESEARCH

The foregoing introduction shows that the reaction between substituted diphosphines and diarsines with various metal carbonyls produce a series of interesting compounds.

Structural evidence based on infrared proton magnetic resonance, dipole moment data and microanalyses allows the classification of these compounds into two distinct types A and B (Fig. 1). The assigment of structures to the type A compounds corresponding to the general structure II presents an interesting problem in that there arise several possibilities (XI, XII, XIII and XIV). Photochemical experiments favour structures XII, XIII or XIV, all of which possess unique CO groups *trans*- to the (M-M) bond. A dipole moment of approximately 1D would suggest a folded molecule (XIV). Since the dipole moments depend on several other measurements (density, refractivity, dielectric constant) there is the possibility that the small dipole moments obtained (<1.5D) are not significant, but are simply due to additive errors. If the dipole moment evidence is discounted this leaves structure XI as a possibility, although this has no unique CO-groups.

Type B compounds were unknown, but the evidence from infrared spectra, proton magnetic resonance and dipole moments suggested structure IV (Fig. 1).

It was thus decided to employ X-ray diffraction methods to resolve the structural problem posed by the type A compounds and to elucidate the structure of the type B compounds whose structures were unknown.

Several compounds could have been chosen from the series as being characteristic of the two types A and B. The molybdenum compounds were selected because it was thought that molybdenum would be sufficiently heavy to facilitate the solving of vector maps arising from three-dimensional Patterson syntheses without giving serious complications in the refinement due to thermal motion. The compounds chosen are products of the same reaction:

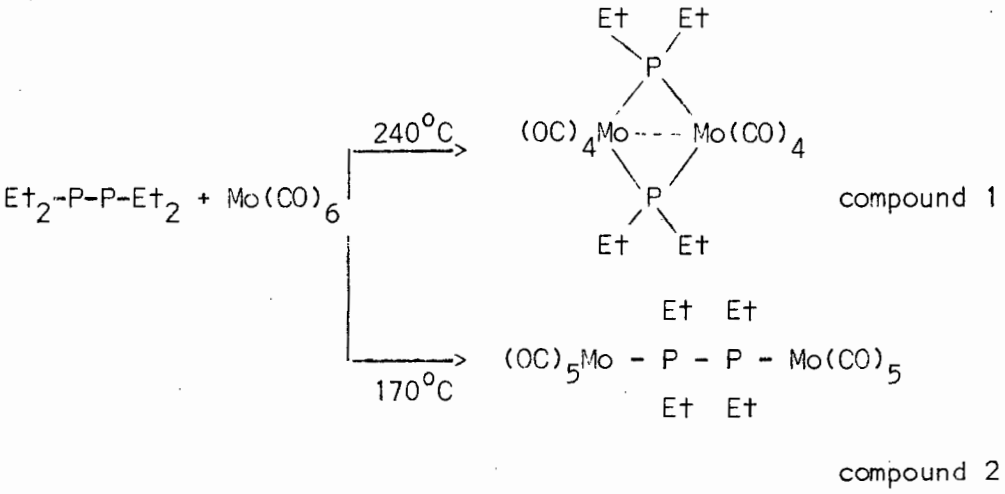

Compound 1 (Type A) di-μ-diethylphosphido-bis-(tetracarbonylmolybdenum).

Compound 2 (Type B) μ-Tetraethyldiphosphine-bis(pentacarbonylmolybdenum).

3. PREPARATION OF THE COMPOUNDS

3.1 PREPARATION OF TETRAETHYLDIPHOSPHINE.

3.1(a) Preparation of thiophosphoryl chloride ($PSC\ell_3$)

The thiophosphoryl chloride was prepared by the Knotz method[23]. Sulphur (36g) and phosphorous trichloride (150g) were heated on a water bath in a 500 ml round bottom flask. Aluminium chloride (6g) was added and the mixture heated to boiling. After approximately 10 minutes the boiling ceased, indicating that the reaction had terminated. The mixture was cooled and transferred to a separating funnel and water (400 ml) was added. The lower layer ($PSC\ell_3$) was removed, dried over calcium chloride and filtered. The thiophosphoryl chloride was distilled and the fraction boiling between 125 - 127°C/760 mm was collected.

$$PC\ell_3 + S \rightarrow PSC\ell_3 \text{ (yield of product 81\%).}$$

3.1(b) Preparation of dry ether.

A winchester quart of ether was filled to a depth of 1" with granular calcium chloride and allowed to stand for 24 hours with occasional shaking. The ether was filtered and placed in a clean dry bottle and sodium wire was pressed into it. The container was gently stoppered and allowed to stand for 24 hours.

3.1(c) Preparation of tetrahydrofuran (T.H.F.).

The T.H.F. was allowed to stand overnight with some KOH pellets in a greased glass stoppered 5ℓ round bottom flask. This was then

distilled and sodium wire pressed into the flask. Under an atmosphere of nitrogen, the T.H.F. was then refluxed for 24 hours, redistilled, and more sodium wire was added to the bottle. 5g of benzophenone were added and the T.H.F. refluxed until a blue colour appeared, indicating that the liquid was now perfectly dry. It was then distilled under nitrogen into a clean dry flask and kept under nitrogen.

3.1(d) Preparation of tetraethyldiphosphine disulphide.

Magnesium turnings (36.4g) were placed in a flask and just covered in dry ether. Ethyl bromide (164g) was dissolved in ether (300 ml) and placed in a dropping funnel. The ethyl bromide was slowly added to the magnesium turnings and the reaction was started with a small crystal of iodine. The solution was stirred and the rate of addition of the ethyl bromide adjusted so that the ether was kept gently refluxing. The mixture was cooled and the dropping funnel replaced with one containing thiophosphoryl chloride (79.5g). The latter was added dropwise and with constant stirring. When the mixture became too viscous to stir, dry T.H.F. was added. When the addition of the thiophosphoryl chloride was complete, the flask was warmed to 45°C and the mixture stirred for 2 hours. The mixture was allowed to cool and H_2SO_4 (2.5N; 500 ml) carefully added with stirring. The T.H.F.-ether layer was separated from the aqueous layer, and the tetraethyldiphosphine disulphide, which is solid, was filtered from the T.H.F.-ether mixture and dried in a vacuum desiccator.

3.2 PREPARATION OF Di-μ-diethylphosphido-bis-(tetracarbonylmolybdenum) (compound 1)

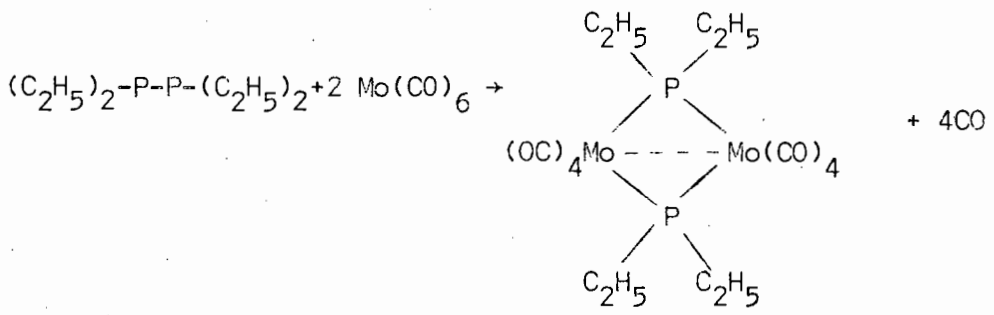

The reaction was carried out in a sealed tube at 240°C for 96 hours. The product was recrystallised 10 times from light petroleum ether (b.p.60-80°) giving small orange crystals. There was no sharp melting point, the crystals slowly decomposing above 130°C. Carbon-hydrogen analysis* gave the following results:

Found C = 32.3%, H = 3.3%

Calculated for $C_{16}H_{20}Mo_2O_8P_2$ C = 32.3%, H = 3.4%

3.3 PREPARATION OF μ-Tetraethyldiphosphine-bis-(pentacarbonylmolybdenum) (compound 2).

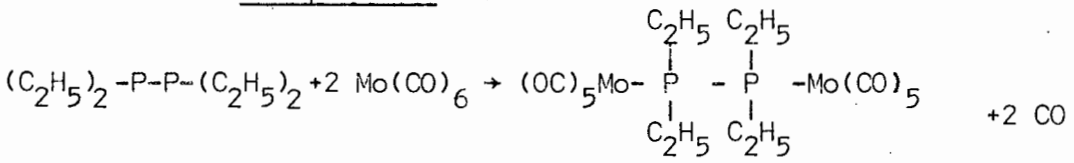

The reaction was carried out in a sealed tube at 170°C for 24 hours. The product was recrystallised 10 times from benzene giving small colourless crystals. The melting point was 156-157°C with some decomposition. Carbon-hydrogen analysis* gave the following results:

*Analysis was carried out by F. Pascher and E. Pascher at the Microanalytisches Laboratorium, Bonn.

Found C = 33.4%, H = 3.0%

Calculated for $C_{18}H_{20}Mo_2O_{10}P_2$ C = 33.3%, H = 3.1%

3.4 INFRARED SPECTRA.

The infrared spectra of the two compounds are shown in Fig. 6 and Fig. 7.

The infrared spectrum of compound 1 (type A) shown in Fig. 6 exhibits bands at 2028, 1963, 1930 cm^{-1} which are due to ν_{CO} of the terminal carbonyl groups. If these were bridging carbonyl groups, these bands would be expected at 1900-1700 cm^{-1} [1]. The bands at 768 and 735 cm^{-1} would, following Adams[8], be assigned to $\nu_{P-C(as)}$ and $\nu_{P-C(s)}$ respectively.

$\nu_{P-C(as)}$ is the phosphorus-carbon asymmetric stretching frequency:

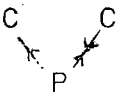

and $\nu_{P-C(s)}$ is the phosphorus-carbon symmetric stretching frequency:

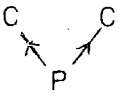

The infrared spectrum of compound 2 (type B) shown in Fig. 7 exhibits bands at 2072, 1963, 1930 and 1920 cm^{-1} which are again attributed to ν_{CO} of the terminal carbonyl groups. The $\nu_{P-C(as)}$ and $\nu_{P-C(s)}$ occur at 762 and 723 cm^{-1} respectively.

In both spectra the C-H frequencies are masked by the mulling agent (nujol).

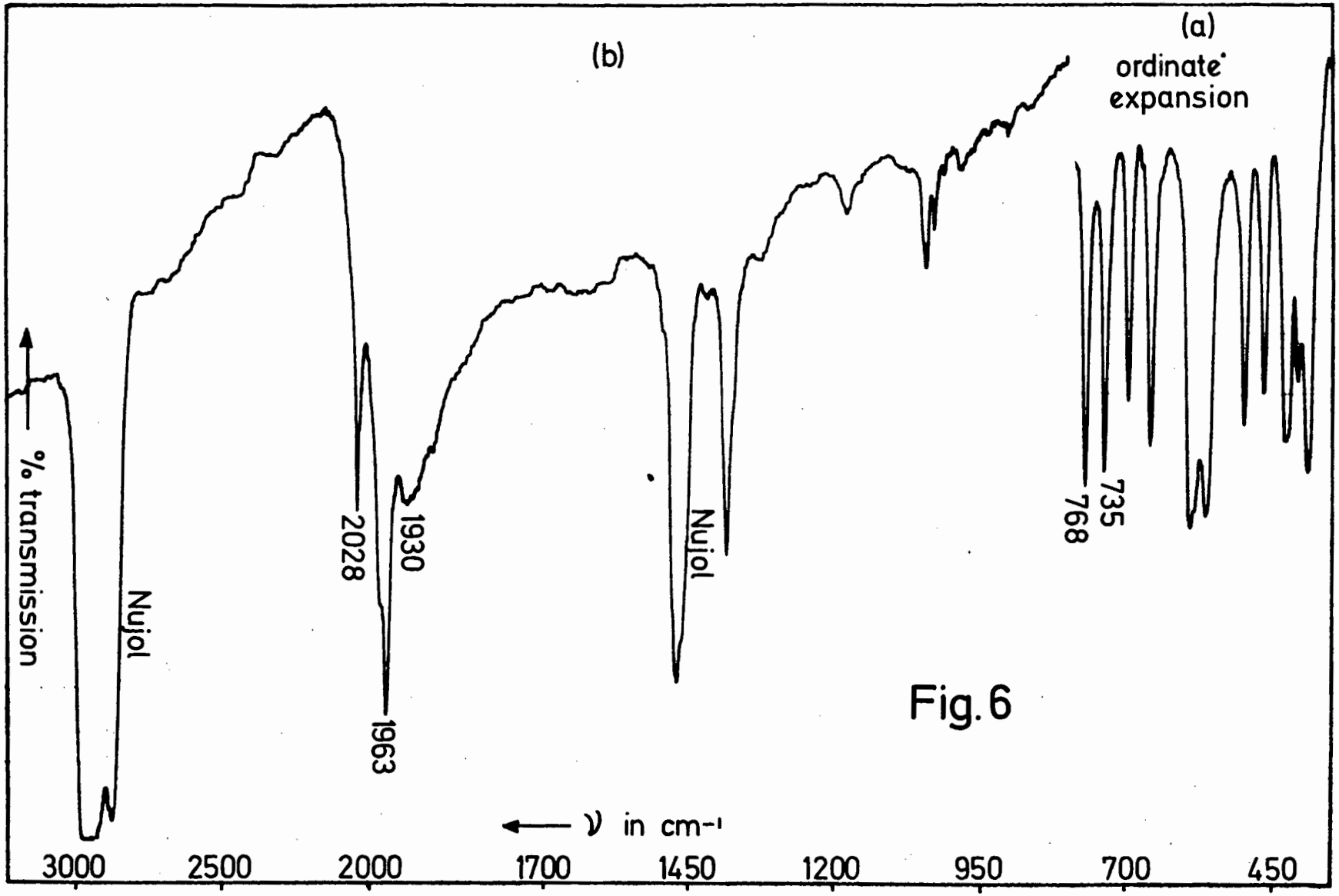
(b)
(a)
ordinate expansion
% transmission
Nujol
2028
1930
1963
Nujol
768
735
ν in cm⁻¹
3000
2500
2000
1700
1450
1200
950
700
450

Fig. 6

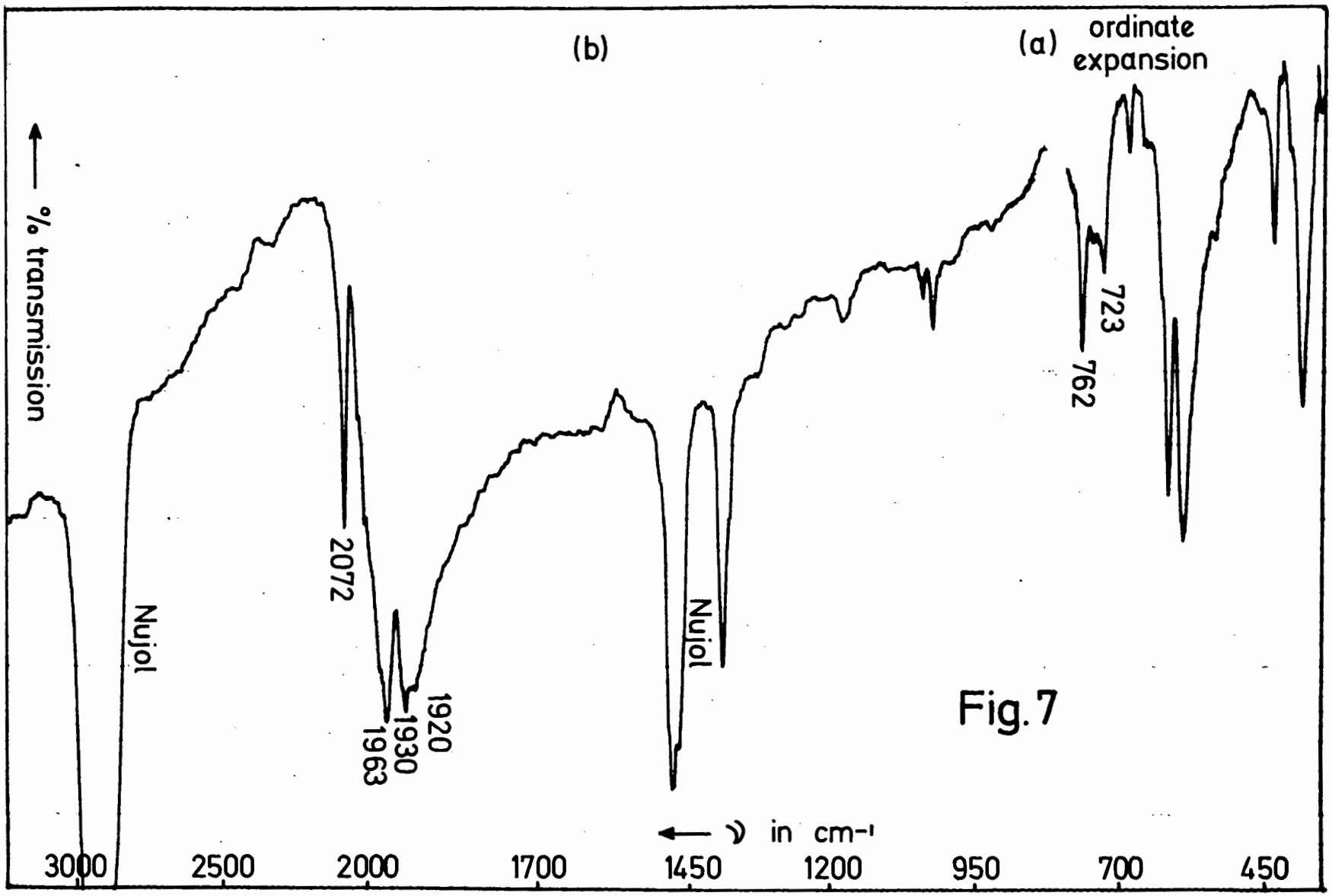
(b)
(a)
ordinate expansion
% transmission
Nujol
2072
1963
1930
1920
Nujol
762
723
ν in cm⁻¹
3000
2500
2000
1700
1450
1200
950
700
450

Fig. 7

4. APPARATUS

4.1 THE X-RAY GENERATORS AND ACCESSORIES.

The generators used in the project were

(a) A Hilger and Watts Microfocus Generator, with an X-ray tube which is continuously evacuated by an oil diffusion pump backed by a rotary oil pump. The generator was operated at 50kv and 3mA and a demountable copper target was used.

(b) Philips PW1009 and P1010 generators, employing sealed X-ray tubes with copper targets. The generators were operated at 40kv and 20mA.

The Laue camera and the rotation and Weissenberg goniometers used were made by Unicam. The integrating Weissenberg was made by Stoe (Heidelberg). The goniometer heads on the instruments are interchangeable and the rotation camera has an optical goniometer.

The film used was Kodak "Kodirex", which was developed in D19b developer for 5 minutes at 20°C, immersed for 5 seconds in a stop bath of 3% acetic acid, and fixed for 5 minutes with agitation in Kodak X-ray fixer. This was followed by a 10 minute suspension in the fixer. The films were then washed in running water for 30 minutes and subsequently dried in a fume cupboard in order to avoid dust.

Kodak 'Industrex D' film, which has no detectable shrinkage on development and fixing, was used in the determination of accurate cell parameters.

4.2 THE DENSITOMETER.

A modified Steinheil densitometer was used to measure the intensities of the diffraction spots. The instrument is shown in Fig. 8. The light source consisted of a Philips cold lamp rated at 50 watts and was cooled by a stream of compressed air. A potential difference of 8 volts was maintained across the lamp, the voltage being kept constant by means of a variable resistance in the circuit.

The light transmission was measured by a photo-emissive search head connected to an electronic photometer, both manufactured by the Photovolt Corporation of New York. The photocell was covered by a head having an adjustable aperture.

Although the system is stable and gives reproducible results, the response of the densitometer is not linear. Thus a calibration curve of spot density versus relative exposure time was drawn up, (Fig. 9). This shows that the densitometer only reads linearly in the density range: 0-0.575, and a correction curve derived from the calibration curve is shown in Fig. 10. This shows the correction factor that must be applied to diffraction spots having a density ranging from 0.575 to 1.2.

MODIFIED STEINHEIL

DENSITOMETER

Fig. 8

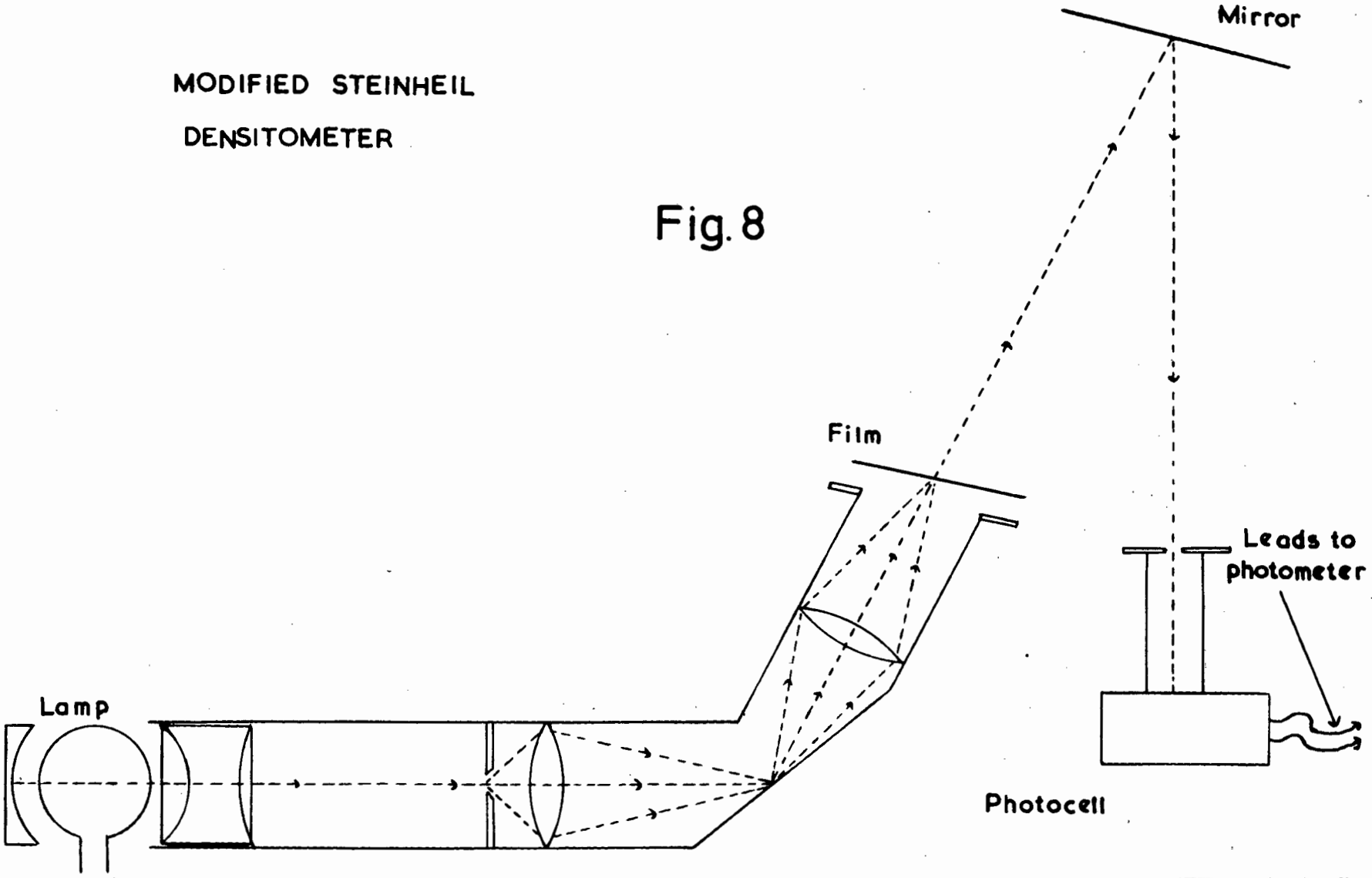

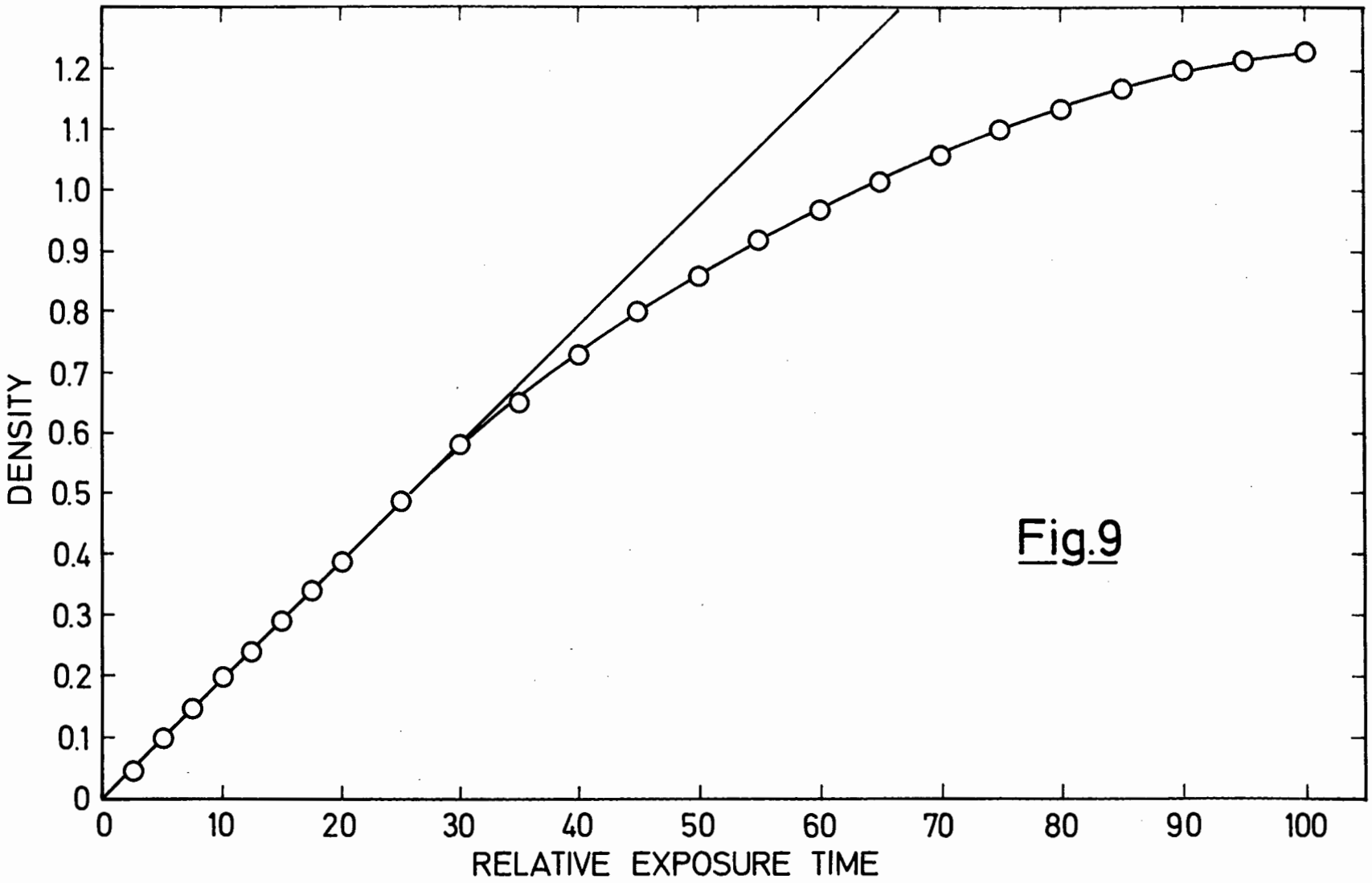
DENSITY
1.2
1.1
1.0
0.9
0.8
0.7
0.6
0.5
0.4
0.3
0.2
0.1
0
0
10
20
30
40
50
60
70
80
90
100
RELATIVE EXPOSURE TIME

Fig.9

Fig. 10

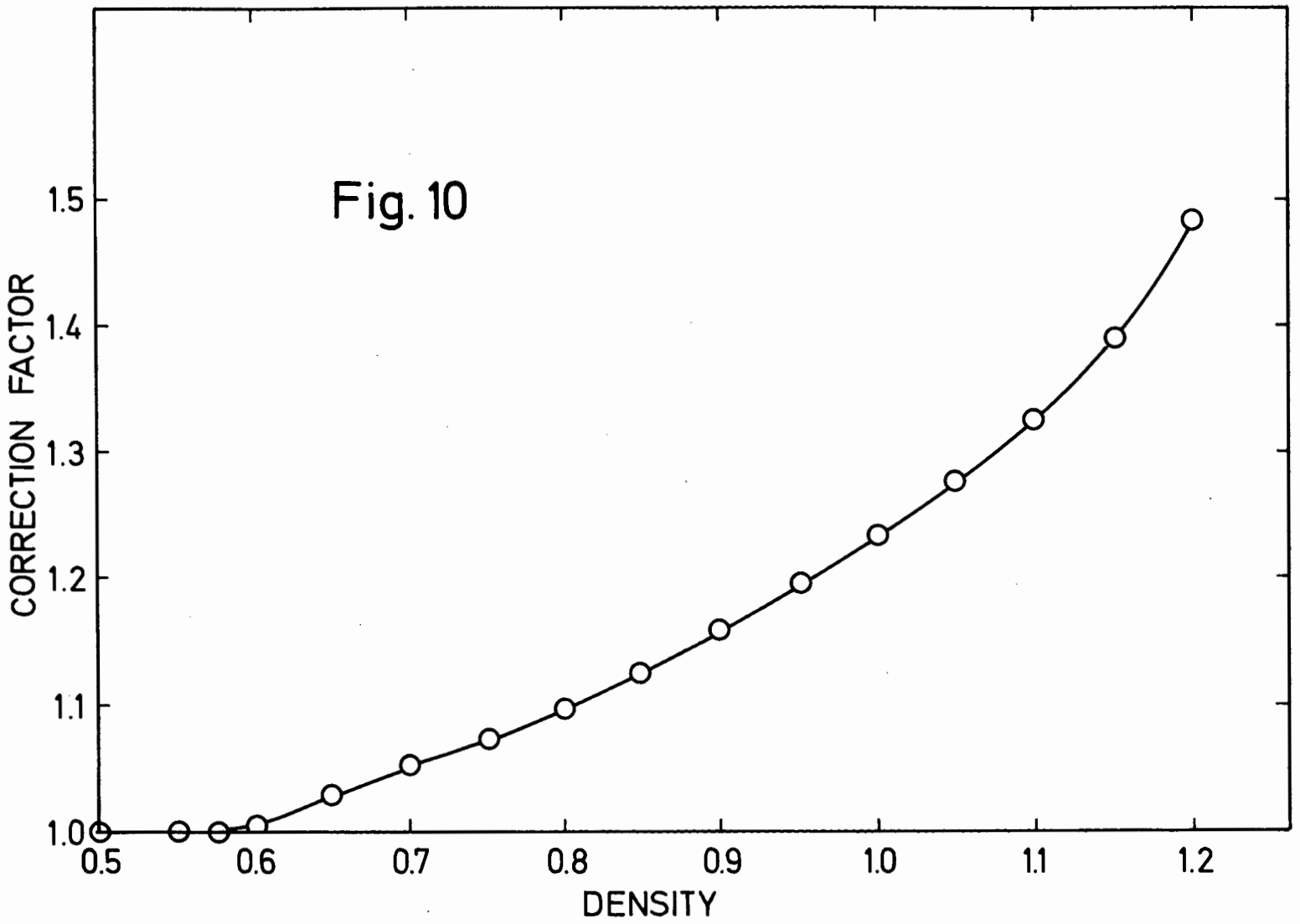
CORRECTION FACTOR
1.0
1.1
1.2
1.3
1.4
1.5
0.5
0.6
0.7
0.8
0.9
1.0
1.1
1.2
DENSITY

5. COMPUTING

The majority of the computing was carried out on the University of Cape Town's I.C.T. 1301 computer. This has an 800 word Immediate Access Store (I.A.S.) and a 16000 word capacity in two storage drums.

Since the I.C.T. computer does not have a sufficiently large storage capacity, the final least squares refinement calculations were carried out on the C.S.I.R. I.B.M. 360/40 and 360/65 computers using the ORFLSRED least squares programme.

The sequence of programmes used on the I.C.T. 1301 is shown schematically (Fig. 11). The programmes are now outlined individually.

5.1 THE SCATTERING FACTOR PROGRAMME.

This programme converts the uncorrected intensity data to F_o or F_o^2 and computes the scattering factors of each atomic species for every reflection. It requires the following input data:

(i) The reciprocal cell dimensions and the X-ray wavelength.

(ii) The Weissenberg inclination angle.

(iii) The scattering factor tables of every element in the structure.

(iv) The absorption correction table.

(v) The Miller Indices and uncorrected intensity of each reflection.

The program then computes any or all of the following for each reflection:

(a) $\sin^2\theta/\lambda^2$

(b) Lorentz-Polarisation correction (Lp)

(c) Absorption correction

(d) F_o or F_o^2

(e) The scattering factors $f_1, f_2, f_3, \ldots, f_n$ for n different elements in the structure.

The $\sin^2\theta/\lambda^2$ values are computed from the equation[24]

$$\sin^2\theta/\lambda^2 = \frac{1}{4}\,(h^2a^{*2} + k^2b^{*2} + \ell^2c^{*2} + 2\,hk\,a^*b^*\cos\gamma^* + 2\,h\ell\,a^*c^*\cos\beta^* + 2\,k\ell\,b^*c^*\cos\alpha^*) \quad \ldots\ldots\ldots \quad 5.1$$

where $a^*, b^*, c^*, \alpha^*, \beta^*, \gamma^*$ are the reciprocal lattice parameters,

h, k, ℓ are the Miller indices, θ is the Bragg angle and

λ the X-ray wavelength.

The polarization factor is a simple function of θ [25]

$$p = \tfrac{1}{2} + \tfrac{1}{2}\cos^2 2\theta \quad \ldots\ldots\ldots \quad 5.2$$

by substituting the trigonometric identity $\cos 2\theta = 1 - 2\sin^2\theta$ the polarization factor reduces to

$$p = 1 - 2\sin^2\theta + 2\sin^4\theta \quad \ldots\ldots\ldots \quad 5.3$$

The Lorentz factor L is given by the equation[26]

$$\frac{1}{L} = \cos\mu\,\cos\nu\,\sin T \quad \ldots\ldots\ldots \quad 5.4$$

where μ is the complement of the angle between the incident beam and the oscillation axis,

ν is the complement of the semi angle of the cone of reflected X-rays,

T is the angle which is proportional to the distance of the reflection from the centre of the cylindrical film. T is thus a film coordinate[27].

It can be shown that[28]

$$\cos 2\theta = 1 - 2\sin^2\theta = \sin\mu\,\sin\nu + \cos\mu\,\cos\nu\,\cos T \quad \ldots\ldots\ldots \quad 5.5$$

For the Equi-Inclination case, where $\mu = -\nu$

$$1 - 2\sin^2 2\theta = -\sin^2\mu + \cos^2\mu\,\cos T \quad \ldots\ldots\ldots \quad 5.6$$

$$\therefore \quad \cos T = \frac{1 - 2\sin^2 2\theta + \sin^2 \mu}{\cos^2 \mu} \qquad \ldots\ldots \quad 5.7$$

$$\therefore \quad \sin T = \left[1 - \left[\frac{(1-2\sin^2 2\theta+\sin^2 \mu)}{\cos^2 \mu}\right]^2\right]^{\frac{1}{2}} \qquad \ldots\ldots \quad 5.8$$

Hence $$\frac{1}{L} = \cos^2 \mu \sin T \qquad \ldots\ldots \quad 5.9$$

$$\frac{1}{L} = \sqrt{\cos^4 \mu - \left[1-2\sin^2 \theta+\sin^2 \mu\right]^2} \qquad \ldots\ldots \quad 5.10$$

For the purpose of computation, the polarization and Lorentz factors are treated together, and the equation takes on the form:-

$$\frac{1}{2Lp} = \frac{\sqrt{\cos^4 \mu - \left[1-2\sin^2 \theta+\sin^2 \mu\right]^2}}{2-4\sin^2 \theta+4\sin^4 \theta} \qquad \ldots\ldots \quad 5.11$$

The absorption correction for a given reflection is calculated by reading into the computer a table of values for A^*, the absorption correction, at various values of $\sin^2\theta/\lambda^2$. The required value of A^* for a given reflection is then calculated by using the linear interpolation formula

$$y = y_2 - \left(\frac{x_2-x}{x_2-x_1}\right)(y_2-y_1) \qquad \ldots\ldots \quad 5.12$$

where in this case $y = A^*$, $x = \sin^2\theta/\lambda^2$

and $y_1, y_2, y_3, \ldots, y_n$ are the tabulated values of A^* at the corresponding values $x_1, x_2, x_3, \ldots, x_n$ values of $\sin^2\theta/\lambda^2$. The scattering factors of the different scattering atoms are calculated in the same way, the A^* correction being substituted by the appropriate scattering factor table.

Since both the scattering factor and the absorption correction fall off rapidly with θ at low θ values, the intervals of $\sin^2\theta/\lambda^2$ were

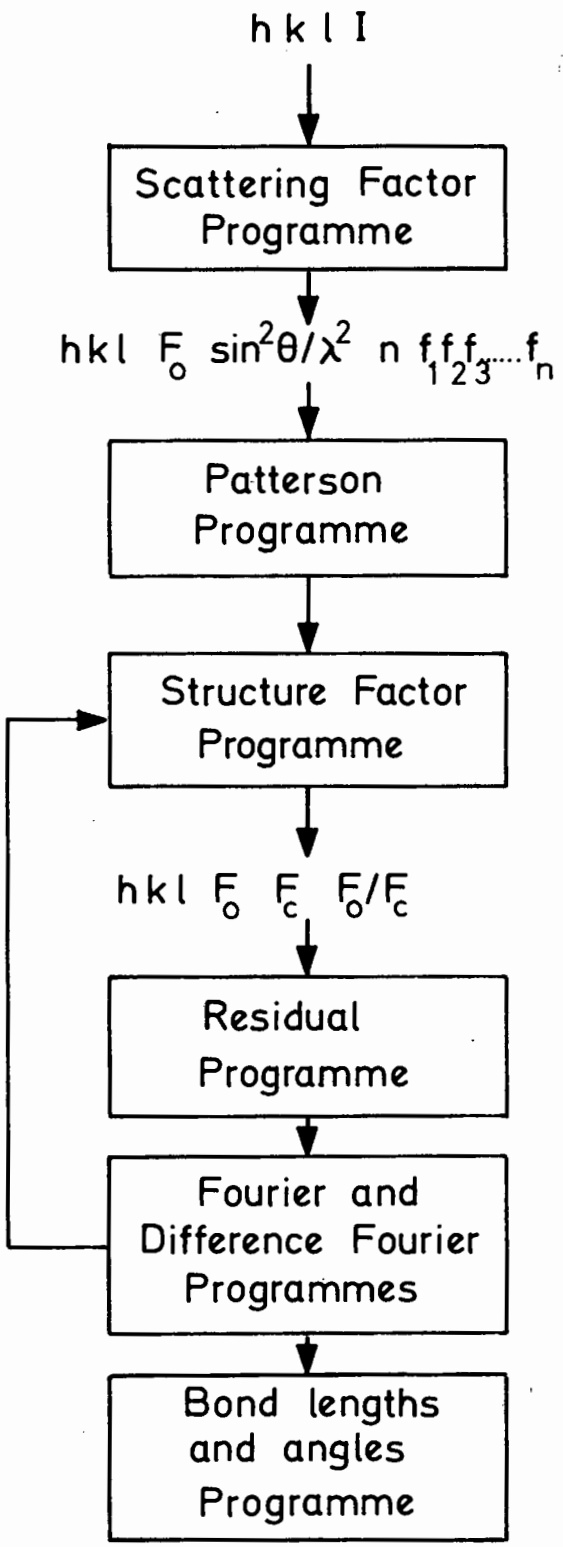
h k l I
Scattering Factor Programme
hkl F_o $\sin^2\theta/\lambda^2$ n $f_1 f_2 f_3 \ldots f_n$
Patterson Programme
Structure Factor Programme
hkl F_o F_c F_o/F_c
Residual Programme
Fourier and Difference Fourier Programmes
Bond lengths and angles Programme

Fig. 11

carefully chosen to obtain a good linear interpolation. The table has 26 values of $\sin^2\theta/\lambda^2$ ranging from 0 to 0.46, but increasing in steps of 0.01 for the first twelve steps.

The output is obtained both as a print output and as punched cards which are used in subsequent programmes.

There is a punched card for each reflection, containing the following information:

(1) 1000 + |h|

(2) 1000 + |k|

(3) 1000 + |ℓ|

(4) p where p = 1 for $hk\ell$

2 " $h\bar{k}\ell$

3 " $\bar{h}k\ell$

4 " $\bar{h}\bar{k}\ell$

5 " $hk\bar{\ell}$

6 " $h\bar{k}\bar{\ell}$

7 " $\bar{h}k\bar{\ell}$

8 " $\bar{h}\bar{k}\bar{\ell}$

(5) 1,000,000 + F_o (or F_o^2) corrected for Lp and A^* factors

(6) 1,000,000 + $10^4 \sin^2\theta/\lambda^2$

(7) $100f_1$, $100f_2$, $100f_3$,...,$100f_n$, where f_n is the scattering factor of the n^{th} element.

The reason for adding 1000 to the Miller indices and 1000000 to F_o and $\sin^2\theta/\lambda^2$ is that there is no facility for field definition on the I.C.T. 1301 computer using the Manchester Auto Code (MAC) language, and this was a suitable method of punching the data in appropiate columns on the cards which could then be sorted as required.

5.2 THE STRUCTURE FACTOR PROGRAMME.

This programme is written for the most general case of a triclinic unit cell and can take up to 35 atoms, with individual temperature factors.

The formula used in the computation is:

$$F_{c(hk\ell)} = \sum_i f_i \sum_j \cos 2\pi(hx_{ij}/a + ky_{ij}/b + \ell z_{ij}/c) e^{-B_j \sin^2\theta/\lambda^2} \quad \ldots\ldots \quad 5.13$$

where j = number of atoms of each element in the unit cell

i = different number of elements

B_j is the isotropic temperature factor of the j^{th} atom.

The programme has the facility of treating any given atom as vibrating anisotropically, in which case

$$B_j \sin^2\theta/\lambda^2 = [-\tfrac{1}{4}(\beta_{11}h^2a^{*2} + \beta_{22}k^2b^{*2} + \beta_{33}\ell^2c^{*2} + 2\beta_{12}hka^*b^*\cos\gamma^* + 2\beta_{13}h\ell a^*c^*\cos\beta^* + 2\beta_{23}k\ell b^*c^*\cos\alpha^*)] \quad \ldots\ldots \quad 5.14$$

The six β parameters serve to describe the ellipsoidal electron distribution of the anisotropically vibrating atom[29].

The programme can be modified for a particular space group so that only the position of the atoms in the asymmetric unit need be read thus shortening the time of computation. The F_o values are scaled to the F_c values by multiplication by a suitable scale factor k, so that

$$\frac{\Sigma kF_o}{\Sigma F_c} = 1$$

The punched cards obtained as output from the scattering factor programme are used as input data. The output is again in two forms:

(a) A print output giving the values of h, k, ℓ, F_o, F_c and F_o/F_c.

(b) A punch output containing the following information on the card

(1) 1000 + |h|

(2) 1000 + |k|

(3) 1000 + |ℓ|

(4) p, the designation number described in the previous programme

(5) 1,000,000 + $10F_o$

(6) 1,000,000 + $10F_o$.

This output is also suitable for sorting the reflection in any required order.

5.3 THE FOURIER PROGRAMME.

The structure factor $F_{hk\ell}$ may be expressed in exponential form by the formula:

$$F_{hk\ell} = \sum j\ f_j e^{2\pi i(hx_j+ky_j+\ell z_j)}$$
$$= \sum j\ f_j e^{i\phi_j} \quad \ldots\ldots \quad 5.15$$

It is a complex quantity, the real and imaginary parts being $A_{hk\ell}$ and $B_{hk\ell}$ respectively:

$$A_{hk\ell} = \sum j\ f_j \cos 2\pi(hx_j+ky_j+\ell z_j)$$
$$= \sum j\ f_j \cos\phi_j \quad \ldots\ldots \quad 5.16$$

$$B_{hk\ell} = \sum j\ f_j \sin 2\pi(hx_j+ky_j+\ell z_j)$$
$$= \sum j\ f_j \sin\phi_j \quad \ldots\ldots \quad 5.17$$

ϕ_j is defined by: $\phi_j = 2\pi(hx_j+ky_j+\ell z_j)$.

The phase angle $\alpha_{hk\ell}$ can be obtained from:

$$\tan \alpha_{hk\ell} = \frac{B_{hk\ell}}{A_{hk\ell}} \quad \ldots\ldots \quad 5.18$$

From 15, 16 and 17 it follows that

$$A_{hk\ell} = |F_{hk\ell}| \cos\alpha_{hk\ell}$$
$$B_{hk\ell} = |F_{hk\ell}| \sin\alpha_{hk\ell} \qquad \ldots\ldots \quad 5.19$$

Method of Summation

The electron density in the unit cell at a point determined by the fractional coordinates X, Y, Z is given by:

$$\rho(XYZ) = \frac{1}{V} \sum_{-\infty}^{+\infty} h \sum_{-\infty}^{+\infty} k \sum_{-\infty}^{+\infty} \ell \; F_{hk\ell} e^{-2\pi i(hX+kY+\ell Z)}$$

If we define θ by : $\theta = 2\pi(hX+kY+\ell Z)$ and use the relations

$$F_{hk\ell} = A_{hk\ell} + iB_{hk\ell}$$

$$F_{\bar{h}\bar{k}\bar{\ell}} = A_{\bar{h}\bar{k}\bar{\ell}} + iB_{\bar{h}\bar{k}\bar{\ell}} = A_{hk\ell} - iB_{hk\ell}\,, \quad \text{we find}$$

$$\rho(XYZ) = \frac{1}{2V} \sum_{-\infty}^{+\infty} \sum \sum \left[F_{hk\ell} e^{-i\theta} + F_{\bar{h}\bar{k}\bar{\ell}}\, e^{i\theta}\right]$$
$$= \frac{1}{2V} \sum_{-\infty}^{+\infty} \sum \sum \left[(A_{hk\ell}+iB_{hk\ell})e^{-i\theta} + (A_{hk\ell}-iB_{hk\ell})e^{i\theta}\right]$$
$$= \frac{1}{V} \sum_{-\infty}^{+\infty} \sum \sum \left[A_{hk\ell}\cos\theta + B_{hk\ell}\sin\theta\right] \qquad \ldots\ldots \quad 5.20$$

where $A_{hk\ell} = \sum j \; f_j \cos 2\pi(hx_j+ky_j+\ell z_j)$

$B_{hk\ell} = \sum j \; f_j \sin 2\pi(hx_j+ky_j+\ell z_j)$

$\theta = 2\pi(hX+kY+\ell Z)$.

For convenience we will henceforth write $\theta = (hx+ky+\ell z)$.

To facilitate computation it is useful to write $\cos\theta$ and $\sin\theta$ as the sum of a set of triple products:

$$\cos\theta = \cos(hx+ky+\ell z)$$

$$= \cos hx \cos(ky+\ell z) - \sin hx \sin(ky+\ell z)$$

$$= (\cos hx \cos ky \cos \ell z$$
$$- \cos hx \sin ky \sin \ell z$$
$$- \sin hx \cos ky \sin \ell z$$
$$+ \sin hx \sin ky \cos \ell z);$$

$$\sin\theta = \sin(hx+ky+\ell z)$$

$$= \sin hx \cos(ky+\ell z) + \cos hx \sin(ky+\ell z)$$

$$= (-\sin hx \sin ky \sin \ell z + \sin hx \cos ky \cos \ell z + \cos hx \sin ky \cos \ell z + \cos hx \cos ky \sin \ell z).$$

Substituting for $\cos\theta$ and $\sin\theta$ in equation 5.20, we get

$$\rho(XYZ) = \frac{1}{V} \sum_{-\infty}^{+\infty} h \sum_{-\infty}^{+\infty} k \sum_{-\infty}^{+\infty} \ell \Big[A_{hk\ell} (\cos hx \cos ky \cos \ell z - \cos hx \sin ky \sin \ell z - \sin hx \cos ky \sin \ell z + \sin hx \sin ky \cos \ell z) + B_{hk\ell} (-\sin hx \sin ky \sin \ell z + \sin hx \cos ky \cos \ell z + \cos hx \sin ky \cos \ell z + \cos hx \cos ky \sin \ell z) \Big]$$

$$= \frac{1}{V} \sum_{0}^{+\infty} h \sum_{0}^{+\infty} k \sum_{0}^{+\infty} \ell \cos hx \cos ky \cos \ell z (A_{hk\ell} + A_{\bar{h}k\ell} + A_{h\bar{k}\ell} + A_{\bar{h}\bar{k}\ell} + A_{hk\bar{\ell}} + A_{\bar{h}k\bar{\ell}} + A_{h\bar{k}\bar{\ell}} + A_{\bar{h}\bar{k}\bar{\ell}})$$

$$+ \cos hx \sin ky \sin \ell z (-A_{hk\ell} - A_{\bar{h}k\ell} + A_{h\bar{k}\ell} + A_{\bar{h}\bar{k}\ell} + A_{hk\bar{\ell}} + A_{\bar{h}k\bar{\ell}} - A_{h\bar{k}\bar{\ell}} - A_{\bar{h}\bar{k}\bar{\ell}})$$

+ similar terms.

Now $A_{hk\ell} = A_{\bar{h}\bar{k}\bar{\ell}}$ $\quad B_{hk\ell} = -B_{\bar{h}\bar{k}\bar{\ell}}$

$A_{\bar{h}k\ell} = A_{h\bar{k}\bar{\ell}}$ $\quad B_{\bar{h}k\ell} = -B_{h\bar{k}\bar{\ell}}$

$A_{h\bar{k}\ell} = A_{\bar{h}k\bar{\ell}}$ $\quad B_{h\bar{k}\ell} = -B_{\bar{h}k\bar{\ell}}$

$A_{\bar{h}\bar{k}\ell} = A_{hk\bar{\ell}}$ $\quad B_{\bar{h}\bar{k}\ell} = -B_{hk\bar{\ell}}$, so the expression becomes:

$$\rho(XYZ) = \frac{2}{V} \sum_{0}^{\infty} h \sum_{0}^{\infty} k \sum_{0}^{\infty} \ell \Big[A^1 \cos hx \cos ky \cos \ell z + A^2 \cos hx \sin ky \sin \ell z + A^3 \sin hx \cos ky \sin \ell z + A^4 \sin hx \sin ky \cos \ell z + B^1 \sin hx \sin ky \sin \ell z + B^2 \sin hx \cos ky \cos \ell z + B^3 \cos hx \sin ky \cos \ell z + B^4 \cos hx \cos ky \sin \ell z \Big]$$

where $A^1 = A_{hk\ell} + A_{\bar{h}k\ell} + A_{h\bar{k}\ell} + A_{\bar{h}\bar{k}\ell}$

$A^2 = -A_{hk\ell} - A_{\bar{h}k\ell} + A_{h\bar{k}\ell} + A_{\bar{h}\bar{k}\ell}$

$A^3 = -A_{hk\ell} + A_{\bar{h}k\ell} - A_{h\bar{k}\ell} + A_{\bar{h}\bar{k}\ell}$

$A^4 = -A_{hk\ell} + A_{\bar{h}k\ell} + A_{h\bar{k}\ell} - A_{\bar{h}\bar{k}\ell}$

$B^1 = -B_{hk\ell} + B_{\bar{h}k\ell} + B_{h\bar{k}\ell} - B_{\bar{h}\bar{k}\ell}$

$B^2 = +B_{hk\ell} - B_{\bar{h}k\ell} + B_{h\bar{k}\ell} - B_{\bar{h}\bar{k}\ell}$

$B^3 = +B_{hk\ell} + B_{\bar{h}k\ell} - B_{h\bar{k}\ell} - B_{\bar{h}\bar{k}\ell}$

$B^4 = +B_{hk\ell} + B_{\bar{h}k\ell} + B_{h\bar{k}\ell} + B_{\bar{h}\bar{k}\ell}$ 5.21

If the unit cell contains symmetry elements, the expressions A^1, A^2,...,B^4 can be simplified.

The Fourier Programme has the possibility of arranging the output of the electron density function in various formats. By reading in appropriate constants, the unit cell axes can be arranged in various combinations. The output is in the form

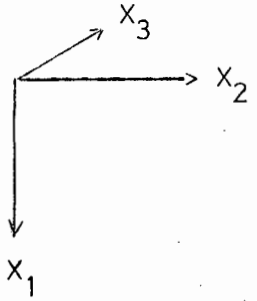

so that if the required format is

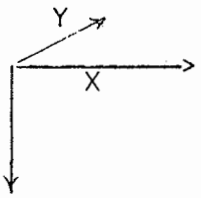

, then the appropriate order constants would be $X_1 = Z$, $X_2 = X$, $X_3 = Y$, which are read into the programme as 3,1,2.

The print output on the computer page can be altered to approximate

the unit cell lengths and angles. Thus it is possible to have the X_1 and X_2 axes inclined to each other at various angles

angle $>90^\circ$ $\quad$ 90° $\quad$ $<90^\circ$

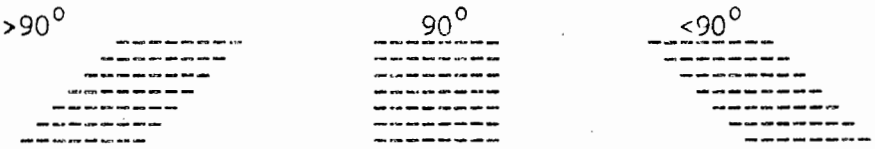

and the length of X_1 can be increased by skipping a given number of lines in the output.

A three dimensional Fourier is obtained by dividing the unit cell into two dimensional sections perpendicular to X_3, the spacing between these can be chosen at will. Thus X_3 may have values of 0, 1/100, 2/100, 3/100 ..... .

As an example, the codeword for the space group Pbca, which was used in the calculation of the Fourier summation of compound 2, is derived. Suppose the axial setting is chosen as

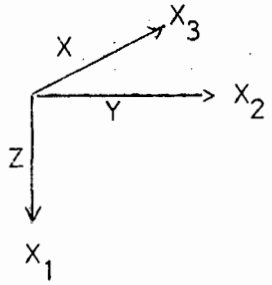

then the appropriate order constants are 3,2,1 i.e. we carry out an 'ℓkh' summation.

Since the space group Pbca is centrosymmetric, the B values in equation 5.21 are all zero.

For this space group there are four sets of relations for $A_{hk\ell}$ depending on the Miller indices:

1 even-even $\begin{cases} h + k = 2n \\ k + \ell = 2n \end{cases}$

2 odd-even $\begin{cases} h + k = 2n+1 \\ k + \ell = 2n \end{cases}$

3 even-odd $\begin{cases} h + k = 2n \\ k + \ell = 2n+1 \end{cases}$

4 odd-odd $\begin{cases} h + k = 2n+1 \\ k + \ell = 2n+1 \end{cases}$

The programme is able to test which of these four conditions is applicable to any one reflection. In this case four codewords must be calculated, i.e. one for each condition.

First codeword: 'even-even' case.

For an 'ℓkh' summation the coefficients in eqn. 5.21 may be written

$$A^1 = A_{\ell kh} + A_{\bar{\ell} kh} + A_{\ell \bar{k} h} + A_{\bar{\ell}\bar{k}h}$$
$$= A_{hk\ell} + A_{hk\bar{\ell}} + A_{h\bar{k}\ell} + A_{h\bar{k}\bar{\ell}}$$
$$= A_{hk\ell} + A_{hk\bar{\ell}} + A_{h\bar{k}\ell} + A_{\bar{h}k\ell} \qquad \text{(Friedel's Law)}$$

For the space group Pbca the following relation holds:

$$A_{hk\ell} = A_{\bar{h}k\ell} = A_{h\bar{k}\ell} = A_{hk\bar{\ell}}$$

and the first codeword is therefore

$$A^1 = A_{hk\ell} + A_{hk\ell} + A_{hk\ell} + A_{hk\ell} = 4A_{hk\ell}$$
$$A^2 = -A_{hk\ell} - A_{hk\ell} + A_{hk\ell} + A_{hk\ell} = 0$$
$$A^3 = -A_{hk\ell} + A_{hk\ell} - A_{hk\ell} + A_{hk\ell} = 0$$
$$A^4 = -A_{hk\ell} + A_{hk\ell} + A_{hk\ell} - A_{hk\ell} = 0$$

$B^1 = 0$

$B^2 = 0$

$B^3 = 0$

$B^4 = 0$

Only values of $A_{hk\ell}$, and not the values of $A_{\bar{h}k\ell}$, $A_{h\bar{k}\ell}$ and $A_{hk\bar{\ell}}$ are read into the computer, however, and consequently the computer memory holds the following values

$A^1 = A_{hk\ell}$

$A^2 = -A_{hk\ell}$

$A^3 = -A_{hk\ell}$

$A^4 = -A_{hk\ell}$

Thus to obtain the correct values the coefficients A^2, A^3, A^4 must be zeroed

Hence $A^1 = A^1 \times 1$
$A^2 = A^2 \times 0$
$A^3 = A^3 \times 0$
$A^4 = A^4 \times 0$

codeword = 1000

The full codeword, including the coefficients B^1, B^2, B^3, B^4 is therefore : 10000000.

The codewords for the other three cases : 'odd-even', 'even-odd' and 'odd-odd' may be similarly derived and the full four part codeword is:

10000000 00100000 00010000 01000000.

5.4 THE PATTERSON PROGRAMME.

The Patterson programme is similar to the Fourier programme but uses F_o^2 as coefficients and uses the formula

$$P(u,v,w) = \sum_{h} \sum_{\underline{k}}^{\infty} \sum_{\ell} F_o^2 \cos 2\pi(hu + kv + \ell w) \qquad \ldots\ldots\ldots \quad 5.22$$

where u, v, w are the fractional coordinates of the unit cell parameters.

Since the Patterson function is centrosymmetric, the codeword is restricted to evaluating the coefficients of A^1, A^2, A^3, A^4, the corresponding B values being zero.

In this case equation 5.19 modifies to

$$A_{(hk\ell)} = F^2_{o(hk\ell)}$$

5.5 THE RESIDUAL PROGRAMME.

This programme calculates the residual index R

$$R = \frac{\sum ||F_o| - |F_c||}{\sum |F_o|} \qquad \ldots\ldots\ldots \quad 5.23$$

from properly scaled F_o and F_c values, and expresses the answer as a percentage.

5.6 THE BOND LENGTHS AND ANGLES PROGRAMME.

This programme requires as input the unit cell parameters: a, b, c, c^*, α, β, γ and the fractional coordinates of each atom. It can then calculate

(a) Interatomic distances
(b) Interatomic angles
(c) The best plane (by least squares) through any number of points
(d) The angles between any given plane
(e) The perpendicular distance between atoms and planes.

The fractional coordinates (x^i) measured in triclinic system are converted to Cartesian coordinates (X^i) by the contravariant transformation[30]

$$(X^i) = (x^i)(\beta^i_j)$$

where $(X^i) = (X^1, X^2, X^3) = (X, Y, Z)$ (Cartesian coordinates)

$(x^i) = (x^1, x^2, x^3) = (x/a, y/b, z/c)$ (Fractional coordinates)

$$(\beta^i_j) = \begin{bmatrix} a & 0 & 0 \\ b\cos\gamma & b\sin\gamma & 0 \\ c\cos\beta & -c\,\dfrac{\cos\beta\cos\gamma - \cos\alpha}{\sin\gamma} & \dfrac{1}{c^*} \end{bmatrix}$$

(a) Interatomic distances are calculated from the formula:

$$r_{AB} = \left[(X_B - X_A)^2 + (Y_B - Y_A)^2 + (Z_B - Z_A)^2\right]^{\frac{1}{2}}$$

(b) Interatomic angles are calculated from the formula:

$$\vec{r}_{AB} \cdot \vec{r}_{BC} = |r_{AB}|\,|r_{BC}| \cos\phi_{ABC}$$

whence $\phi_{ABC} = \text{Arc cos}\dfrac{|(X_A - X_B)(X_B - X_C) + (Y_A - Y_B)(Y_B - Y_C) + (Z_A - Z_B)(Z_B - Z_c)|}{|r_{AB}| - |r_{BC}|}$

(c) The best plane through any number of points.

Equations of a plane are: $\ell X + mY + nZ - p = 0$

and $\ell^2 + m^2 + n^2 = 1$

this then means then ℓ, m, n are the direction cosines of the plane.

Let eq. of the plane be $Y = m'X + n'Z + c$

If (X_i, Y_i, Z_i) lies off the plane then $m'X_i + n'Z_i + c = Y \neq Y_i$.

then $Y_i - Y = Y_i - (m'X_i + n'Z_i + c)$

then by principles of least Sq. which states that the sum of the square of these differences = min. for the best plane.

Let there be "N" points then

$$U = \sum_{i=1}^{N} \left[m' X_i + n' Z_i + c - Y_i\right]^2$$

then $\frac{\partial U}{\partial m'} = \frac{\partial U}{\partial n'} = \frac{\partial U}{\partial c} = 0$

which gives rise to the equations.

$$\sum_{i=1}^{N} Y_i = m' \sum_{i=1}^{N} X_i + n' \sum_{i=1}^{N} Z_i + Nc$$

$$\sum_{i=1}^{N} X_i Y_i = m' \sum_{i=1}^{N} X_i^2 + n' \sum_{i=1}^{N} X_i Z_i + c \sum_{i=1}^{N} X_i$$

$$\sum_{i=1}^{N} Z_i Y_i = m' \sum_{i=1}^{N} X_i Z_i + n' \sum_{i=1}^{N} Z_i^2 + c \sum_{i=1}^{N} Z_i$$

then solving for m' n' and c.

$$\sum Y_i = m' \sum X_i + n' \sum Z_i + Nc$$

$$\sum X_i Y_i = m' \sum X_i^2 + n' \sum X_i Z_i + c \sum X_i$$

$$\sum Z_i Y_i = m' \sum X_i Z_i + n' \sum Z_i^2 + c \sum Z_i$$

$$n' = \frac{(\Sigma X \Sigma Y - N\Sigma XY)(\Sigma X \Sigma Z - N\Sigma XZ) - (\Sigma Z \Sigma Y - N\Sigma YZ)(\Sigma X \Sigma X - N\Sigma X^2)}{(\Sigma Z \Sigma X - N\Sigma XZ)(\Sigma X \Sigma Z - N\Sigma XZ) - (\Sigma X \Sigma X - N\Sigma X^2)(\Sigma Z \Sigma Z - N\Sigma Z^2)}$$

$$m' = \frac{(\Sigma X \Sigma Y - N\Sigma XY)(\Sigma Z \Sigma Z - N\Sigma Z^2) - (\Sigma Z \Sigma X - N\Sigma XZ)(\Sigma Z \Sigma Y - N\Sigma ZY)}{(\Sigma X \Sigma X - N\Sigma X^2)(\Sigma Z \Sigma Z - N\Sigma Z^2) - (\Sigma Z \Sigma X - N\Sigma XZ)(\Sigma X \Sigma Z - N\Sigma XZ)}$$

$$c = \frac{\Sigma Y - m' \Sigma X - n' \Sigma Z}{N}$$

From these values of m' n' and c

$$\ell = -m' / \sqrt{1 + (m')^2 + (n')^2}$$

$$m = 1 / \sqrt{1 + (m')^2 + (n')^2}$$

$$n = -n' / \sqrt{1 + (m')^2 + (n')^2}$$

$$p = c / \sqrt{1 + (m')^2 + (n')^2}$$

(d) The angle between two planes.

If the two planes have the equations

$$\ell_1 X + m_1 Y + n_1 Z - p_1 = 0 \quad \text{and} \quad \ell_1^2 + m_1^2 + n_1^2 = 1$$

and $\ell_2 X + m_2 Y + n_2 Z - p_2 = 0$ and $\ell_2^2 + m_2^2 + n_2^2 = 1$

then the angle between them, θ, has the value.

$$\theta = \text{Arc cos } (\ell_1 \ell_2 + m_1 m_2 + n_1 n_2)^{31}$$

(e) The perpendicular distance between a point and a plane.

Let the point concerned have the coordinates (X_1, Y_1, Z_1) and let the plane concerned have the equation

$$\ell X + mY + nZ - p = 0 \quad \text{with} \quad \ell^2 + m^2 + n^2 = 1$$

then the (perpendicular)distance D from the point to the plane is

$$D = \ell X_1 + mY_1 + nZ_1 - p$$

Where D is positive if the point (X_1, Y_1, Z_1) is on the side of the plane opposite to that containing the origin.

6. THE CRYSTAL STRUCTURE OF Di-μ-diethylphosphido-bis-(tetracarbonylmolybdenum)(compound 1).

6.1 OPTICAL GONIOMETRIC STUDY.

A drawing of the crystal and a stereographic projection are shown in Fig. 12. A goniometric study was carried out using a two circle optical goniometer. The readings obtained are only accurate to within 20 minutes of a degree because the crystals were very small and the reflections obtained were not always good.

Several crystals were examined and the quoted angles are the means of measurements independently carried out on five different crystals.

6.1 (a) Procedure. The crystal was mounted with the large face b (Fig. 12) in a horizontal position. Interfacial angles were measured in the following zones

Zone A a ^ b ^ c ^ d ^ e ^ f

$(1\bar{1}1) \wedge (100) \wedge (11\bar{1}) \wedge (\bar{1}1\bar{1}) \wedge (\bar{1}00) \wedge (\bar{1}\bar{1}1)$

Zone B g ^ b ^ h ^ i ^ e ^ k

$(1\bar{1}\bar{1}) \wedge (100) \wedge (111) \wedge (\bar{1}11) \wedge (\bar{1}00) \wedge (\bar{1}\bar{1}\bar{1})$

Interfacial angles between similar faces were found to be

$(100) \wedge (111) = 56^{\circ}30'$

$(100) \wedge (11\bar{1}) = 68^{\circ}51'$

and the obtuse angle between zone A and B was measured and found to be $100^{\circ}43'$.

6.1 (b) Determination of the angle β.

In determining the angle β between the X and Z axes it

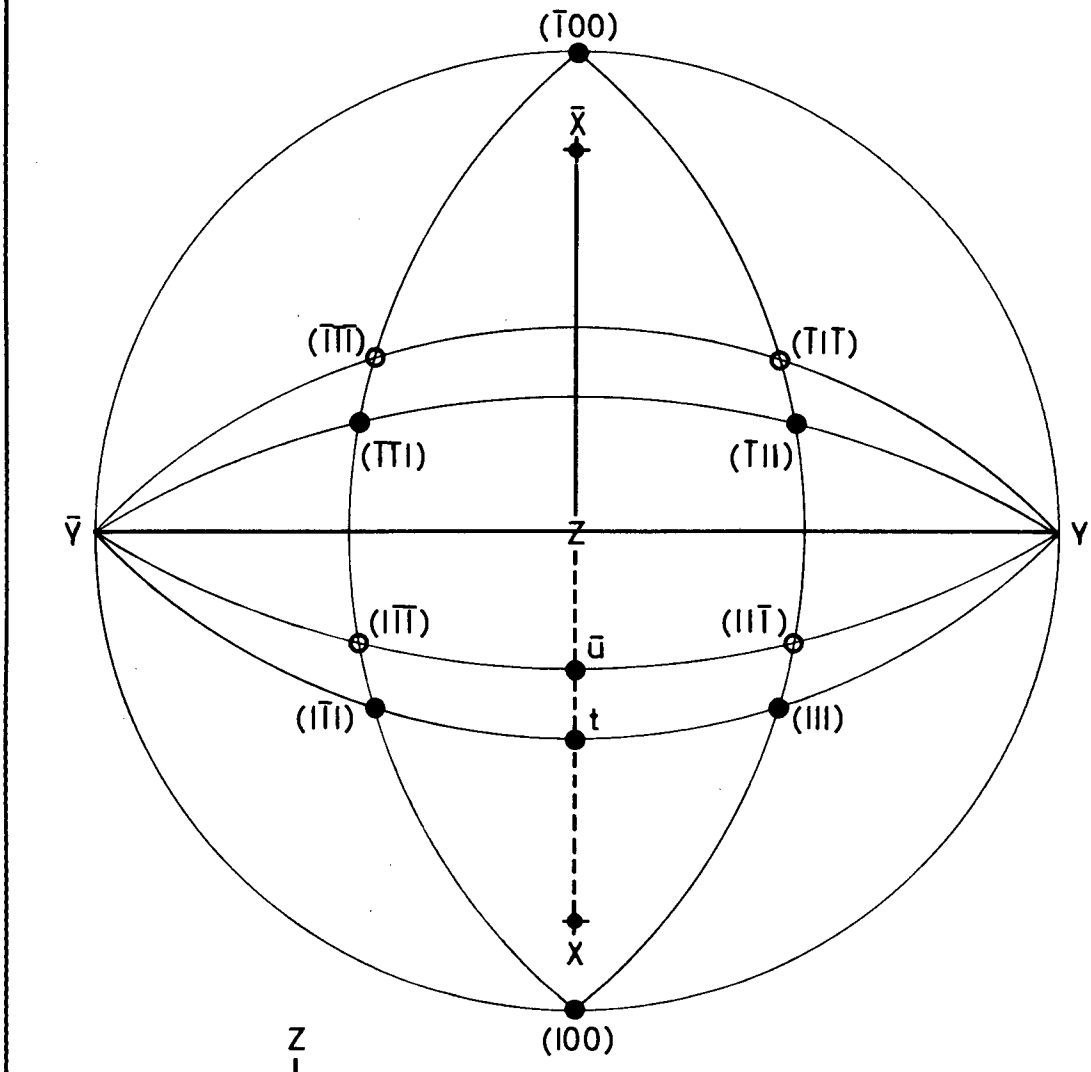

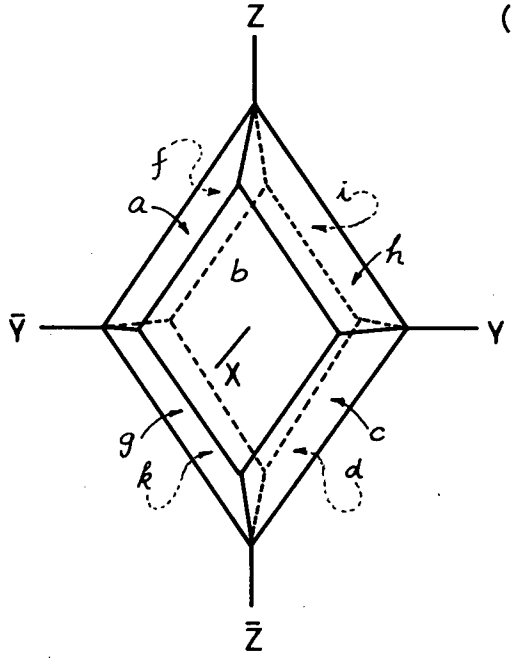

FORMS PRESENT:

(100) ORTHOPINACOID

(111) -ve HEMI-BIPYRAMID

(T11) +ve HEMI-BIPYRAMID

Fig. 12

was assumed that the face which is cozonal with $(1\bar{1}1,111)$ and (100,001) is the negative hemi-orthodome (101). This is the hypothetical face † labelled on the stereogram (Fig. 12). By considering the face (100) together with the hypothetical face (101), the following equations may be derived:-

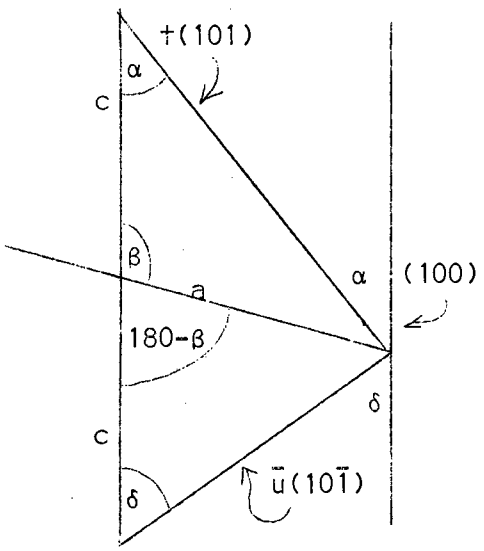

$$\frac{c}{\sin\ 180-(\alpha+\beta)} = \frac{a}{\sin\ \alpha} = \frac{c}{\sin(\alpha+\beta)}$$

$$\therefore\ \sin(\alpha+\beta) = \frac{c \sin \alpha}{a} \qquad \text{.....(i)}$$

$$\frac{c}{\sin\ 180-\left|(180-\beta)+\delta\right|} = \frac{a}{\sin\ \delta}$$

$$\therefore\ \sin(\beta-\delta) = \frac{c \sin \delta}{a} \qquad \text{.....(ii)}$$

$$\frac{(i)}{(ii)} = \frac{\sin(\alpha+\beta)}{\sin(\beta-\delta)} = \frac{\sin \alpha}{\sin \delta}$$

$$\therefore\ \frac{\sin \alpha \cos \beta + \cos \alpha \sin \beta}{\sin \beta \cos \delta - \cos \beta \sin \delta} = \frac{\sin \alpha}{\sin \delta}$$

$$\therefore \sin\alpha\cos\beta\sin\delta + \cos\alpha\sin\beta\sin\delta = \sin\alpha\sin\beta\cos\delta - \sin\alpha\cos\beta\sin\delta$$

$$\therefore \cos\beta(\sin\alpha\sin\delta + \sin\alpha\sin\delta) = \sin\beta(\sin\alpha\cos\delta - \cos\alpha\sin\delta)$$

$$\therefore\ \frac{\sin \beta}{\cos \beta} = \frac{2 \sin\alpha\sin\delta}{\sin(\alpha-\delta)} \qquad \text{.....(iii)}$$

To determine the angle α, which is the angle between (100) and the hypothetical face (101), consider the following Napierian triangle

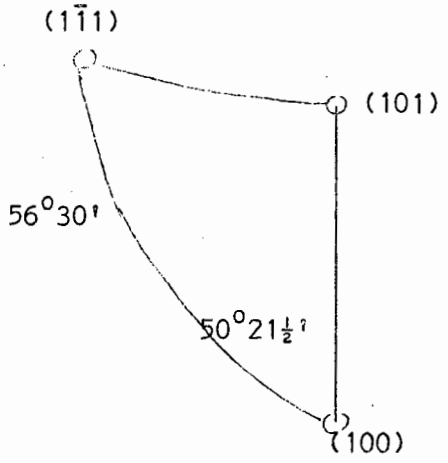

By goniometry, the angle (100) ^ (1$\bar{1}$1) = 56°30', and the angle between the zone (100,101) and (100,1$\bar{1}$1) is half the angle 100°43' = 50°21'30"

$$\sin 90\text{-}50^\circ 21\tfrac{1}{2}' = \tan 90\text{-}56^\circ 30' \cdot \tan (100) \wedge (101)$$

$$\therefore \tan (100) \wedge (101) = \frac{\sin 39^\circ 38\frac{1}{2}'}{\tan 33^\circ 30'}$$

hence α = (100) ^ (101) = 43°57'.

To determine the angle δ, which is the angle between the face (100) and the hypothetical face (10$\bar{1}$) consider the following Napierian triangle

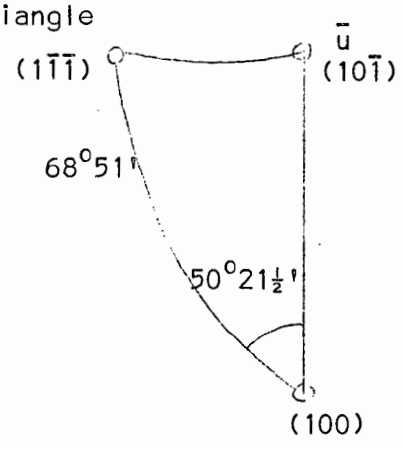

By goniometry the angle (100) ^ $(1\bar{1}\bar{1})$ = $68^{\circ}51'$ and the angle between the zone (100, $10\bar{1}$) and (100, $1\bar{1}\bar{1}$) is half the angle $100^{\circ}43' = 50^{\circ}21'30''$

sin $90-50^{\circ}21\frac{1}{2}'$ = tan $90-68^{\circ}51'$ tan (100) ^ $(10\bar{1})$

$\therefore$ tan (100) ^ $(10\bar{1}) = \frac{\sin 39^{\circ}38\frac{1}{2}'}{\tan 21^{\circ}9'}$

hence δ = (100) ^ $(10\bar{1})$ = $58^{\circ}46'$

$\therefore$ tan $\beta = \frac{2 \sin 43^{\circ}47' \sin 58^{\circ}46'}{\sin 14^{\circ}49'}$

$\therefore$ $\beta = 75^{\circ}01'$ (acute)

or $\beta = 104^{\circ}59'$ (obtuse)

6.1 (c) Calculation of axial ratios.

Considering the following Napierian triangle

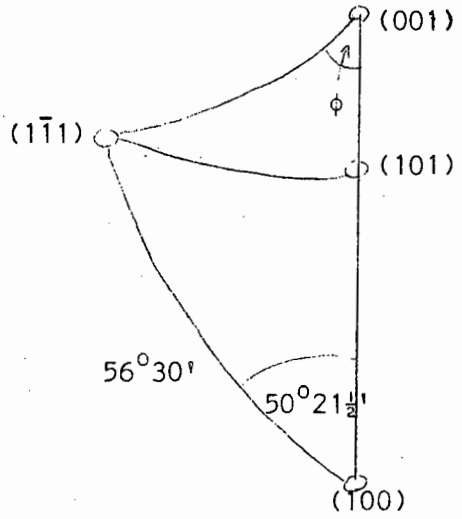

(1) By calculation (100) ^ (101) = $43^{\circ}57'$

and (101) ^ (001) = $\beta - 43^{\circ}57' = 31^{\circ}04'$

(2) To obtain the angular distance $(1\bar{1}1)$ ^(101):-

$$\sin 43^\circ 57' = \tan 90\text{-}50^\circ 21\tfrac{1}{2}' \tan (1\bar{1}1) \wedge (101)$$

$$\tan (1\bar{1}1) \wedge (101) = \frac{\sin 43^\circ 57'}{\tan 39^\circ 38\tfrac{1}{2}'}$$

$$(1\bar{1}1) \wedge (101) = 39^\circ 57'$$

(3) To obtain the angular value ϕ :-

$$\sin 31^\circ 4' = \tan 39^\circ 57' \tan 90\text{-}\phi$$

$$\tan 90\text{-}\phi = \frac{\sin 31^\circ 4'}{\tan 39^\circ 57'}$$

$$\phi = 58\ 23'$$

$$\tan \phi = \frac{a}{b} = 1.6244$$

The axial ratio $\frac{c}{a} = \frac{\sin (001) \wedge (101)}{\sin (100) \wedge (101)}$

$$= \frac{\sin 31^\circ 4'}{\sin 43^\circ 57'}$$

$$\frac{c}{a} = 0.7433$$

$$\frac{c}{b} = \frac{c}{a} \times \frac{a}{b} = 0.7433 \times 1.6244 = 1.207$$

Hence a : b : c

1.624 : 1 : 1.207

Change of axes.

In the subsequent X-ray analysis it was necessary, in order to comply with space group conditions of $C_{2/c}$ to relabel the axes : Goniometric study a b c

↓ ↓ ↓

X-ray study c b a

and the angle β was, unconventionally, chosen as acute.

6.2 THE DETERMINATION OF THE UNIT CELL AND SPACE GROUP.

6.2(a). The measurements of the unit cell parameters.

The unit cell lengths were measured from layer-line spacings

of single crystal rotation photographs[32]. The values were refined by taking zero layer Weissenberg photographs about each axis and extrapolating the interplanar spacings in accordance with Bradley and Jay's extrapolation[33].

The angle β^* was measured accurately from Weissenberg photographs in two ways

(a) by the method of ω separations[34], yielding a value of $\beta^* = 102^\circ 31'$

$\beta = 77^\circ 29'$

(b) by the method of triangulation[35], yielding a value of $\beta^* = 102^\circ 32'$

$\beta = 77^\circ 28'$

This value compared favourably with the value $\beta = 75^\circ 1'$ obtained by optical goniometry. In the accurate determination of the unit cell lengths, Kodak Industrex D film, which has no significant shrinkage, was used.

The final values of the unit cell parameters obtained were

$a = 13.21 \pm .01$ Å	$\alpha = 90^\circ$
$b = 10.85 \pm .01$ Å	$\beta = 77.46^\bullet \pm .08^\circ$
$c = 16.48 \pm .02$ Å	$\gamma = 90^\circ$

Several methods for accurately setting crystals were employed[36-38]. The one which proved the most successful was the double Laue method of Weist and Cole[39]: this consists of taking a Laue photograph of a crystal on a cylindrical camera and having one of the arcs of the goniometer head parallel to the incident beam. A second photograph is superimposed on the first by turning the crystal through

180°. From the resulting composite photograph it is possible to determine both the magnitudes and directions of the arc errors.

6.2 (b) The measurement of the crystal density.

The density of the crystals was measured by the flotation method. The liquid used was a mixture of bromoform and ethyl alcohol in which the crystals were insoluble. This method yielded a value of

$$\rho = 1.633 \pm .003 \text{ g/cm}^3.$$

6.2 (c) The number of molecules/unit cell.

The volume of the unit cell of a monoclinic crystal is given by the formula $V = abc \sin \beta$.

The number of molecules in the unit cell can therefore be calculated from the formula

$$nM = abc \sin \beta \rho N \quad \ldots\ldots\ldots \quad 6.1$$

where M is the molecular weight of the compound

ρ_m is the crystal density (measured)

N is the Avogadro number.

By appropriate substitution of the measured constants

$$n = \frac{13.21 \times 10.85 \times 16.48 \times .9762 \times 1.633 \times 6.023 \times 10^{23} \times 10^{-24}}{594.2}$$

$n = 3.817 = 4$ molecules/unit cell.

The calculated crystal density ρ_c, assuming four molecules per unit cell, is 1.711 g/cm^3.

6.2(d) The examination of systematic absences and the determination of the space group.

Zero and upper layer Weissenberg photographs were taken with the crystal oscillating about all three principal axes. The reflections were indexed and an examination of the indices was carried out.

The conditions limiting the possible reflections were

$hk\ell$: $h + k = 2n$

$h0\ell$: $\ell = 2n$, $h = 2n$

$0k0$: $k = 2n$

The diffraction symbol (Monoclinic second setting) was therefore 12/m1C.c. which corresponds to two possible space groups : $C_{2/c}$ (No 15) or C_c (No 9), the latter being non-centrosymmetric. Attempts to establish whether the crystals were centrosymmetric and thus uniquely determine the space group were carried out by applying tests for pyro-electricity[40] and by carrying out a Wilson plot[41]. Both of these methods, however, yielded non-definitive results, and the space group was uniquely determined by subsequent analysis of the Patterson synthesis.

6.3 THE SELECTION OF A CRYSTAL SUITABLE FOR INTENSITY DATA COLLECTION.

From consideration of elementary X-ray absorption theory it can be shown that[42]

$$I = I_o e^{-\mu t} \qquad \ldots\ldots\ldots \quad 6.2$$

where I = intensity of the X-ray beam,

I_o = initial intensity of X-ray beam,

μ = linear absorption coefficient,

t = thickness of crystal traversed by the X-ray beam,

and further that the optimum crystal size is of the order of $2/\mu$ cm. The size and shape of the crystal are important because it is difficult to correct diffraction intensities for absorption if the crystal is not either cylindrical or spherical.

In order to minimize absorption errors attempts were made to grind the crystal into a sphere[43], but the crystals invariably shattered.

Calculation of the linear absorption coefficient μ.

The linear absorption coefficient may be calculated from the formula

$$\mu = \rho \Sigma p\mu_m \quad \ldots\ldots\ldots\ldots \quad 6.3$$

where ρ = density of the compound

p = the proportion of each element by weight in the compound

μ_m = mass absorption coefficient of each element[44].

For the compound under analysis and using CuK_α radiation of wavelength 1.5418 Å

$$\rho = 1.633 \text{ g/cm}^3$$

$$\mu_m(Mo) = 162 \text{ cm}^2\text{g}^{-1}$$

$$\mu_m(P) = 74.1 \text{ "}$$

$$\mu_m(O) = 11.7 \text{ "}$$

$$\mu_m(C) = 4.60 \text{ "}$$

$$\mu_m(H) = 0.435 \text{ "}$$

This gives $\mu = 104.6\ cm^{-1}$, and an optimum crystal size of $2/\mu = 0.019$ cm = 0.2 mm.

6.4 THE COLLECTION AND MEASUREMENT OF INTENSITY DATA.

A single crystal, having dimensions .12 mm ×.10 mm × .07 mm was selected. The mean radius was taken as 0.049 mm. Hence $\mu R = 0.51$.

The absorption correction A^* for $\mu R = .51$ varies only from 2.08 at $\theta = 0^\circ$ to 1.90 at $\theta = 90^\circ$. This was not deemed significant and therefore no absorption correction was applied to the intensity data.

An integrating Weissenberg goniometer was used to collect the intensity data. In order to overcome the lack of range of a single film, the multiple film technique[45] was employed. The crystal was set with the Y axis parallel to the axis of oscillation and upper layer intensities were collected using the equi-inclination technique. Data was collected from the h0ℓ, h1ℓ, h2ℓ, h3ℓ, h4ℓ, h5ℓ, and h6ℓ layer lines. The integrated intensities of the reflections were measured on the densitometer and the appropiate corrections to account for the non-linearity of the densitometer response were applied (Section 4.2). The intensity data from the different layers was scaled by measuring the reflections obtained from a zero layer integrated Weissenberg photograph taken about the Z axis (hk0 reflections).1027 reflections were measured.

The intensities were punched on computer cards and corrected for various geometric and physical factors as discussed in Section 5.1 A Patterson synthesis was then computed.

6.5 THE PATTERSON SYNTHESIS.

A three dimensional Patterson synthesis was computed (equation 5.22) for the fraction of the unit cell $0 \rightarrow \frac{1}{2}$ along a, $0 \rightarrow \frac{1}{2}$ along b and $0 \rightarrow \frac{1}{2}$ along c. The three dimensional map was drawn on glass sheets and photographed (Fig. 13).

Since molybdenum is considerably heavier than any other atoms in the molecule, the vector peaks arising from Mo - Mo interactions can be expected to be considerably larger than those arising from any other atoms.

The interpretation of the Patterson synthesis was carried out using an analytical method. The structure has four molecules, and hence eight molybdenum atoms per unit cell. There are two possible space groups $C_{2/c}$ (centrosymmetric) and C_c (non-centrosymmetric).

The eight molybdenum atoms were placed in the general positions as required by the space group $C_{2/c}$[46] and 8×8 positions of the vector peaks arising from the Mo - Mo interactions are shown in Table 4. Not all of these peaks are unique, however, since there are eight vector peaks at the origin (0,0,0), there are four peaks at $(\frac{1}{2},\frac{1}{2},0)$ and four at $(-\frac{1}{2},-\frac{1}{2},0)$: this is analogous to a peak of multiplicity 8 at (2,2,0), and similarly for other peaks.

6.5 (a) Calibration of Patterson peaks[47].

The volume of a Patterson peak due to a pair of atoms i and j is Z_iZ_j where Z is the number of electrons in an atom.

$$V_{ij} = Z_iZ_j \qquad \ldots\ldots\ldots \quad 6.4$$

ATOMIC POSITION	1 x y z	2 $\bar{x}\ \bar{y}\ \bar{z}$	3 $\bar{x}$ y $\frac{1}{2}$-z	4 x $\bar{y}$ $\frac{1}{2}$+z	5 $\frac{1}{2}$+x $\frac{1}{2}$+y z	6 $\frac{1}{2}$-x $\frac{1}{2}$-y $\bar{z}$	7 $\frac{1}{2}$-x $\frac{1}{2}$+y $\frac{1}{2}$-z	8 $\frac{1}{2}$+x $\frac{1}{2}$-y $\frac{1}{2}$+z
1 x y z	1-1 0 0 0	1-2 2x 2y 2z	1-3 2x 0 $\frac{1}{2}$	1-4 0 2y $-\frac{1}{2}$	1-5 $-\frac{1}{2}$ $-\frac{1}{2}$ 0	1-6 2x-$\frac{1}{2}$ 2y-$\frac{1}{2}$ 2z	1-7 2x-$\frac{1}{2}$ $-\frac{1}{2}$ 2z-$\frac{1}{2}$	1-8 $-\frac{1}{2}$ 2y-$\frac{1}{2}$ $-\frac{1}{2}$
2 $\bar{x}\ \bar{y}\ \bar{z}$	2-1 -2x -2y -2z	2-2 0 0 0	2-3 0 -2y $-\frac{1}{2}$	2-4 -2x 0 -2z-$\frac{1}{2}$	2-5 -2x-$\frac{1}{2}$ -2y-$\frac{1}{2}$ -2z	2-6 $-\frac{1}{2}$ $-\frac{1}{2}$ 0	2-7 $-\frac{1}{2}$ -2y-$\frac{1}{2}$ $-\frac{1}{2}$	2-8 -2x-$\frac{1}{2}$ $-\frac{1}{2}$ -2z-$\frac{1}{2}$
3 $\bar{x}$ y $\frac{1}{2}$-z	3-1 -2x 0 $\frac{1}{2}$-2z	3-2 0 2y $\frac{1}{2}$	3-3 0 0 0	3-4 -2x 2y -2z	3-5 $-\frac{1}{2}$-2x $-\frac{1}{2}$ $\frac{1}{2}$-2z	3-6 $-\frac{1}{2}$ 2y-$\frac{1}{2}$ $\frac{1}{2}$	3-7 $-\frac{1}{2}$ $-\frac{1}{2}$ 0	3-8 $-\frac{1}{2}$-2x 2y-$\frac{1}{2}$ -2z
4 x $\bar{y}$ $\frac{1}{2}$+z	4-1 0 -2y $\frac{1}{2}$	4-2 2x 0 $\frac{1}{2}$+2z	4-3 2x -2y 2z	4-4 0 0 0	4-5 $-\frac{1}{2}$ $-\frac{1}{2}$-2y $\frac{1}{2}$	4-6 2x-$\frac{1}{2}$ $-\frac{1}{2}$ $\frac{1}{2}$+2z	4-7 2x-$\frac{1}{2}$ $-\frac{1}{2}$-2y 2z	4-8 $-\frac{1}{2}$ $-\frac{1}{2}$ 0
5 $\frac{1}{2}$+x $\frac{1}{2}$+y z	5-1 $\frac{1}{2}$ $\frac{1}{2}$ 0	5-2 $\frac{1}{2}$+2x $\frac{1}{2}$+2y 2z	5-3 $\frac{1}{2}$+2x $\frac{1}{2}$ 2z-$\frac{1}{2}$	5-4 $\frac{1}{2}$ $\frac{1}{2}$+2y $-\frac{1}{2}$	5-5 0 0 0	5-6 2x 2y 2z	5-7 2x 0 2z-$\frac{1}{2}$	5-8 0 2y $-\frac{1}{2}$
6 $\frac{1}{2}$-x $\frac{1}{2}$-y $\bar{z}$	6-1 $\frac{1}{2}$-2x $\frac{1}{2}$-2y -2z	6-2 $\frac{1}{2}$ $\frac{1}{2}$ 0	6-3 $\frac{1}{2}$ $\frac{1}{2}$-2y $-\frac{1}{2}$	6-4 $\frac{1}{2}$-2x $\frac{1}{2}$ $-\frac{1}{2}$-2z	6-5 -2x -2y -2z	6-6 0 0 0	6-7 0 -2y $-\frac{1}{2}$	6-8 -2x 0 $-\frac{1}{2}$-2z
7 $\frac{1}{2}$-x $\frac{1}{2}$+y $\frac{1}{2}$-z	7-1 $\frac{1}{2}$-2x $\frac{1}{2}$ $\frac{1}{2}$-2z	7-2 $\frac{1}{2}$ $\frac{1}{2}$+2y $\frac{1}{2}$	7-3 $\frac{1}{2}$ $\frac{1}{2}$ 0	7-4 $\frac{1}{2}$-2x $\frac{1}{2}$+2y -2z	7-5 -2x 0 $\frac{1}{2}$-2z	7-6 0 2y $\frac{1}{2}$	7-7 0 0 0	7-8 -2x 2y -2z
8 $\frac{1}{2}$+x $\frac{1}{2}$-y $\frac{1}{2}$+z	8-1 $\frac{1}{2}$ $\frac{1}{2}$-2y $\frac{1}{2}$	8-2 $\frac{1}{2}$+2x $\frac{1}{2}$ $\frac{1}{2}$+2z	8-3 $\frac{1}{2}$+2x $\frac{1}{2}$-2y 2z	8-4 $\frac{1}{2}$ $\frac{1}{2}$ 0	8-5 0 -2y $\frac{1}{2}$	8-6 2x 0 $\frac{1}{2}$+2z	8-7 2x -2y 2z	8-8 0 0 0

TABLE 8

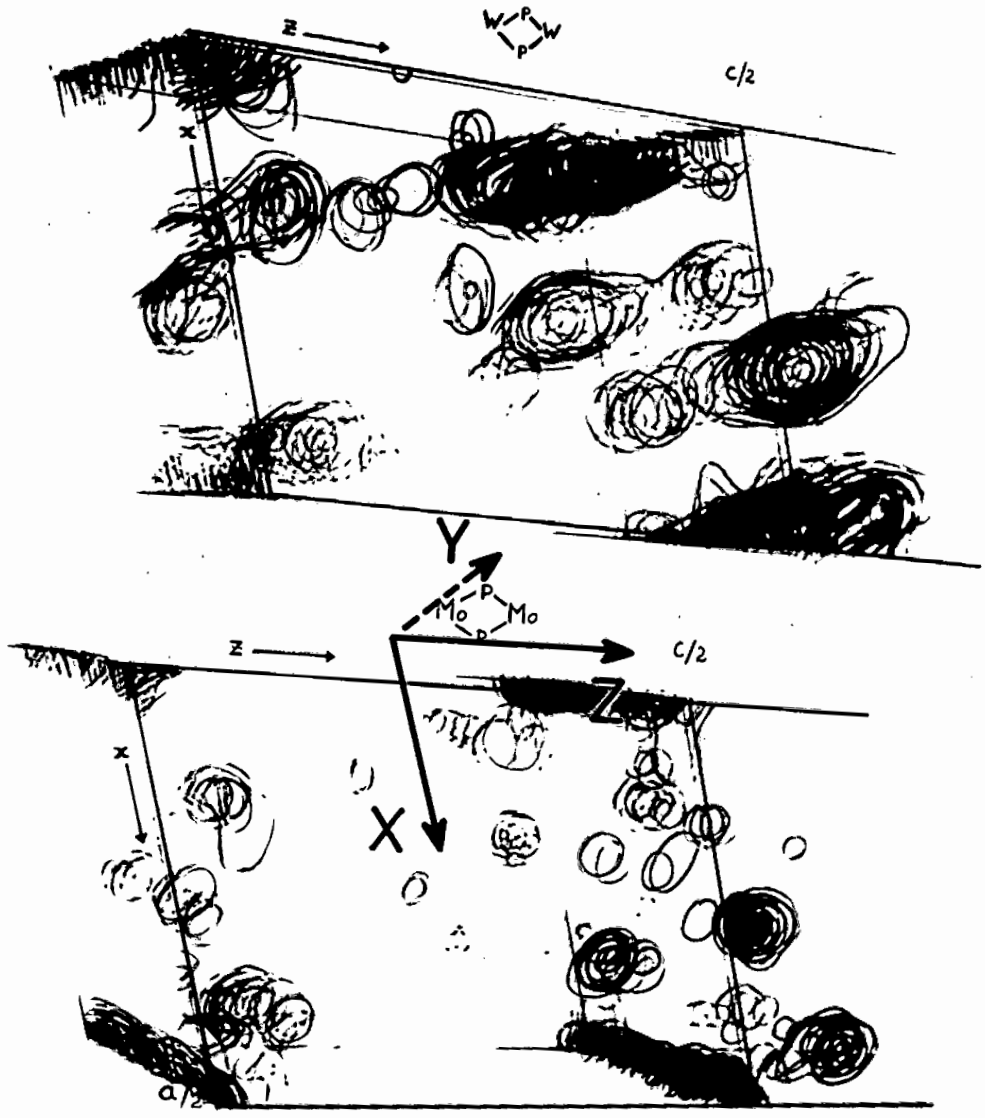

Fig. 13

The volume of the origin peak is multiple and contains a volume

$$V \text{ origin} = \sum_n Z_n^2 \qquad \ldots\ldots\ldots \quad 6.5$$

where n is the number of atoms in the unit cell.

The volume of a peak is not easy to measure, so one can use the approximation that the height of a peak is proportional to its volume

$$H \approx KV \qquad \ldots\ldots\ldots \quad 6.6$$

Thus the expected peak heights for all expected pairs of atoms can be tabulated on an absolute scale.

For compound 1, $\sum_n Z_n^2 = 20344$ = height of the origin peak. A single Mo-Mo interaction will therefore have an expected peak height = 42×42 = 1764, a double Mo-Mo interaction a peak height of 2 × 1764 = 3528 etc.

An analysis of Table 4 yields the expected peak positions and heights shown in Table 5. Since the Patterson synthesis was only computed over 1/8 of the volume of the unit cell, only a fraction of the total number of peaks are expected on the Patterson map as computed. These are marked with an asterisk in Table 5.

TABLE 5

Peak position	Multiplicity	Expected in Patterson map	Expected peak height
0, 0, 0	8	*	20344
$\frac{1}{2}$, $\frac{1}{2}$, 0	8	*	20344
0, 2y, $\frac{1}{2}$	4	*	7056
0, -2y, $\frac{1}{2}$	4		
2x, 0, $\frac{1}{2}$+2z	4		
-2x, 0, $\frac{1}{2}$-2z	4		
$\frac{1}{2}$, $\frac{1}{2}$+2y, $\frac{1}{2}$	4		
$\frac{1}{2}$, $\frac{1}{2}$-2y, $\frac{1}{2}$	4	*	7056
$\frac{1}{2}$+2x, $\frac{1}{2}$, $\frac{1}{2}$+2z	4		
$\frac{1}{2}$-2x, $\frac{1}{2}$, $\frac{1}{2}$-2z	4	*	7056
2x, 2y, 2z	2	*	3528
-2x, -2y, -2z	2		
2x, -2y, 2z	2		
-2x, 2y, 2z	2		
$\frac{1}{2}$+2x, $\frac{1}{2}$-2y, 2z	2		
$\frac{1}{2}$+2x, $\frac{1}{2}$+2y, 2z	2		
$\frac{1}{2}$-2x, $\frac{1}{2}$-2y, -2z	2		
$\frac{1}{2}$-2x, $\frac{1}{2}$+2y, -2z	2		

6.5 (b) Analysis of the Patterson synthesis and the unambiguous determination of the space group.

The peaks obtained in the Patterson synthesis are shown in Table 6. The heights of the peaks are scaled so that the origin peak has a value = $\sum_n Z_n^2$ = 20344. The position of the rotation peak was found as follows:

Table 5 shows that there should be a peak at $(0, 2y, \frac{1}{2})$ of height 7056. The only corresponding two peaks found (Table 6) are peak 6 (height 1610) and peak 13 (height 7798). The latter peak was chosen because its height closely matched the expected height. Hence $2y = 39/100$. The rotation peak was then sought in the Patterson map at the section where $2y = 39/100$. The only peak corresponding to this was peak 15 at $2x = 28/100$, $2y = 40/100$, $2z = 4/100$. This was checked by seeking the satellite peaks at $(\frac{1}{2}, \frac{1}{2}-2y, \frac{1}{2})$ and at $(\frac{1}{2}-2x, \frac{1}{2}, \frac{1}{2}-2z)$. The result (Table 6) shows that not only do the peaks appear in the correct positions, but that their heights compare remarkably well with the expected heights.

The Patterson synthesis also established the space group of the structure uniquely as $C_{2/c}$. The vector peaks arising from the other possible space group, C_c[48], were analysed in a similar manner, but gave no vector peak at $(\frac{1}{2}-2x, \frac{1}{2}, \frac{1}{2}-2z)$ which was found on the vector map (Table 6, peak 19). The space group $C_{2/c}$ was thus taken as correct and was confirmed subsequently by the successful structural analysis.

TABLE 6

List of peak heights and positions for compound 1 and its tungsten isomorph. Positions are listed as hundredths of the unit cell parameters.

	Mo compound				W compound			
Peak Number	Position	Height Observed:x	Height Expected	General Coordinates	Position	Height Found:y	Height Expected	Ratio y/x
1	0, 0, 0	20344	20344	0 0 0	0, 0, 0	50024	50024	-
2	15, 0, 6	2628			15, 0, 6	3543		1.34
3	50, 0, 0	3009			-	-		-
4	13, 0,18	975			13,0,18	1829		1.88
5	22, 0,45	932			-	-		-
6	0, 8,50	1610			-	-		-
7	50,11,50	7798	7056	$\frac{1}{2},\frac{1}{2}-2y,\frac{1}{2}$	50,12,50	24879	21904	3.38 *
8	42,32,12	2839			42,32,12	2896		1.02
9	8,20,37	1144			8,20,36	1181		1.03
10	34,16,45	2119			34,16,44	2438		1.15
11	0,20, 0	2161			0,23, 0	4572		2.11
12	50,30, 0	2161			50,29, 0	4572		2.11
13	0,39,50	7798	7056	$0, 2y, \frac{1}{2}$	0,38,50	24879	21904	3.38 *
14	50,42,50	1610			-	-		-
15	28,40, 4	2967	3528	2x,2y,2z	28,39, 4	11430	10952	3.85 *
16	0,50, 0	3009			-	-		-
17	6,50,39	2712			6,50,40	4724		1.74
18	50,50, 0	20344	20344	$\frac{1}{2}, \frac{1}{2}, 0$	50,50, 0	50024	50024	-
19	22,50,45	7205	7056	$\frac{1}{2}-2x,\frac{1}{2},\frac{1}{2}-2z$	22,50,46	22403	21904	3.11 *

6.5 (C) Analysis of the Patterson synthesis by the isomorphous substitution method.

The Patterson map of the molybdenum compound was compared with that of the isomorphous tungsten compound[49]. The peaks of the Patterson synthesis of the tungsten compound were put on an absolute scale ($\sum_n Z_n^2 = 50024$) and compared in position and height with those obtained from the molybdenum compound (Table 6). The peaks due to the heavy atom interactions only, may be expected to have heights in the ratio $\frac{Z_W^2}{Z_{Mo}^2} = \frac{74^2}{42^2} = 3.10$, while the other peaks, due to interaction of the heavy metal with P,O or C and of the light atoms with each other, may be expected to have a lower ratio.

Table 6 shows that peaks 7, 13, 15 and 19 comply with the required ratio ≈ 3.1 while the others do not. This offers a second proof that peak 15 is the rotation peak at $2x = .28$, $2y = .40$, $2z = .04$ and that the molybdenum atom therefore lies at $x = .14$, $y = .20$, $z = .02$.

6.6 THE LOCATION OF THE LIGHT ATOMS.

Structure factors were calculated with the molybdenum atom alone, located at $x = .14$, $y = .20$, $z = .02$ and with a tentative B value of $2\ \text{Å}^2$. These gave an R value of 0.37. A Fourier synthesis, followed by a difference Fourier synthesis, showed the locations of all the light atoms with the exception of C_2 and C_4.

The positions of the atoms as found from the first difference Fourier are shown in Table 7. (Fig. 16 shows the atomic nomenclature).

TABLE 7

Atomic positional parameters in fractions of the unit cell lengths a, b, c.

	x	y	z
Mo	.140	.195	.022
P	.296	.136	.087
O_1	.068	.380	.150
O_2	.029	.008	.151
O_3	.565	.261	.040
O_4	.300	.515	.098
C_1	.274	.180	.196
C_3	-.340	-.030	.076
C_5	.100	.314	.102
C_6	.069	.075	.105
C_7	.501	.276	.017
C_8	.328	.440	.055

Structure factors were again calculated including all the atoms listed in Table 7. The following tentative B values were assigned:

Mo	B = 1.8	$\mathring{A}^2$
P	B = 1.8	"
O_1	B = 5	"
O_2	B = 5	"
O_3	B = 5	"
O_4	B = 5	"
C_1	B = 4	"
C_3	B = 4	"
C_5	B = 4	"
C_6	B = 4	"
C_7	B = 4	"
C_8	B = 4	"

A second difference Fourier synthesis carried out with the latter structure factors showed the positions of the atoms C_2 and C_4 at

C_2 x = .381 y = .203 z = .224

C_4 x = .230 y = -.090 z = .100

The second difference Fourier synthesis also showed characteristic peaks in the vicinity of the Mo atom implying anisotropic thermal motion.

6.7 REFINEMENT.

The structure was refined by least squares method using the C.S.I.R. ORFLSRED programme. In the refinement, the scattering factor of the molybdenum atom was corrected for dispersion[50].

The first two cycles were devoted only to refining the scale factors, thus placing the observed and calculated structure factors on the same scale. This was followed by three cycles where the scale factors, the atomic positions and the isotropic temperature factors were all allowed to vary. At this stage of the refinement the value of the residual, R, was 0.116.

The isotropic temperature factor of atom C_4, however, was noted to be somewhat high and oscillating with each cycle of refinement:

after 3^{rd} cycle B = 8.7 $\mathring{A}^2$

after 4^{th} cycle B = 12.5 "

after 5^{th} cycle B = 10.6 "

It was thought that the atom had been misplaced and a further calculation of structure factors, omitting the atom C_4, followed by a three dimensional difference Fourier synthesis was carried out. The resulting map was featureless except for a large peak at x = .25 y = -.09 z = .10 which was in good agreement with the position obtained from the fifth cycle of refinement : x = .2746 y = -.1069 z = .1057.

This proved that atom C_4 had, in fact, been correctly located, so three more cycles of refinement were carried out, again varying the positions and isotropic temperature factors of all the atoms. The temperature factor of atom C_4 remained steady:

after the 6^{th} cycle B = 12.46 $\mathring{A}^2$

after the 7^{th} cycle B = 12.22 "

after the 8^{th} cycle B = 12.48 "

Finally three cycles of refinement were carried out varying the positions of all the atoms and treating the temperature factor of the Mo atom anisotropically (section 5.2). The final R value for the structure was 0.110.

The final atomic positions, with estimated standard deviations, are given in Table 8. The final values of the temperature factors are given in Table 9.

The value of 12.48 $\mathring{A}^2$ obtained for the temperature factor of C_4 is considerably higher than the values obtained for the other C atoms (B = 4.04 average) and would only be reasonably possible if the atom were located in a large vacant space in the structure, thus allowing it free movement. However the C_4 - P distance is 3.2 $\mathring{A}$, which is smaller than the van der Waals interaction force distance, taken as approximately 3.5 $\mathring{A}$.

The temperature factor corresponds to a mean atomic vibration amplitude of $\approx$ 0.4 $\mathring{A}$ which is somewhat high but not unreasonable. However no explanation can be given for the rather high value of the temperature factor of atom C_4.

The Fourier synthesis, computed from the structure factors obtained from the final values of the atomic parameters is shown in Fig. 14. The Fourier map shows the positions of the atoms in the complete molecule.

An accurate model of the molecule was constructed (scale 4 cm = 1 $\mathring{A}$) and photographed in colour (Fig. 15). The colour photograph of the model gives a good three dimensional impression of the relative location

of the atoms to each other. (Mo atoms brown

P atoms blue

O atoms red

C atoms black)

An idealised drawing of the molecule is shown in Fig. 16, in which all the atoms have been labelled.

The values of observed and calculated structure factors are tabulated in Appendix I.

6.8 CALCULATION OF INTERATOMIC BOND LENGTHS AND ANGLES.

Interatomic bond lengths and angles and their estimated standard deviations were calculated by using the formulae discussed in section 5.6 These are shown in Tables 10 and 11.

The best planes going through the atoms O_2', O_3', C_6', C_7', Mo', P', P, Mo, C_7, C_6, O_3, O_2 (the 'horizontal' plane - see Fig. 16) and the atoms O_1', C_5', Mo', C_8', O_4', O_4, C_8, Mo, C_5, O_1 (the 'vertical' plane - see Fig. 16) were computed. The interplanatory angle was found to be 89.95° which is in excellent agreement with the expected value of 90°. The perpendicular distances of these atoms to their respective planes are shown in Table 12.

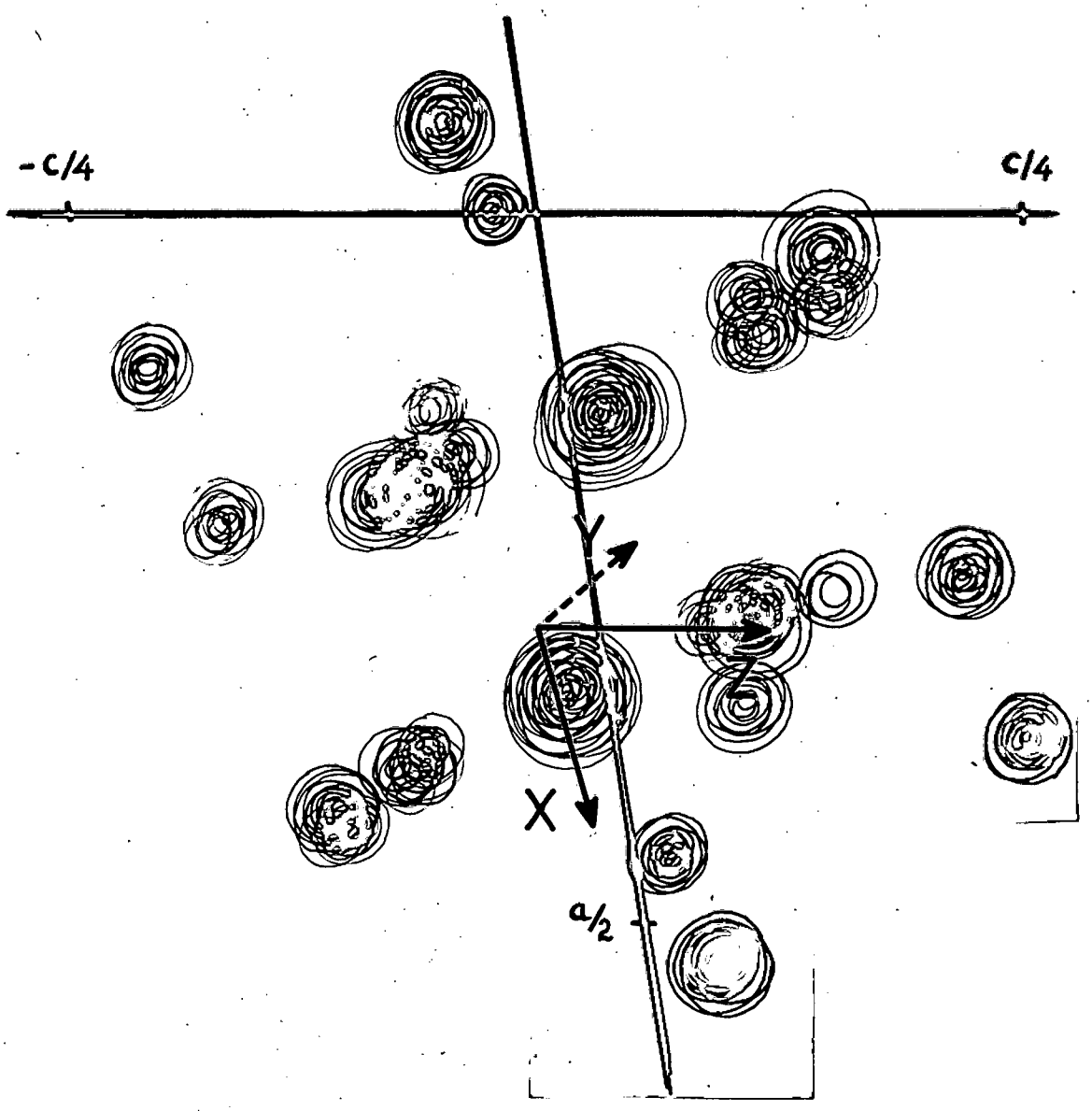

Fig. 14

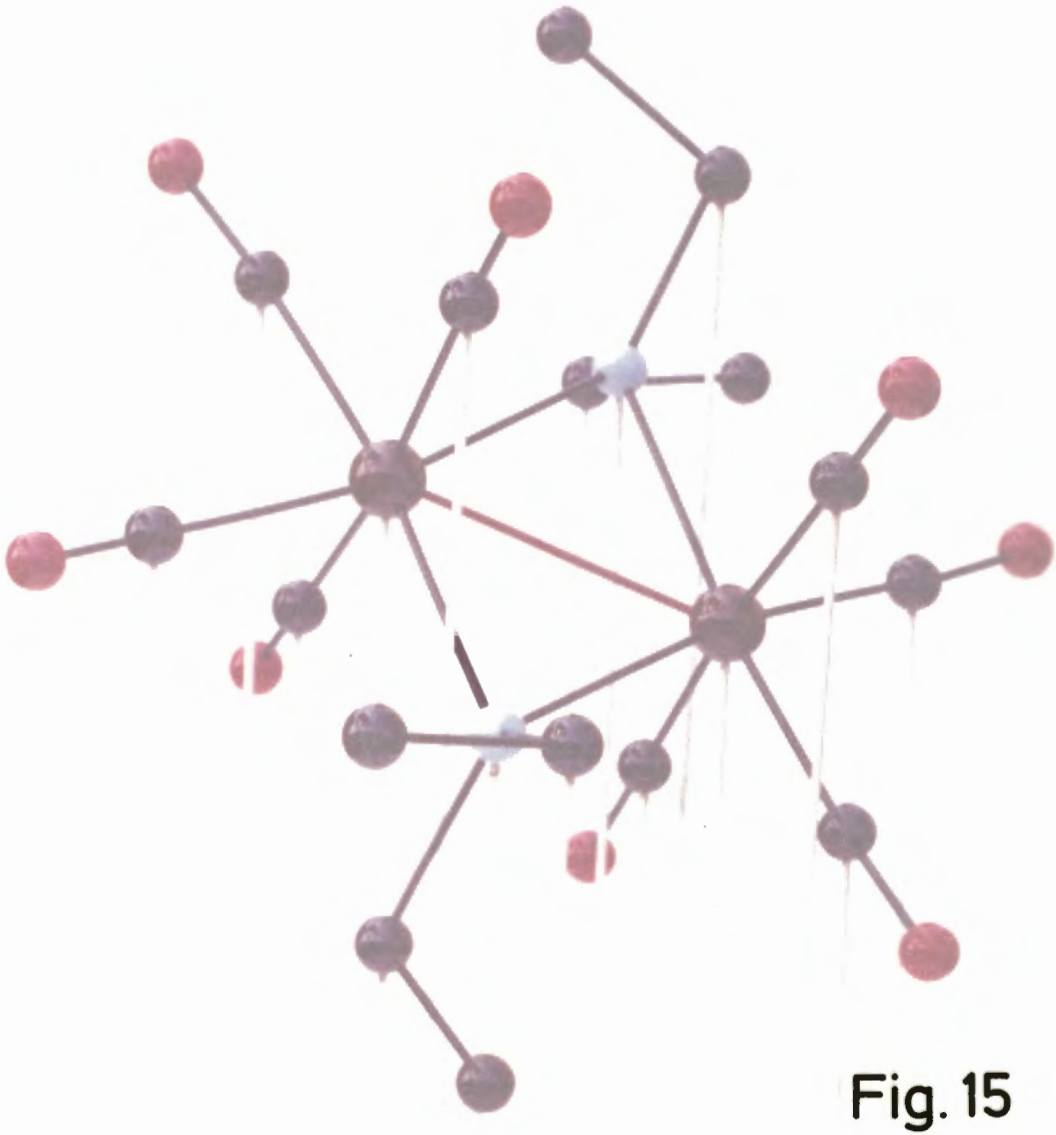

Fig. 15

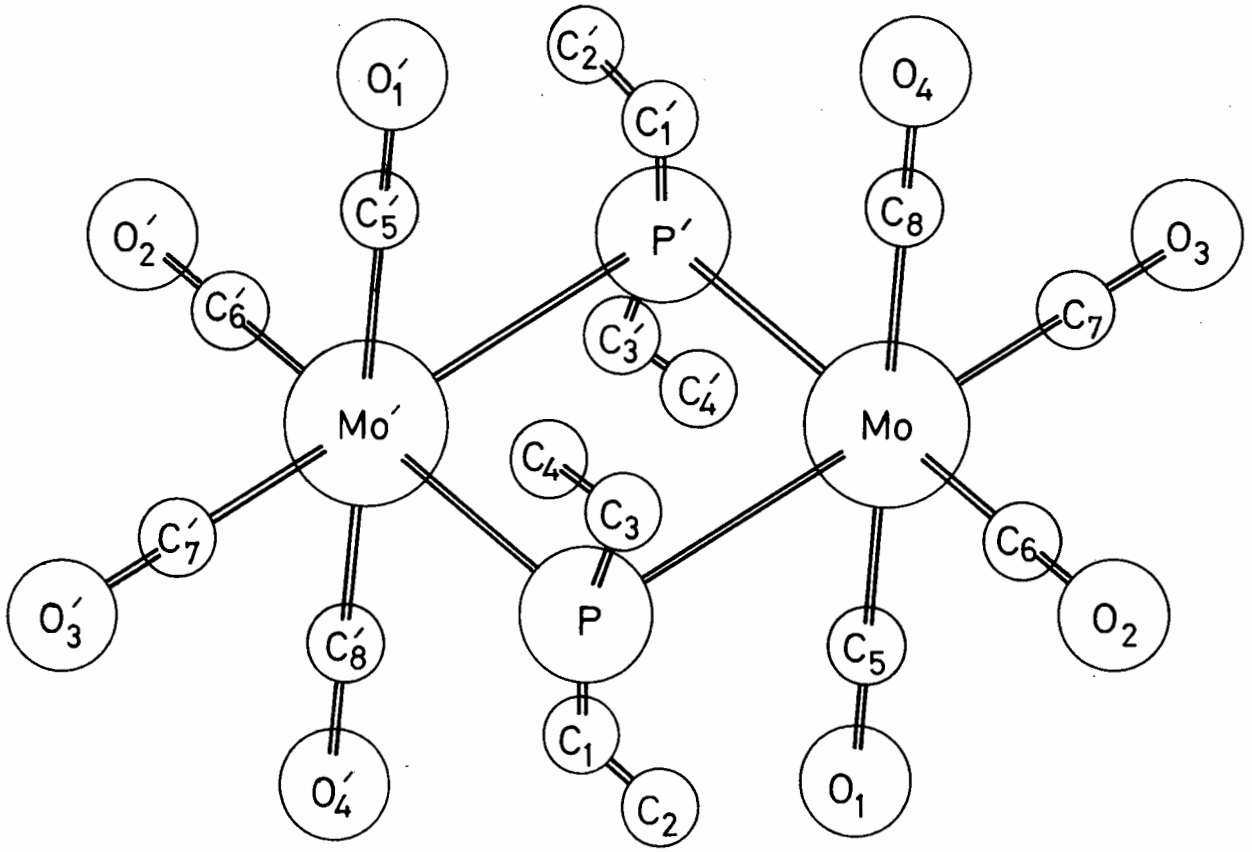
O'1
C'2
C'1
O4
O'2
C'5
C8
O3
C'6
P'
C7
C'3
C'4
Mo'
Mo
C4
C3
C'7
C6
O'3
P
O2
C'8
C5
C1
O'4
O1
C2

Fig. 16

TABLE 8

Atomic positional parameters and their standard deviations in fractions of the unit cell lengths a, b, c.

	x	y	z	σx	σy	σz
Mo	0.1408	0.1953	0.0216	0.0001	0.0003	0.0001
P	0.2923	0.1456	0.0854	0.0005	0.0008	0.0004
O_1	0.0655	0.3954	0.1551	0.0019	0.0029	0.0015
O_2	0.0219	0.0114	0.1556	0.0018	0.0027	0.0015
O_3	-0.0658	0.2389	-0.0381	0.0017	0.0024	0.0013
O_4	0.2005	-0.0283	-0.1060	0.0019	0.0028	0.0015
C_1	0.2720	0.1806	0.1965	0.0022	0.0037	0.0017
C_2	0.3809	0.1896	0.2268	0.0024	0.0040	0.0019
C_3	0.3477	0.0002	0.0730	0.0021	0.0036	0.0016
C_4	0.2739	-0.0983	0.1115	0.0049	0.0065	0.0039
C_5	0.0994	0.3244	0.1045	0.0022	0.0040	0.0018
C_6	0.0637	0.0764	0.1043	0.0022	0.0036	0.0017
C_7	0.0061	0.2198	-0.0171	0.0023	0.0037	0.0017
C_8	0.1763	0.0550	-0.0575	0.0022	0.0036	0.0018

TABLE 9

Final temperature factors with standard deviations

Mo	β_{11}	= 0.00212 ± 0.00008
	β_{22}	= 0.00302 ± 0.00033
	β_{33}	= 0.00123 ± 0.00005
	β_{12}	= 0.00041 ± 0.00018
	β_{13}	= -0.00056 ± 0.00005
	β_{23}	= -0.00004 ± 0.00013
P	B	= 1.78 ± .12
O_1	B	= 6.07 ± .62
O_2	B	= 5.88 ± .60
O_3	B	= 4.95 ± .53
O_4	B	= 6.03 ± .62
C_1	B	= 4.26 ± .66
C_2	B	= 5.00 ± .74
C_3	B	= 3.55 ± .63
C_4	B	= 12.48 ± 1.96
C_5	B	= 4.14 ± .67
C_6	B	= 3.55 ± .62
C_7	B	= 4.14 ± .67
C_8	B	= 3.64 ± .64

TABLE 10

Bond lengths (Å) with estimated standard deviations.

Mo - Mo'	3.057(6)	P - C_1	1.83(3)
P - P'	3.96(1)	P - C_3	1.73(3)
Mo - P	2.51(1)	C_5 - O_1	1.15(5)
Mo - P'	2.49(1)	C_6 - O_2	1.15(4)
Mo - C_5	1.95(4)	C_7 - O_3	1.10(4)
Mo - C_6	1.99(3)	C_8 - O_4	1.20(5)
Mo - C_7	2.03(3)	C_1 - C_2	1.62(5)
Mo - C_8	1.99(4)	C_3 - C_4	1.49(4)

(The figure in parentheses represents the estimated standard deviation of the last significant digit).

TABLE 11

Bond angles (°) with estimated standard deviation.

$Mo' - Mo - P$	52.0 (3)	$P - Mo - C_7$	171.8 (15)
$Mo' - Mo - P'$	52.7 (3)	$P' - Mo - C_6$	170.3 (16)
$P - Mo - P'$	104.6 (3)	$C_8 - Mo - C_5$	175.8 (17)
$Mo' - P - Mo$	75.4 (3)	$Mo - C_5 - O_1$	173.3 (16)
$P - Mo - C_6$	84.8 (5)	$Mo - C_6 - O_2$	175.8 (16)
$C_6 - Mo - C_7$	87.0 (5)	$Mo - C_7 - O_3$	176.6 (17)
$C_7 - Mo - P'$	83.5 (6)	$Mo - C_8 - O_4$	178.1 (18)
$P - Mo - C_8$	90.8 (6)	$P - C_3 - C_4$	112.4 (9)
$C_8 - Mo - C_7$	89.6 (5)	$P - C_1 - C_2$	111.9 (9)
$C_7 - Mo - C_5$	89.7 (6)	$Mo' - P - C_1$	121.1 (9)
$C_5 - Mo - P$	89.4 (6)	$C_1 - P - Mo$	114.6 (10)
$P' - Mo - C_8$	94.0 (6)	$C_3 - P - Mo'$	118.2 (12)
$C_8 - Mo - C_6$	88.0 (5)	$C_3 - P - C_1$	105.9 (11)
$C_6 - Mo - C_5$	87.8 (6)	$C_3 - P - Mo$	120.0 (14)
$C_5 - Mo - P'$	90.0 (6)		

(The figure in parentheses represents the estimated standard deviation in the last significant digit).

TABLE 12

Perpendicular distances between atoms and planes.

(a) Distances between atoms and horizontal plane

Atom	Perp. Distance
O_2'	-0.043 Å
O_3'	-0.021 Å
C_6'	0.028 Å
C_7'	0.031 Å
Mo'	0.044 Å
P'	0.029 Å
P	-0.029 Å
Mo	-0.044 Å
C_7	-0.031 Å
C_6	-0.028 Å
O_3	0.021 Å
O_2	0.043 Å

(b) Distances between atoms and vertical plane

Atom	Perp. distance
O_1'	0.020 Å
C_5'	-0.001 Å
Mo'	-0.042 Å
C_8'	-0.002 Å
O_4'	0.021 Å
O_4	-0.021 Å
C_8	0.002 Å
Mo	0.042 Å
C_5	0.001 Å
O_1	0.020 Å

7. THE CRYSTAL STRUCTURE OF μ-Tetraethyldiphosphine-bis-(pentacarbonylmolybdenum)(compound 2).

7.1 OPTICAL GONIOMETRIC STUDY.

An accuarte drawing of the crystal and a stereogram are shown in Fig. 17. The crystals are bipyramidal.

The angles $e \wedge e'$, $e \wedge e'''$ and $e \wedge e''$ were measured on five independently chosen crystals. The crystals were very well formed and good signals were obtained experimentally, all readings being accurate to $\pm$ 3 minutes of a degree.

The mean valuesobtained were:

$e \wedge e'$	$62^{\circ}22'$
$e \wedge e'''$	$94^{\circ}8\frac{1}{2}'$
$e \wedge e''$	$94^{\circ}8\frac{1}{2}'$

The fact that $e \wedge e''$ is exactly equal to $e \wedge e'''$ shows that, on optical goniometrical evidence alone, the crystals are tetragonal.

7.1 (a) Calculation of axial ratio.

(i) if the face e is assumed to be (101) (as drawn on the stereogram Fig. 17)

the axial ratio $c/a = \frac{\tan 94^{\circ}8\frac{1}{2}'}{2}$

$= 1.0851$

(ii) if the face e is assumed to be (111)

the axial ratio $c/a = \frac{\tan 94^{\circ}8\frac{1}{2}'}{2} \times \cos 45^{\circ}$

$= 0.7602$

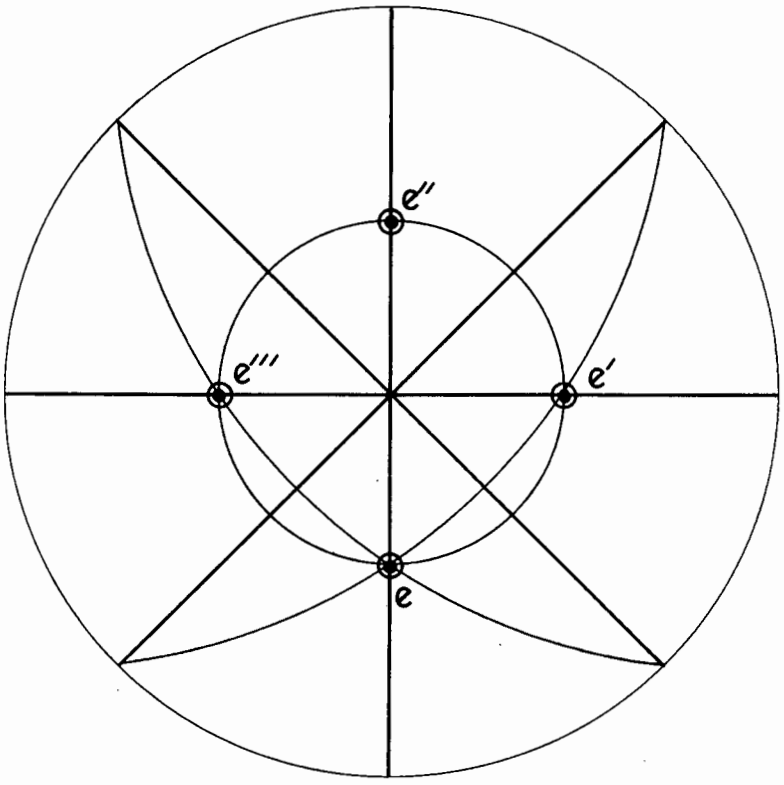

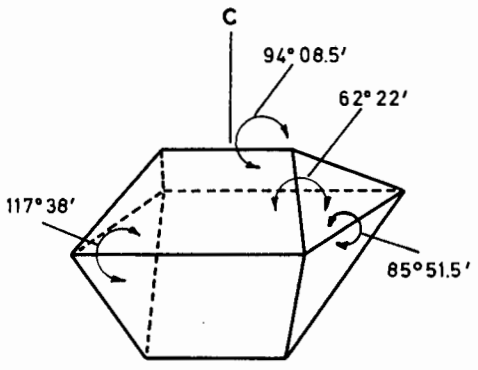

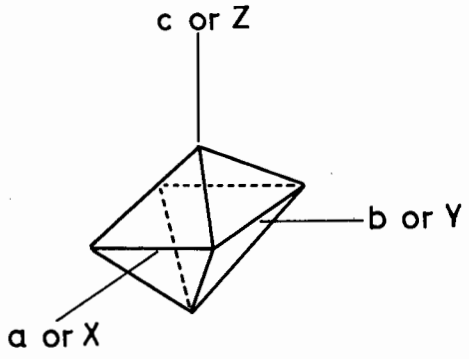

Fig. 17

If it is tetragonal, the angle $e \wedge e'$ can be checked by calculation

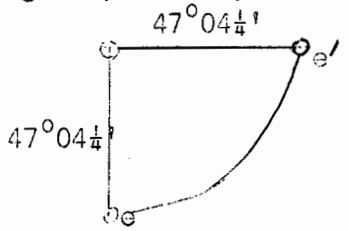

Considering the Napierian triangle above,

$$\sin (90 - e\wedge e') = \cos 47^\circ 04\tfrac{1}{4}' \cos 47^\circ 04\tfrac{1}{4}'$$

$$\underline{e \wedge e' = 62^\circ 21'}$$

this is within $0^\circ 01'$ of the measured value.

7.1 (b) Optical characteristics.

The crystals were examined under the polarising microscope and found to be definitely biaxial ($2V = 72^\circ$). This posed a direct problem, and the only possible explanation for the above evidence was that perhaps the uniaxial crystal is a polymorph which is truly tetragonal at the temperature of crystallisation but passes through an inversion at lower temperature rendering it optically biaxial. There are many examples of minerals which should be uniaxial but are, in fact, markedly biaxial, e.g. apatite. Normally, however, 2V of the anomalous minerals is small, and from a random batch of crystals some will be uniaxial and some biaxial. The large number of crystals examined, however, were <u>all</u> biaxial with large 2V.

The problem was later solved by considering the symmetry of the Patterson projections which proved that the crystal is orthorhombic.

It is of interest at this point to note that the classification of crystals in many texts is based on a consideration of crystal axes,

and in particular their lengths and directions. This approach gives correct assignments in a great majority of cases but occasionally leads to error. Thus a unit cell with $a \neq b \neq c$ and $\alpha = \beta = \gamma = 90^{\circ}$ does not necessarily mean that the crystal has orthorhombic symmetry. In the tabulation of Donnay and Nowacki[51] there are over fifty monoclinic substances listed having unit cells of the above shape. Crystals should therefore be classified not according to axial lengths and angles, but by considering the minimum number of symmetry axes present. Thus the tetragonal system may be defined as having one four fold axis, 4 (or $\bar{4}$) only; while the orthorhombic system may be defined as having more than one two fold axis, 2 (or $\bar{2}$), and no axes of higher symmetry.

The above discussion may be summarised by quoting the International Tables[52], which state "The symbol $\neq$ implies non-equality by reason of symmetry; accidental equality may, of course occur".

Change of axes.

In the subsequent X-ray analysis it was necessary, in order to comply with the space group conditions of Pbca, to relabel the axes:

Goniometric study	a	b	c
	↓	↓	↓
X-ray study	c	b	a

7.2 THE DETERMINATION OF THE UNIT CELL AND SPACE GROUP.

7.2 (a) The measurement of the unit cell parameters.

The unit cell parameters were measured from layer-line spacings of single crystal rotation photographs[32]. The values were refined by taking zero layer Weissenberg photographs about each axis

and extrapolating the interplanar spacings in accordance with Bradley and Jay's extrapolation[33]. In the accurate determination of the unit cell lengths, Kodak Industrex D film was used, as this has no significant shrinkage on development.

The final values of the unit cell parameters obtained were

$$a = 11.43 \pm .01 \text{ Å} \qquad \alpha = 90^{\circ}$$

$$b = 14.95 \pm .02 \text{ Å} \qquad \beta = 90^{\circ}$$

$$c = 14.95 \pm .02 \text{ Å} \qquad \gamma = 90^{\circ}$$

The methods of accurately aligning the crystals have been previously described (Section 6.2).

7.2 (b) The measurement of the crystal density.

The density of the crystal was measured by the flotation method. The liquid used was a mixture of bromoform and ethyl alcohol in which the crystals were insoluble.

The measured value of the density was

$$\rho = 1.679 \text{ g/cm}^3$$

7.2 (c) The number of molecules/unit cell.

The number of molecules/unit cell was calculated from the formula

$$nM = abc\, \rho_m N$$

where M is molecular weight of the compound
ρ_m is the measured crystal density
a,b,c are the unit cell lengths
N is the Avogadro number

By appropiate substitution of the measured constants

$$n = \frac{11.34 \times 14.95 \times 14.95 \times 1.679 \times 6.023 \times 10^{23} \times 10^{-24}}{650.2}$$

$n = 3.974 = 4$ molecules/unit cell.

The calculated crystal density ρ_c, assuming four molecules per unit cell, is $1.690\ g/cm^3$.

7.2 (d) The examination of systematic absences and the determination of the space group.

Laue photographs were taken with the X-ray beam accurately aligned to the three principal axes in each case. All three photographs displayed mm symmetry, giving the crystal a Laue symmetry of mmm, thus placing it uniquely in the orthorhombic system.

Zero and upper layer Weissenberg photographs were taken with the crystal oscillating in turn about all three principal axes. The reflections were indexed and an examination of the indices was carried out.

The upper layer photographs showed that there were no restrictions for $h + k + \ell$, thus the crystal has a primitive lattice P. The reflections from the zero layer photographs showed the following conditions for the indices:

Reflection	Condition
0kℓ	k = 2n
h0ℓ	ℓ = 2n
hk0	h = 2n
h00	h = 2n
0k0	k = 2n
00ℓ	ℓ = 2n

The diffraction symbol was therefore mmmPbca which uniquely corresponds to the space group Pbca.

7.3 THE SELECTION OF A CRYSTAL SUITABLE FOR INTENSITY DATA COLLECTION.

From consideration of elementary absorption theory it can be shown that the optimum size of a crystal = $2/\mu$ (Section 6.3)

where μ = linear absorption coefficient.

Attempts to grind the crystal into a sphere[43] failed, because, as in the case of compound 1, the crystals invariably shattered.

Calculation of the linear absorption coefficient μ.

The linear absorption coefficient was calculated as previously described (Section 6.3) and found to have a value $\mu = 99.46\ cm^{-1}$. A single crystal, having dimensions .15 mm × .15 mm × .12 mm was selected. This was treated as a sphere having a mean radius of 0.07 mm. Thus $\mu R = 0.695 \approx 0.7$. The absorption correction A^* for $\mu R = 0.7$

varies from 2.75 at $\theta = 0^{\circ}$ to 2.32 at $\theta = 90^{\circ}$. Although small, this correction was deemed significant and therefore the intensity data was corrected for absorption.

7.4 THE COLLECTION AND MEASUREMENT OF INTENSITY DATA.

Intensity data were collected using an integrating Weissenberg goniometer and employing the multiple film technique[45]. The crystal was set with the X-axis parallel to the axis of oscillation and upper layer intensities were collected using the equi-inclination method. Data were collected from the $0k\ell$, $1k\ell$, $2k\ell$, $3k\ell$ and $4k\ell$ layer lines. The intensities of the reflections were measured as described in Section 6.4. The intensity data from the different layers were scaled by measuring the reflections obtained from a zero layer Weissenberg photograph taken about the Y axis ($h0\ell$ reflections). The number of reflections measured was 705.

The intensities were punched on computer cards and corrected for various geometric and physical factors as discussed in Section 5.1. A Patterson synthesis was then computed.

7.5 THE PATTERSON SYNTHESIS.

A three dimensional Patterson synthesis was computed (Equation 5.22) for the fraction of the unit cell $0 \rightarrow \frac{1}{2}$ along a, $0 \rightarrow \frac{1}{2}$ along b and $0 \rightarrow \frac{1}{2}$ along c. Two dimensional Patterson syntheses were also calculated and the three vector maps, computed for the (001), (100) and (010) projections all displayed symmetry characteristic of the plane group pgm[55] which is consistent with the space group Pbca[56].

This is a further proof that the crystal is orthorhombic and that the space group Pbca is correct.

The interpretation of the Patterson map was carried out using an analytical method, similar in procedure to the one employed in solving the vector map of compound 1 (Section 6.5).

The structure has four molecules and hence eight molybdenum atoms per unit cell. The eight molybdenum atoms were placed in the general positions as required for the space group Pbca. The 8×8 positions of the vector peaks arising from the Mo-Mo interactions were derived in terms of general coordinates and are shown in Table 13. Analysis of table 13 showed that only seven non origin peaks may be expected to appear in the Patterson map as computed. These peaks and their multiplicity are marked with an asterisk in Table 14.

The Patterson vector peaks were calibrated as discussed in Section 6.5(a), $\sum_n Z_n^2$ for the compound being 21144 = height of the origin peak.

7.5 (a) Analysis of the Patterson synthesis.

The peaks obtained in the Patterson synthesis are shown in Table 15. The heights of the peaks are scaled so that the origin peak has a value $= \sum_n Z_n^2 = 21144$. The position of the rotation peak was found as follows:-

Table 14 shows that there should be a peak at 0, $\frac{1}{2}$-2y, $\frac{1}{2}$ of expected height 7056. The only corresponding peak in Table 15 is peak 4, at 0, 0.16, 0.50 of height 7786.

ATOMIC POSITION	1 x y z	2 $\frac{1}{2}+x\ \frac{1}{2}-y\ \bar{z}$	3 $\bar{x}\ \frac{1}{2}+y\ \frac{1}{2}-z$	4 $\frac{1}{2}-x\ \bar{y}\ \frac{1}{2}+z$	5 $\bar{x}\ \bar{y}\ \bar{z}$	6 $\frac{1}{2}-x\ \frac{1}{2}+y\ z$	7 $x\ \frac{1}{2}-y\ \frac{1}{2}+z$	8 $\frac{1}{2}+x\ y\ \frac{1}{2}-z$
1 x y z	1-1 0 0 0	1-2 $-\frac{1}{2}\ 2y-\frac{1}{2}\ 2z$	1-3 $2x\ -\frac{1}{2}\ 2z-\frac{1}{2}$	1-4 $2x-\frac{1}{2}\ 2y\ -\frac{1}{2}$	1-5 2x 2y 2z	1-6 $2x-\frac{1}{2}\ -\frac{1}{2}\ 0$	1-7 $0\ 2y-\frac{1}{2}\ -\frac{1}{2}$	1-8 $-\frac{1}{2}\ 0\ 2z-\frac{1}{2}$
2 $\frac{1}{2}+x\ \frac{1}{2}-y\ \bar{z}$	2-1 $\frac{1}{2}\ \frac{1}{2}-2y\ -2z$	2-2 0 0 0	2-3 $\frac{1}{2}+2x\ -2y\ -\frac{1}{2}$	2-4 $2x\ \frac{1}{2}\ -2z-\frac{1}{2}$	2-5 $\frac{1}{2}+2x\ \frac{1}{2}\ 0$	2-6 2x -2y -2z	2-7 $\frac{1}{2}\ 0\ -\frac{1}{2}-2z$	2-8 $0\ \frac{1}{2}-2y\ -\frac{1}{2}$
3 $\bar{x}\ \frac{1}{2}+y\ \frac{1}{2}-z$	3-1 $-2x\ \frac{1}{2}\ \frac{1}{2}-2z$	3-2 $-\frac{1}{2}-2x\ 2y\ \frac{1}{2}$	3-3 0 0 0	3-4 $-\frac{1}{2}\ \frac{1}{2}+2y\ -2z$	3-5 $0\ \frac{1}{2}+2y\ \frac{1}{2}$	3-6 $-\frac{1}{2}\ 0\ \frac{1}{2}-2z$	3-7 -2x 2y -2z	3-8 $-\frac{1}{2}-2x\ \frac{1}{2}\ 0$
4 $\frac{1}{2}-x\ \bar{y}\ \frac{1}{2}+z$	4-1 $\frac{1}{2}-2x\ -2y\ \frac{1}{2}$	4-2 $-2x\ -\frac{1}{2}\ \frac{1}{2}+2z$	4-3 $\frac{1}{2}\ -\frac{1}{2}-2y\ 2z$	4-4 0 0 0	4-5 $\frac{1}{2}\ 0\ \frac{1}{2}+2z$	4-6 $0\ -\frac{1}{2}-2y\ \frac{1}{2}$	4-7 $\frac{1}{2}-2x\ -\frac{1}{2}\ 0$	4-8 -2x -2y 2z
5 $\bar{x}\ \bar{y}\ \bar{z}$	5-1 -2x -2y -2z	5-2 $-\frac{1}{2}-2x\ -\frac{1}{2}\ 0$	5-3 $0\ -\frac{1}{2}-2y\ -\frac{1}{2}$	5-4 $-\frac{1}{2}\ 0\ -\frac{1}{2}-2z$	5-5 0 0 0	5-6 $-\frac{1}{2}\ -\frac{1}{2}-2y\ -2z$	5-7 $-2x\ -\frac{1}{2}\ -\frac{1}{2}-2z$	5-8 $-\frac{1}{2}-2x\ -2y\ -\frac{1}{2}$
6 $\frac{1}{2}-x\ \frac{1}{2}+y\ z$	6-1 $\frac{1}{2}-2x\ \frac{1}{2}\ 0$	6-2 -2x 2y 2z	6-3 $\frac{1}{2}\ 0\ -\frac{1}{2}+2z$	6-4 $0\ \frac{1}{2}+2y\ -\frac{1}{2}$	6-5 $\frac{1}{2}\ \frac{1}{2}+2y\ 2z$	6-6 0 0 0	6-7 $\frac{1}{2}-2x\ 2y\ -\frac{1}{2}$	6-8 $-2x\ \frac{1}{2}\ -\frac{1}{2}+2z$
7 $x\ \frac{1}{2}-y\ \frac{1}{2}+z$	7-1 $0\ \frac{1}{2}-2y\ \frac{1}{2}$	7-2 $-\frac{1}{2}\ 0\ \frac{1}{2}+2z$	7-3 2x -2y 2z	7-4 $-\frac{1}{2}+2x\ \frac{1}{2}\ 0$	7-5 $2x\ \frac{1}{2}\ \frac{1}{2}+2z$	7-6 $-\frac{1}{2}+2x\ -2y\ \frac{1}{2}$	7-7 0 0 0	7-8 $-\frac{1}{2}\ \frac{1}{2}-2y\ 2z$
8 $\frac{1}{2}+x\ y\ \frac{1}{2}-z$	8-1 $\frac{1}{2}\ 0\ \frac{1}{2}-2z$	8-2 $0\ -\frac{1}{2}+2y\ \frac{1}{2}$	8-3 $\frac{1}{2}+2x\ -\frac{1}{2}\ 0$	8-4 2x 2y -2z	8-5 $\frac{1}{2}+2x\ 2y\ \frac{1}{2}$	8-6 $2x\ -\frac{1}{2}\ \frac{1}{2}-2z$	8-7 $\frac{1}{2}\ -\frac{1}{2}+2y\ -2z$	8-8 0 0 0

TABLE 13

TABLE 14

Peak position	Multiplicity	Expected in Patterson map	Expected peak Height
0 0 0	8	*	21144
0 $\frac{1}{2}$+2y $\frac{1}{2}$	4		
0 $\frac{1}{2}$-2y $\frac{1}{2}$	4	*	7056
$\frac{1}{2}$ 0 $\frac{1}{2}$+2z	4		
$\frac{1}{2}$ 0 $\frac{1}{2}$-2z	4	*	7056
$\frac{1}{2}$+2x $\frac{1}{2}$ 0	4		
$\frac{1}{2}$-2x $\frac{1}{2}$ 0	4	*	7056
$\frac{1}{2}$ $\frac{1}{2}$+2y 2z	2		
$\frac{1}{2}$ $\frac{1}{2}$-2y 2z	2	*	3528
$\frac{1}{2}$ $\frac{1}{2}$+2y -2z	2		
$\frac{1}{2}$ $\frac{1}{2}$-2y -2z	2		
2x $\frac{1}{2}$ $\frac{1}{2}$+2z	2		
2x $\frac{1}{2}$ $\frac{1}{2}$-2z	2	*	3528
-2x $\frac{1}{2}$ $\frac{1}{2}$+2z	2		
-2x $\frac{1}{2}$ $\frac{1}{2}$-2z	2		
$\frac{1}{2}$+2x 2y $\frac{1}{2}$	2		
$\frac{1}{2}$+2x -2y $\frac{1}{2}$	2		
$\frac{1}{2}$-2x 2y $\frac{1}{2}$	2	*	3528
$\frac{1}{2}$-2x -2y $\frac{1}{2}$	2		
2x 2y 2z	1	*	1764
2x 2y -2z	1		
2x -2y 2z	1		
2x -2y -2z	1		
-2x 2y -2z	1		
-2x -2y 2z	1		
-2x 2y 2z	1		
-2x -2y -2z	1		

TABLE 15

List of peak heights and positions for compound 2

Positions are listed as hundredths of unit cell parameters.

Peak No.	Position	Height Observed	Height Expected	General Coordinates
1	0, 0, 0	21144	21144	0, 0, 0
2	0, 14, 11	2346		
3	0, 0, 36	2791		
4	0, 16, 50	7786	7056	0, $\frac{1}{2}$-2y, $\frac{1}{2}$
5	0, 30, 40	1268		
6	9, 34, 26	1939	1764	2x, 2y, 2z
7	9, 50, 24	4068	3528	2x, $\frac{1}{2}$, $\frac{1}{2}$-2z
8	13, 36, 34	1561		
9	13, 20, 16	1277		
10	12, 36, 10	965		
11	12, 50, 0	1901		
12	16, 38, 50	1183		
13	27, 0, 0	4446		
14	24, 0, 23	2176		
15	25, 15, 27	832		
16	26, 14, 50	1731		
17	40, 50, 0	9365	7056	$\frac{1}{2}$-2x, $\frac{1}{2}$, 0
18	41, 34, 50	3784	3528	$\frac{1}{2}$-2x, 2y, $\frac{1}{2}$
19	38, 36, 10	1656		
20	36, 22, 40	1135		
21	50, 30, 16	1438		
22	50, 50, 37	1078		
23	50, 0, 0	2611		
24	50, 0, 24	9271	7056	$\frac{1}{2}$, 0, $\frac{1}{2}$-2z
25	50, 16, 26	3831	3528	$\frac{1}{2}$, $\frac{1}{2}$-2y, 2z
26	50, 13, 34	2157		
27	50, 0, 38	2223		

Hence $\frac{1}{2}-2y = 0.16$

$2y = 0.34$

There are two possible peaks corresponding to the general position $\frac{1}{2}$, 0, $\frac{1}{2}-2z$: peak 24 of height 9271 and peak 27 of height 2223. The former was chosen because its height was much closer to the expected height of 7056

Hence $\frac{1}{2}-2z = 0.24$

$2z = 0.26$

There are also two possible peaks corresponding to the general position $\frac{1}{2}-2x$, $\frac{1}{2}$, 0 : peak 11 of height 1901 and peak 17 of height 9365. The latter was chosen because its height matched the expected height of 7056 more closely

Hence $\frac{1}{2}-2x = 0.40$

$2x = 0.10.$

The values $2x = 0.10$, $2y = 0.34$ and $2z = 0.26$ were checked by seeking the peaks in the general positions $\frac{1}{2}$, $\frac{1}{2}-2y$, $2z$; $2x$, $\frac{1}{2}$, $\frac{1}{2}-2z$; $\frac{1}{2}-2x$, $2y$, $\frac{1}{2}$; all of expected height 3528, and the rotation peak at $2x$, $2y$, $2z$ of expected height 1764. The result, listed in Table 15, shows that these values fit remarkably well. In all cases the peak heights are somewhat higher than expected, indicating that not only the molybdenum atoms, but the light atoms as well are contributing to the vector peaks.

Peak 16 was therefore chosen as the rotation peak, having coordinates $2x = 0.09$, $2y = 0.34$, $2z = 0.26$, and the molybdenum atom therefore lies at $x = 0.045$, $y = 0.17$, $z = 0.13$.

7.6 THE LOCATION OF THE LIGHT ATOMS.

Structure factors were calculated with the molybdenum atom alone, located at $x = 0.045$ $y = 0.17$ $z = 0.13$ and with a tentative value of $B = 2$ $\mathring{A}^2$. These gave an R value of 0.42.

A Fourier synthesis was then computed for the fraction of the unit cell $0 \rightarrow \frac{1}{2}$ along a, $0 \rightarrow \frac{1}{2}$ along b and $0 \rightarrow \frac{1}{2}$ along c. This showed the positions of the following atoms:

P, C_6, C_8, C_9, O_1, C_2, O_2, C_3, O_3, O_4 and O_5 (see Fig. 23 for the atomic nomenclature in the molecule).

The peaks corresponding to atoms O_4 and O_5 were considerably higher than those of the other three oxygen atoms. In addition a peak, with height approximately $\frac{1}{4}$ of the height of the molybdenum peak was found at position $x = .04$ $y = .17$ $z = .37$. This posed an immediate problem, because by virtue of its position it could not be reasonably linked to any of the light atoms in the molecule and thus made no chemical sense. The peak was of such magnitude, however, that it could not be neglected.

The possibility of impurties in the compound, or of water molecules occluded in the structure was discarded in view of the accurate results of the elemental analysis (Section 3.3) and the infrared spectrum (Section 3.4).

It was thought that the Fourier programme might be at fault and an exhaustive check of the latter was carried out culminating in the computation of a three dimensional Fourier synthesis of a published heavy

atom structure. The programme, however, yielded the correct results.

A three dimensional Fourier synthesis was therefore computed over the whole unit cell, in order to see the location of the unexplained peak in relation to the crystal structure as a whole. The Fourier map was drawn on glass sheets and photographed. The result is shown in Fig. 18. On careful analysis of this Fourier synthesis it was realised that the unexplained peak, when translated in accordance with the requirements of the space group Pbca, lay exactly between two molybdenum atoms which do not belong to the same molecule.

	x	y	z
molybdenum atom (molecule 1)	0.04	.17	.13
unexplained peak	0.54	.17	.13
molybdenum atom (molecule 2)	1.04	.17	.13

In accordance with the space group Pbca, whose equivalent positions are listed in Table 13, this would correspond to translating the unexpected peak from x,y,z (.04, .17, .37) to $\frac{1}{2}+x$, y, $\frac{1}{2}-z$ (.54, .17, .13). It was assumed therefore that this unexpected peak was a heavy atom - heavy atom interaction Fourier peak. This was proved by the fact that, on calculation of the difference Fourier, the peak disappeared, while the peaks of the other light atoms remained.

The positions of the atoms as found from the first difference Fourier are shown in Table 16.

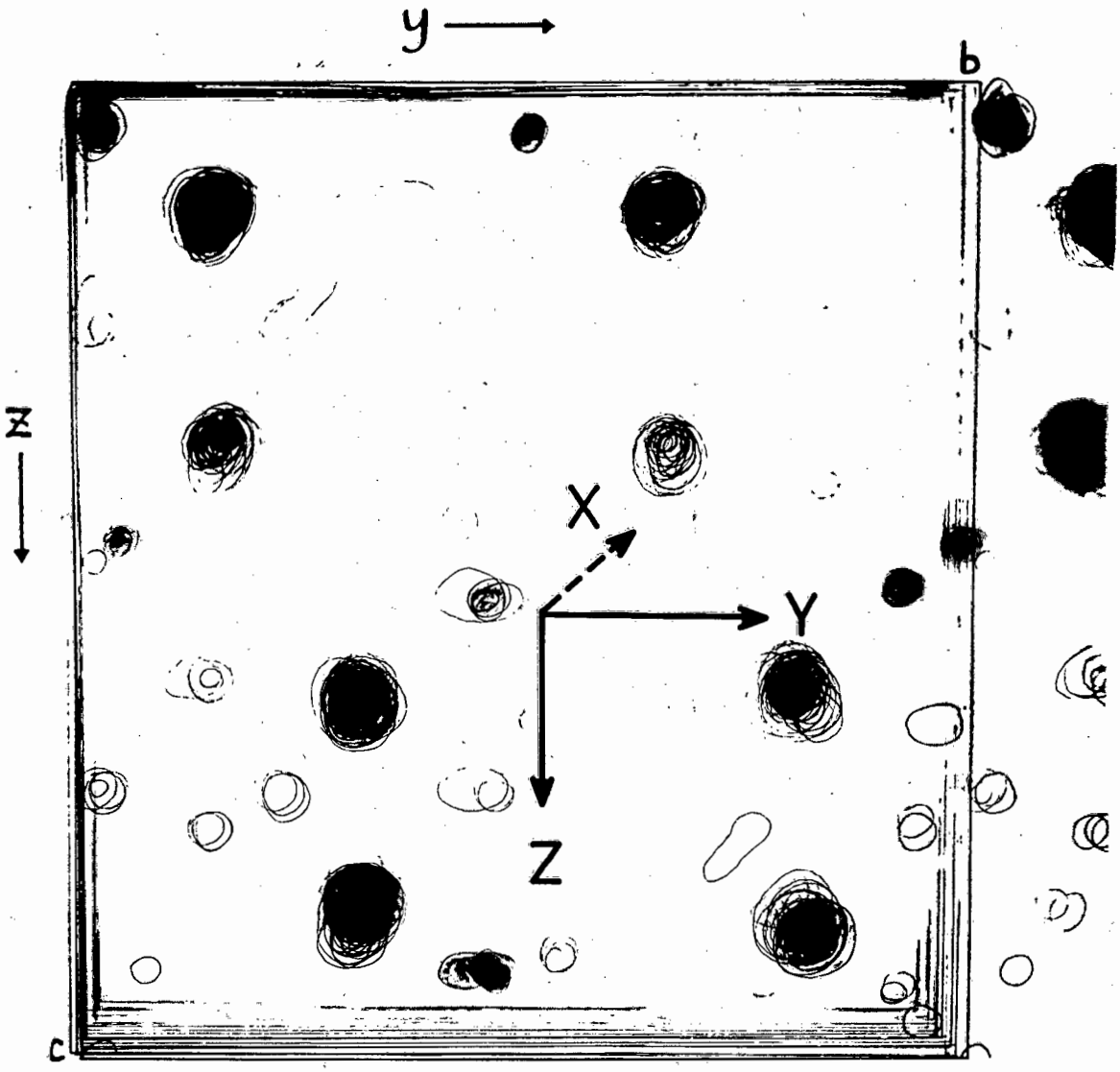

Fig. 18

TABLE 16

Atomic positional parameters in fractions of the unit cell lengths a, b, c.

	x	y	z
Mo	.039	.169	.130
P	.076	.036	.029
O_1	.039	.045	.303
O_2	.012	.331	.253
O_3	.032	.296	.034
O_4	-.230	.170	.135
O_5	.310	.175	.135
C_1	.043	.089	.241
C_2	.016	.270	.208
C_3	.041	.249	.022
C_6	.152	.059	-.084
C_8	.156	-.063	.081

The difference Fourier synthesis did not give a clear indication of the atomic positions of atoms C_4 and C_5, probably due to interference effects of the Mo-Mo interaction peak in this region. Their position was thus calculated by assuming the Mo-C and C-O bond lengths, which were taken as Mo $\underset{}{\overset{2.08\ \text{Å}}{\text{———}}}$ C $\overset{1.15\ \text{Å}}{\text{———}}$ O

$\longleftarrow$ 3.23 Å $\longrightarrow$

and they were thus placed collinearly with the Mo and O atoms in the following positions C_4 x = -.140 y = .170 z = .133

C_5 x = .220 y = .173 z = .133

Structure factors were again calculated including all the atoms in Table 16 as well as atoms C_4 and C_5. The following tentative temperature factors were assigned to the atoms:

Mo	B = 1.8 Å^2	C_1	B = 4 Å^2
P	B = 1.8 "	C_2	B = 4 "
O_1	B = 5 "	C_3	B = 4 "
O_2	B = 5 "	C_4	B = 4 "
O_3	B = 5 "	C_5	B = 4 "
O_4	B = 5 "	C_6	B = 4 "
O_5	B = 5 "	C_8	B = 4 "

This trial structure yielded a residual value of R = 0.25.

A second difference Fourier synthesis, carried out with the latter structure factors showed the positions of the atoms C_7 and C_9 at

C_7 x = .286 y = .070 z = -.075

C_9 x = .268 y = -.040 z = .135

The second difference Fourier synthesis also showed characteristic peaks in the vicinity of both the Mo and P atoms, implying anisotropic thermal motion.

7.7 REFINEMENT.

The structure was refined by least squares method using the C.S.I.R. ORFLSRED programme. In the refinement, the scattering factor of the molybdenum atom was corrected for dispersion[50].

In order to place the observed and calculated structure factors on the same scale, the first two cycles were devoted only to refining the scale factors. This was followed by three cycles where the scale factors, the atomic positions and the isotropic temperature factors were all allowed to vary. At this stage of the refinement the value of the residual, R, was 0.095. The temperature factors of the atoms O_4, O_5 and C_7 were noticed to be somewhat higher than those of the other atoms and oscillating with each cycle. Therefore three more cycles of refinement were carried out varying the same parameters as before. The residual R at this stage was 0.094.

A final three cycles of refinement, in which all the atomic positions were allowed to vary and in which the temperature factors of the Mo and phosphorus atoms were treated anisotropically, were carried out. The final R value for the structure was 0.091.

The final atomic positions, with estimated standard deviations, are given in Table 17 and the final values of the temperature factors are given in Table 18.

The Fourier synthesis, computed from the structure factors obtained from the final values of the atomic parameters, was drawn on glass and photographed (Figs. 19 and 20). The Fourier map shows the positions of the atoms in the asymmetric unit, together with the P' atom belonging to the other half of the molecule. Fig. 19 shows the structure as viewed along the X axis, with atoms O_4, C_4, Mo, C_5, O_5 superimposed .

Fig. 20 gives a perspective view, clearly showing the different positions of atoms which are collinear with the X axis. In both Figs. 19 and 20 the Fourier ripple peak is directly beneath the peak of the Mo atom, near the bottom of the picture.

A section of the electron density distribution through the unit cell at $y = 0.17$ and $z = 0.13$ is shown in Fig. 21. The figure shows the Fourier interaction ripple located halfway between the molybdenum atoms of adjacent molecules.

An accurate model of the molecule was constructed (scale 4cm = 1 Å) and photographed in colour. (Fig. 22). The colour photograph of the model gives a good three dimensional impression of the relative location of the atoms to each other. (Mo atoms brown

P atoms blue

O atoms red

C atoms black)

An idealised drawing of the molecule is shown in Fig. 23, in which all the atoms have been labelled. The final values of the observed and calculated structure factors are tabulated in Appendix II.

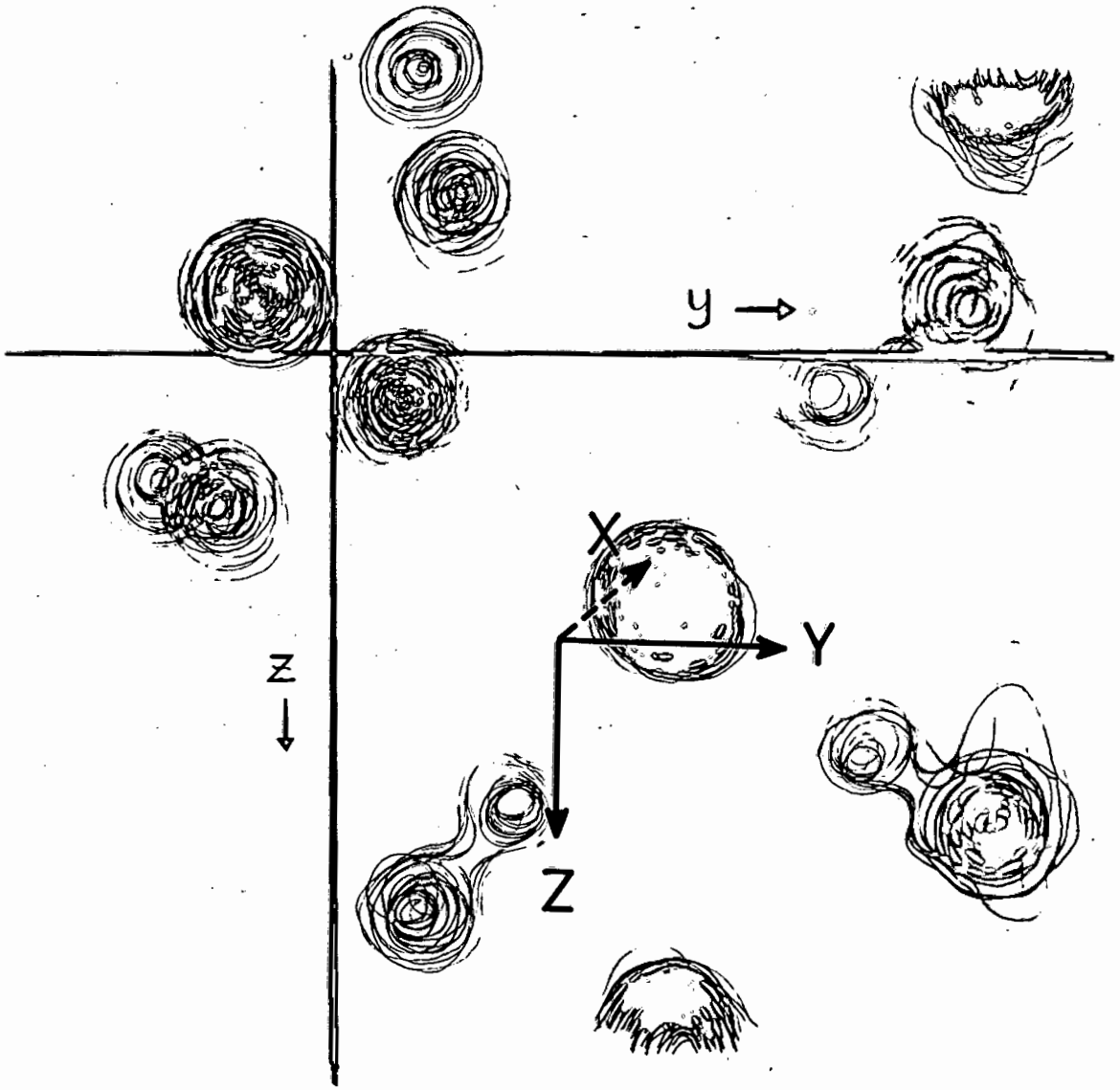

Fig. 19

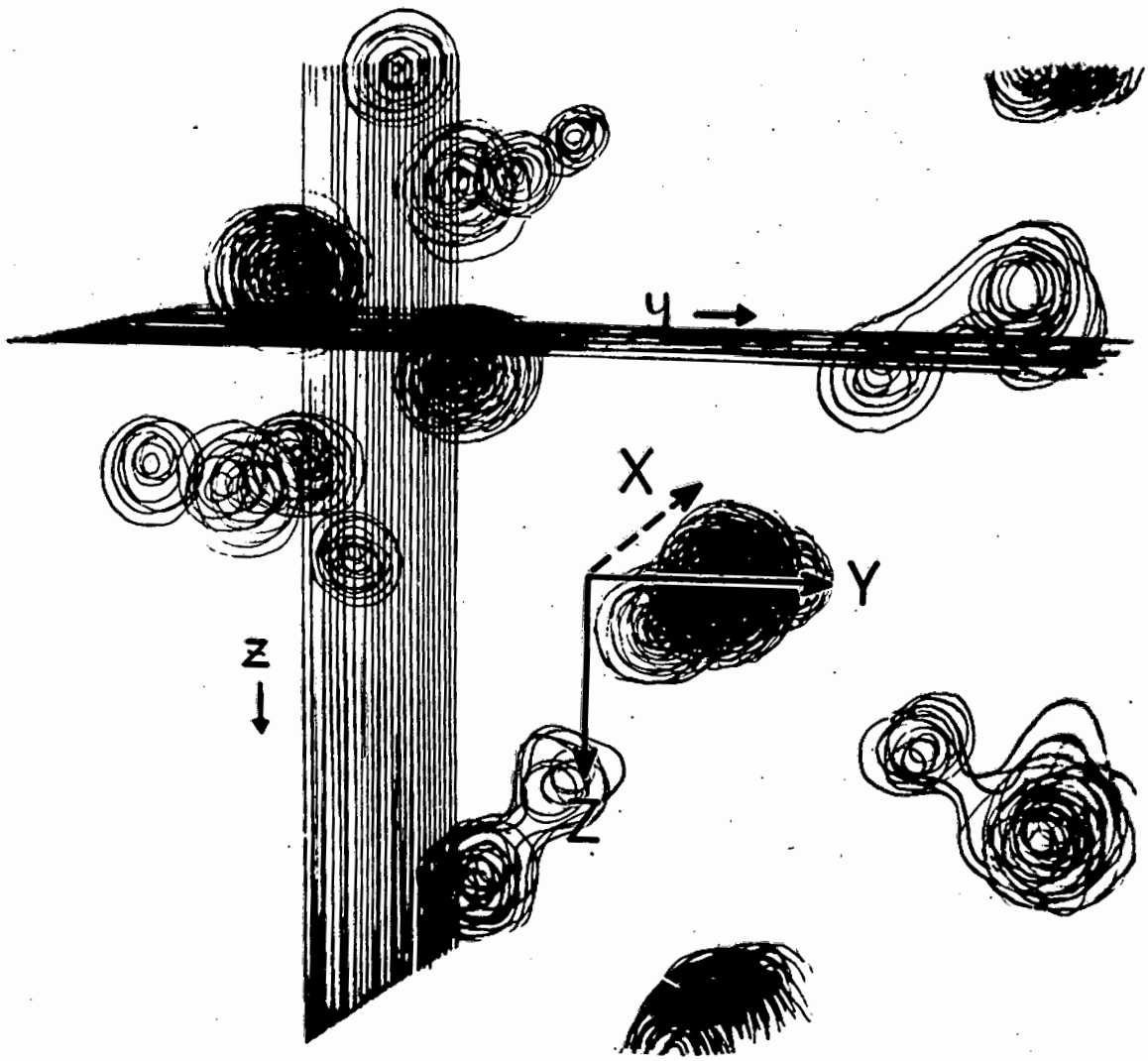

Fig.20

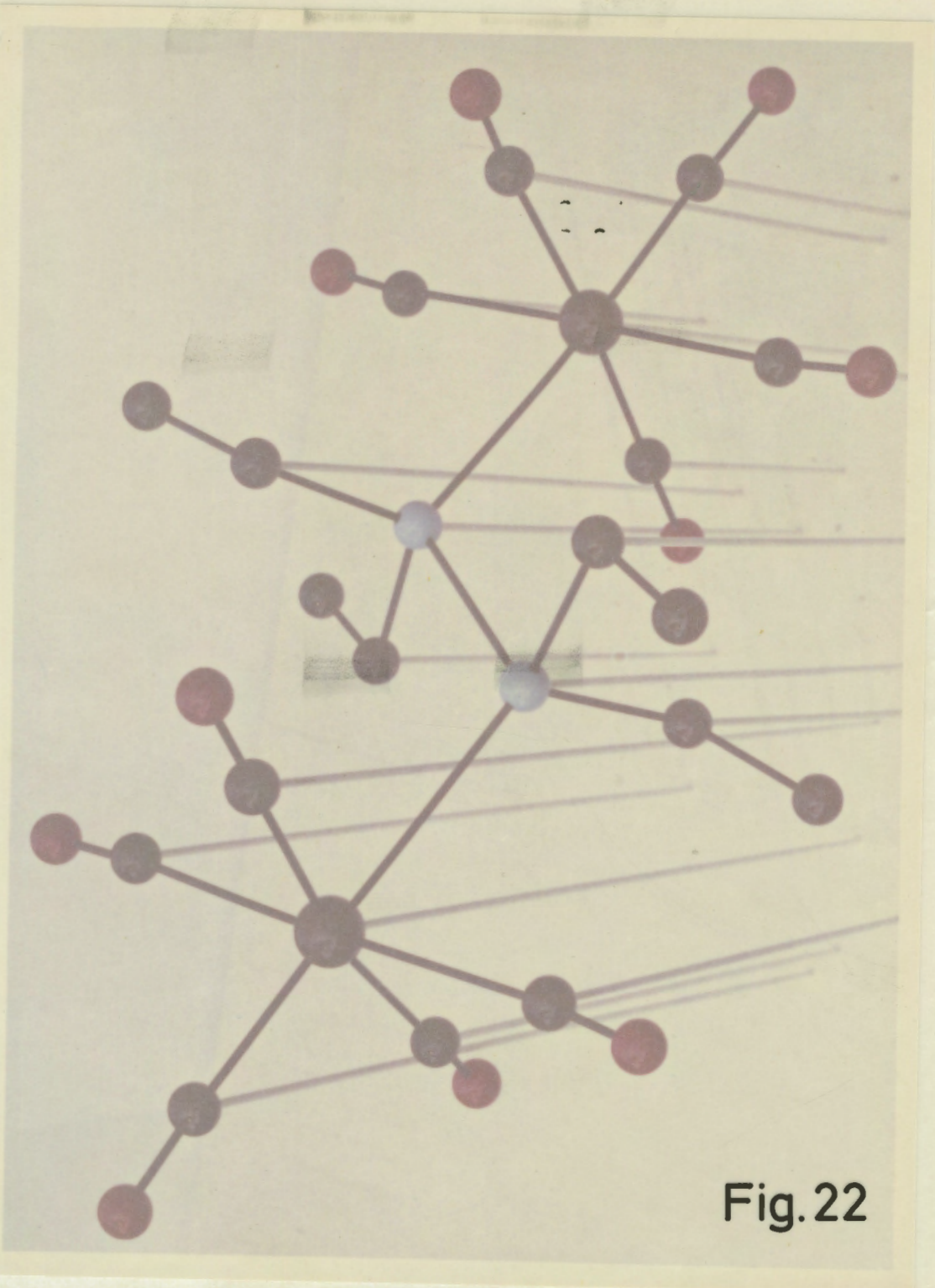

Fig. 22

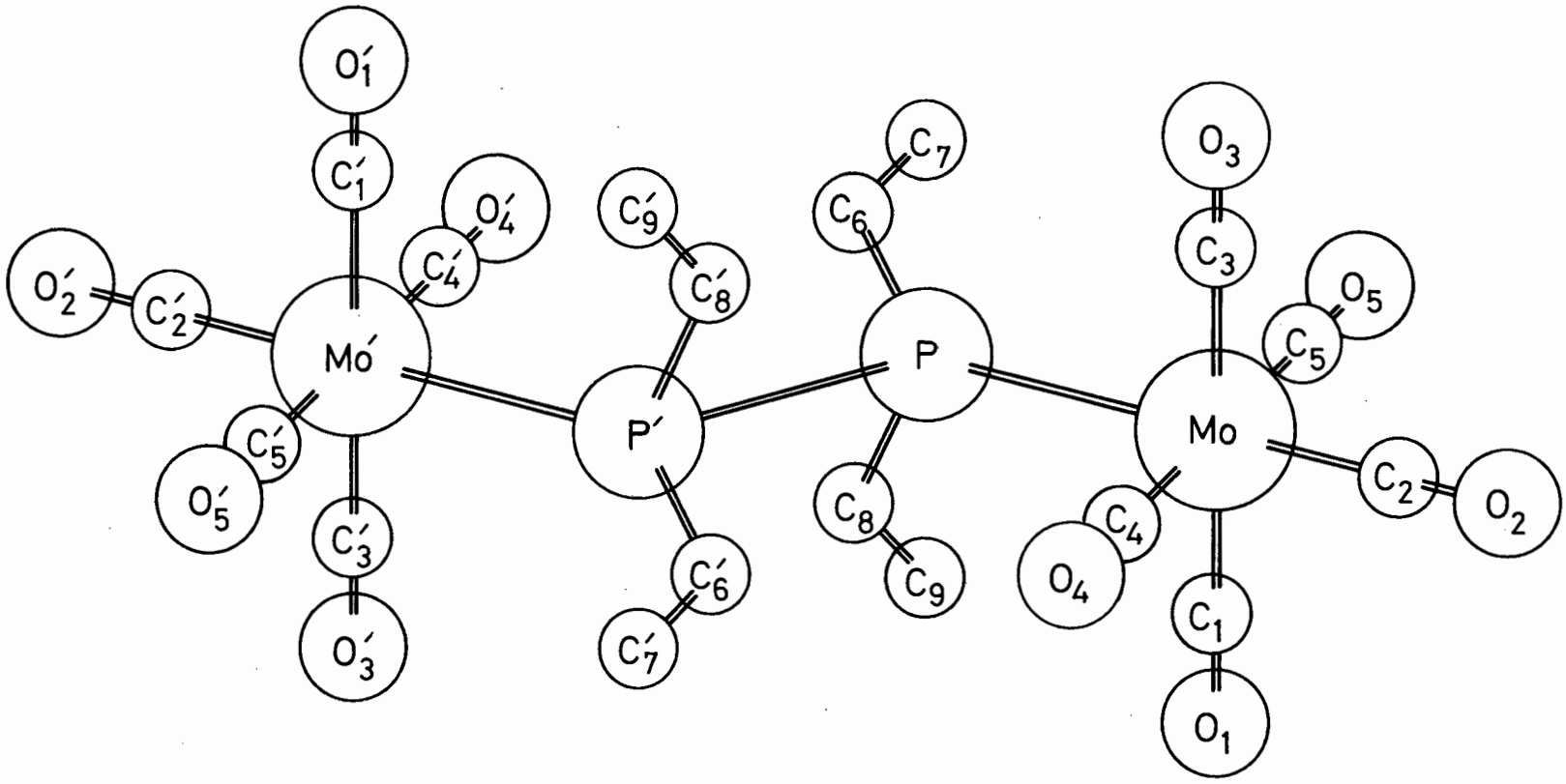
O'1
C'1
O'4
C'4
O'2
C'2
Mo'
C'5
O'5
C'3
O'3
C'9
C'8
P'
C'6
C'7
C7
C6
P
C8
C9
O3
C3
O5
C5
Mo
C2
O2
C4
O4
C1
O1

Fig. 23

7.8 CALCULATION OF INTERATOMIC BOND LENGTHS AND ANGLES.

Interatomic bond lengths and angles and their estimated standard deviations were calculated by using the formulae discussed in Section 5.6. These are shown in Tables 19 and 20.

Three "best planes" going through atoms in the molecule were calculated.

(a) plane "1", going through the atoms:

$O_2', C_2', O_5', C_5', Mo', C_4', O_4', P', P, O_4, C_4, Mo, C_5, O_5, C_2, O_2$

(b) plane "2", going through the atoms:

$P, O_3, C_3, Mo, C_1, O_1, C_2, O_2$

(c) plane "3", going through the atoms:

$O_4, C_4, O_3, C_3, Mo, C_1, O_1, C_5, O_5$

The interplanatory angles were found to be

plane "1" ^ plane "2" = 90.09°

plane "1" ^ plane "3" = 89.13°

plane "2" ^ plane "3" = 84.51°

The angles are in good agreement with the expected value of 90°. The perpendicular distances of these atoms to their respective planes are shown in Table 21.

TABLE 17

Atomic positional parameters and their standard deviations in fractions of the unit cell parameters a, b, c.

	x	y	z	σx	σy	σz
Mo	0.0395	0.1690	0.1304	0.0005	0.0001	0.0001
P	0.0759	0.0357	0.0289	0.0013	0.0004	0.0004
O_1	0.0379	0.0452	0.3020	0.0033	0.0014	0.0015
O_2	0.0087	0.3346	0.2523	0.0028	0.0014	0.0016
O_3	0.0339	0.2979	-0.0351	0.0034	0.0015	0.0015
O_4	-0.2333	0.1710	0.1385	0.0040	0.0023	0.0025
O_5	0.2997	0.1950	0.1474	0.0041	0.0020	0.0022
C_1	0.0386	0.0862	0.2444	0.0045	0.0021	0.0025
C_2	0.0120	0.2724	0.2042	0.0043	0.0018	0.0018
C_3	0.0365	0.2522	0.0219	0.0040	0.0016	0.0016
C_4	-0.1524	0.1652	0.1323	0.0059	0.0022	0.0024
C_5	0.2176	0.1736	0.1351	0.0066	0.0022	0.0025
C_6	0.1459	0.0556	-0.0811	0.0050	0.0021	0.0022
C_7	0.2738	0.0809	-0.0649	0.0066	0.0030	0.0032
C_8	0.1478	-0.0637	0.0774	0.0043	0.0019	0.0022
C_9	0.2626	-0.0429	0.1375	0.0050	0.0022	0.0026

TABLE 18

Final temperature factors with standard deviations ($Å^2$)

Mo	β_{11}	0.00327 ± 0.00108
	β_{22}	0.00242 ± 0.00007
	β_{33}	0.00235 ± 0.00007
	β_{12}	-0.00044 ± 0.00020
	β_{13}	0.00003 ± 0.00023
	β_{23}	-0.00039 ± 0.00008
P	β_{11}	0.00360 ± 0.00244
	β_{22}	0.00219 ± 0.00024
	β_{33}	0.00261 ± 0.00028
	β_{12}	-0.00076 ± 0.00058
	β_{13}	0.00008 ± 0.00067
	β_{23}	-0.00007 ± 0.00022

O_1	B = 5.75 ± 0.61
O_2	B = 5.60 ± 0.52
O_3	B = 6.29 ± 0.65
O_4	B = 8.53 ± 1.75
O_5	B = 7.97 ± 1.50
C_1	B = 5.03 ± 0.76
C_2	B = 3.78 ± 0.66
C_3	B = 2.98 ± 0.59
C_4	B = 3.47 ± 1.06
C_5	B = 3.91 ± 0.91
C_6	B = 3.76 ± 0.81
C_7	B = 8.18 ± 1.44
C_8	B = 3.36 ± 0.78
C_9	B = 5.69 ± 0.96

TABLE 19

Bond lengths (Å) with estimated standard deviations

P' - P	2.21 (2)	P - C_6	1.85 (4)
Mo' - Mo	6.45 (1)	P - C_8	1.85 (4)
P - Mo	2.54 (1)	C_6 - C_7	1.53 (8)
Mo - C_1	2.11 (4)	C_8 - C_9	1.62 (7)
Mo - C_2	1.93 (3)	C_7 - C_9'	6.25 (9)
Mo - C_3	2.04 (3)	C_7 - C_8'	4.83 (9)
Mo - C_4	2.19 (7)	C_6 - C_9'	4.75 (8)
Mo - C_5	2.04 (7)	C_6 - C_8'	3.36 (8)
C_1 - O_1	1.06 (5)		
C_2 - O_2	1.18 (4)		
C_3 - O_3	1.09 (3)		
C_4 - O_4	.93 (8)		
C_5 - O_5	1.01 (8)		

The figure in parentheses represents the estimated standard deviation of the last significant digit.

TABLE 20

Bond angles (°) with estimated standard deviations.

P' - P - Mo	118.9 (5)	C_3 - Mo - C_1	178.1 (12)
P' - P - C_8	96.6 (6)	Mo - C_4 - O_4	171.6 (19)
C_8 - P - Mo	118.0 (4)	Mo - C_1 - O_1	179.4 (15)
C_6 - P - P'	94. 0 (5)	Mo - C_2 - O_2	172.1 (12)
C_6 - P - C_8	106.6 (5)	Mo - C_5 - O_5	161.2 (19)
C_6 - P - Mo	118.4 (4)	Mo - C_3 - O_3	178.6 (15)
		P - C_6 - C_7	108.2 (9)
P - Mo - C_3	90.4 (4)	P - C_8 - C_9	115.1 (8)
C_5 - Mo - P	83.3 (6)		
C_3 - Mo - C_2	87.9 (5)		
C_2 - Mo - C_1	90.4 (6)		
C_1 - Mo - P	91.3 (5)		
C_4 - Mo - C_3	90.5 (4)		
C_3 - Mo - C_5	91.4 (4)		
C_5 - Mo - C_1	89.8 (4)		
P - Mo - C_4	98.7 (5)		
C_4 - Mo - C_2	81.4 (6)		
C_2 - Mo - C_5	96.7 (4)		
P - Mo - C_2	178.3 (12)		
C_4 - Mo - C_5	177.3 (13)		

The figure in parentheses represents the estimated standard deviation of the last significant digit.

TABLE 21

Perpendicular distances between atoms and planes.

(a) Distances between atoms and plane "1"

Atom	Perp.distance (Å)
O_2'	-.053
C_2'	-.057
O_5'	.017
C_5'	.054
Mo'	.014
C_4'	.042
O_4'	.051
P'	.029
P	-.029
O_4	-.051
C_4	-.042
Mo	-.014
C_5	-.054
O_5	-.017
C_2	.057
O_2	.053

(b) Distances between atoms and plane "2"

Atom	Perp.distance (Å)
P	.047
O_3	-.026
C_3	-.013
Mo	-.001
C_1	-.027
O_1	-.041
C_2	-.036
O_2	.097

TABLE 21 (continued)

(c) Distances between atoms and plane "3"

Atoms	Perp.distance (Å)
O_4	.160
C_4	-.010
O_3	-.020
C_3	-.061
Mo	-.090
C_1	-.065
O_1	-.042
C_5	-.095
O_5	.224

8. DISCUSSION

8.1 ELECTRONIC CONFIGURATION OF THE COMPOUNDS.

8.1 (a) Electronic configuration in terms of the Valence Bond theory.

Molybdenum (atomic number 42) has the electronic configuration:

$1s^2 2s^2 2p^6 3s^2 3p^6 3d^{10} 4s^2 4p^6 4d^5\ 5s^1$

and forms a neutral hexacarbonyl $[Mo(CO)_6]$ known to have the octahedral structure expected from its coordination number of 6. This structure, on the Valence Bond theory, would involve d^2sp^3 hybridisation:

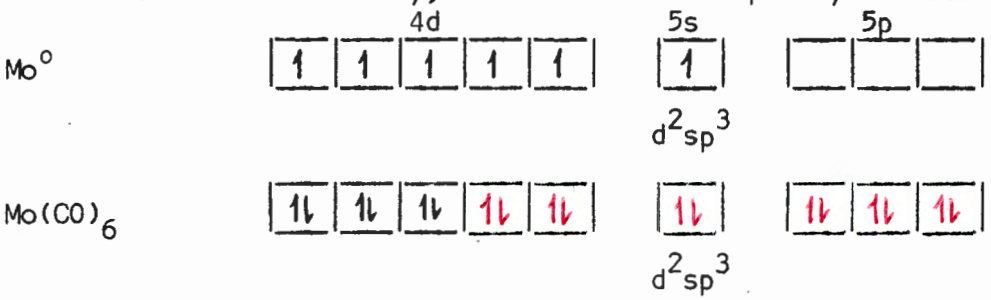

[For clarity, electrons donated by Mo are denoted as 1
electrons donated by CO are denoted as 1↓]

The six carbonyl groups each contribute two electrons, thus molybdenum attains the xenon configuration. There are no unpaired electrons, hence the compound is diamagnetic.

In the type A compound di-μ-diethylphosphido-bis(tetracarbonyl-molybdenum) the evidence obtained from infrared spectra suggests that the structure is fundamentally octahedral as the I.R. spectra are similar to those observed for compounds of the type $[M(CO)_5L]$ where

L is a monodentate, neutral ligand.

There are two ways of formulating the electronic configuration of the compound which is shown below:-

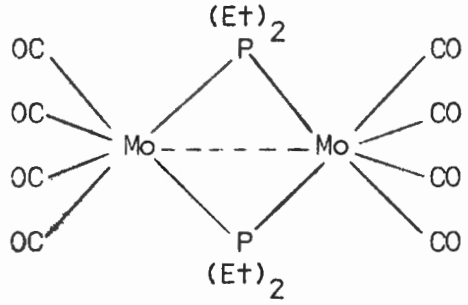

(a) The PEt_2 groups arise from cleavage of the P-P bond in Et_2-P-P-Et_2. This leads to two $\overset{xx}{\cdot}PEt_2$ radicals which implies formally zerovalent molybdenum. The compound may then be formulated as follows

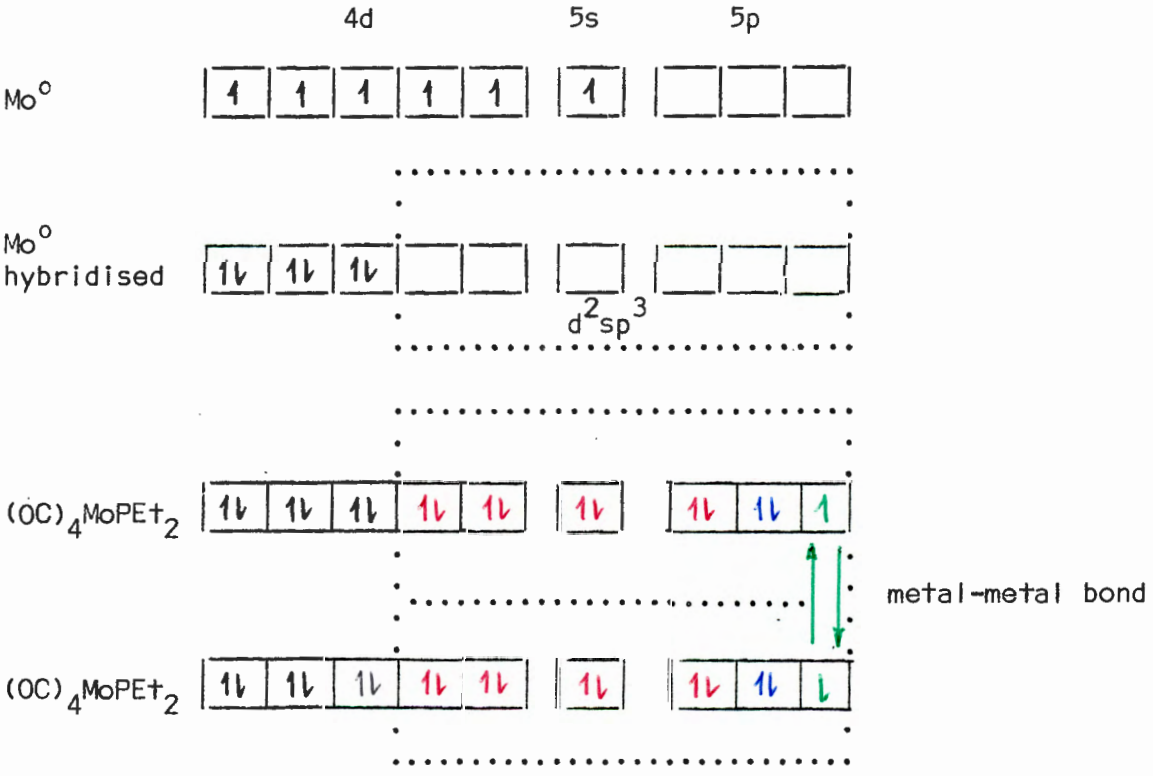

For clarity, the electrons donated by the Mo are denoted as 1
the electrons donated by the CO are denoted as 1
the electrons donated by the P(lone pair) as 1
the electrons donated by the P(single e) as 1

(b) The PEt_2 group may be regarded as a charged anion as is formed in the reaction

$$Et_2P + Na \rightarrow PEt_2^- + Na^+$$

In this case the formal valence of Mo is +1 and the compound may be formulated as follows

$$Mo \rightarrow Mo^+ + e'$$

$$Et_2P\text{-}PEt_2 \rightarrow 2\ Et_2P^{\cdot\,\times\times}$$

$$Et_2P^{\cdot\,\times\times} + e' \rightarrow Et_2P^{\times\times}_{\circ}$$

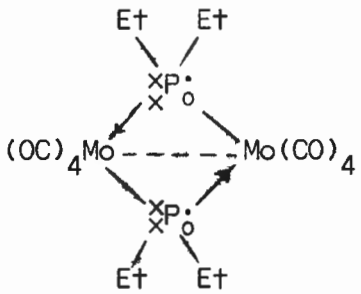

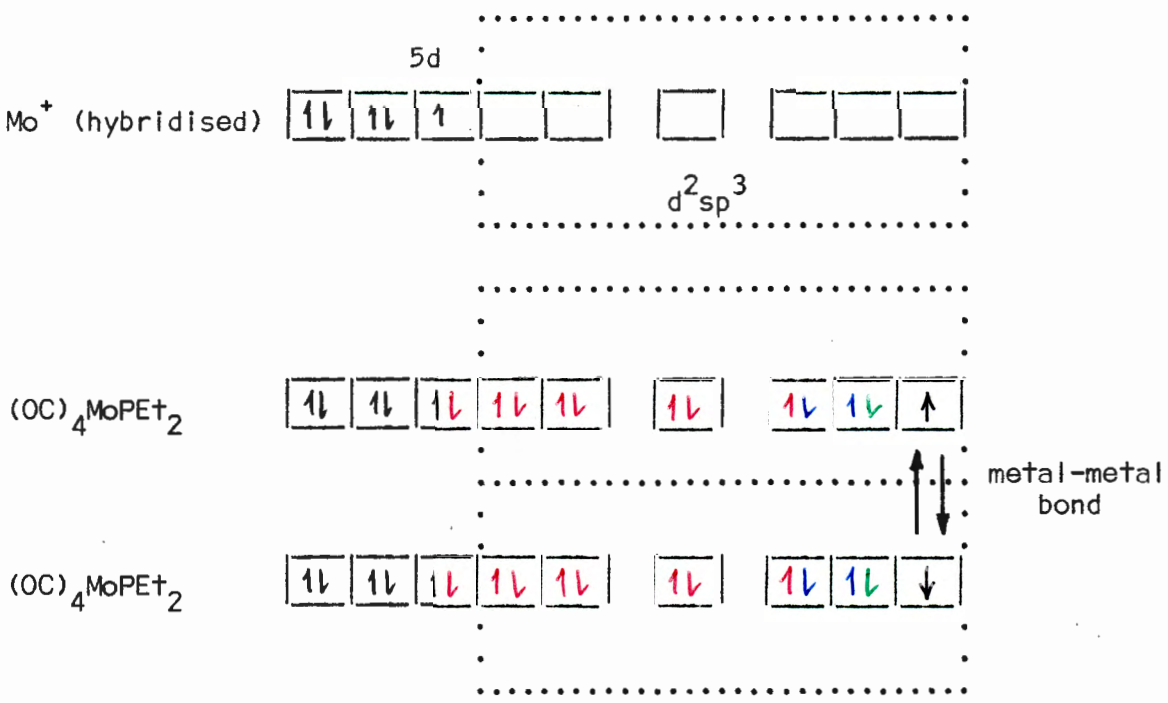

As before, the electrons donated by the Mo are denoted as ↿

the electrons donated by the CO are denoted as ↿

the electrons donated by the P (lone pair)" as ↿

the electron donated by the P are denoted as ↿

the electron donated by the P are denoted as ↿

both these explanations (a) and (b) satisfy Sidgwick's Effective Atomic Number (EAN) concept.

(a)			(b)		
Mo^0	42	electrons	Mo^+	41	electrons
from four CO groups	8	"	from four CO groups	8	"
from PEt_2 group	3	"	from PEt_2 group	4	"
from Mo-Mo bond	1	"	from Mo-Mo bond	1	"
Total	54	"	Total	54	"
(Xenon structure)			(Xenon structure)		

The first explanation is favoured by Thomson's photochemical experiments, which imply the formation of PEt_2 radicals, whilst the latter explanation is favoured by the known existence of the PEt_2^- anion in compounds such as $Na^+(PEt_2)^-$. There is no further experimental evidence available which elucidates the mechanism of the formation of the compound.

In the type B compound μ-Tetraethyldiphosphine-bis(pentacarbonyl-molybdenum)

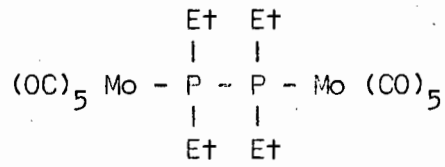

we have octahedral structure about the Mo and tetrahedral structure about the phosphorus. Thus the same considerations as with $|Mo(CO)_6|$ apply with regard to electronic configuration of the metal atom. These were discussed previously, so that no further elucidation is necessary.

8.1(b) ELECTRONIC CONFIGURATION IN TERMS OF THE CRYSTAL FIELD THEORY

The bonding may also be discussed in terms of the crystal field theory, in which the bonding is regarded as purely electrostatic in origin and amounts to considering the interaction between the electrostatic field of the ligands and the d electrons of the metal ion.

To describe this interaction, the d orbitals of the metal are shown in diag. A. If six ligands in an octahedral array are placed around the metal ion, two of the metal orbitals, $d_{x^2-y^2}$ and d_{z^2} (the e_g orbitals) are disposed along the ligand-to-metal bonds. The remaining orbitals, d_{xz}, d_{yz}, d_{xy} (collectively designated the t_{2g} orbitals) are orientated so that each lobe is directed towards a point midway between any two ligands. Because of the electrostatic field of the ligands the potential energy of an electron in the e_g orbitals will be higher than that of an electron in the t_{2g} orbitals. Now an electron will seek a position of lowest potential energy and the

first three electrons will occupy the d_{xy}, dx_{xz} and d_{yz} orbitals. The orbital taken by the fourth electron will depend on the magnitude of the crystal field splitting parameter, Δ_o.

If the electrostatic field produced by the ligand is small (small Δ_o) then the energy required to pair the fourth electron with one already present will be greater than the energy required for its promotion to the e_g level. Under these circumstances the configuration $t_{2g}^{3} e_g^{1}$ will be realised. If the field is strong the configuration will be t_{2g}^{4}.

This may be illustrated schematically as shown in diag.A in which the energy of the d orbitals before and after splitting is shown.

Diag. A

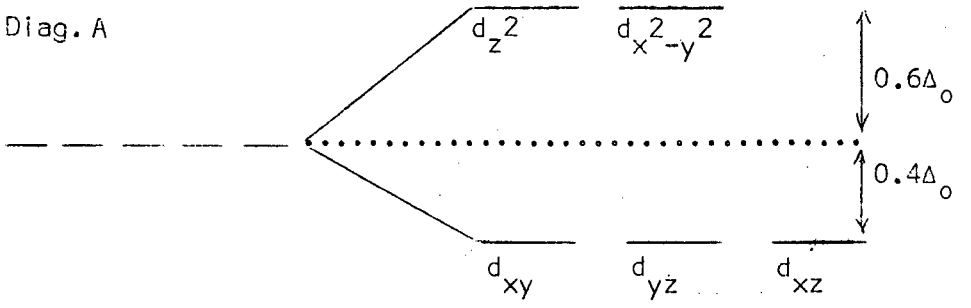

Δ_o represents the total energy separation

$0.4\Delta_o$ represents the energy lost by the system for each electron occupying the low energy level.

$0.6\Delta_o$ represents the energy gained by the system for each electron occupying the low energy level.

In particular, considering the d orbitals of the Mo atom there arise two possibilities, depending on whether the ligand produces a small or large Crystal field.

(a) The ligand produces a small crystal field:

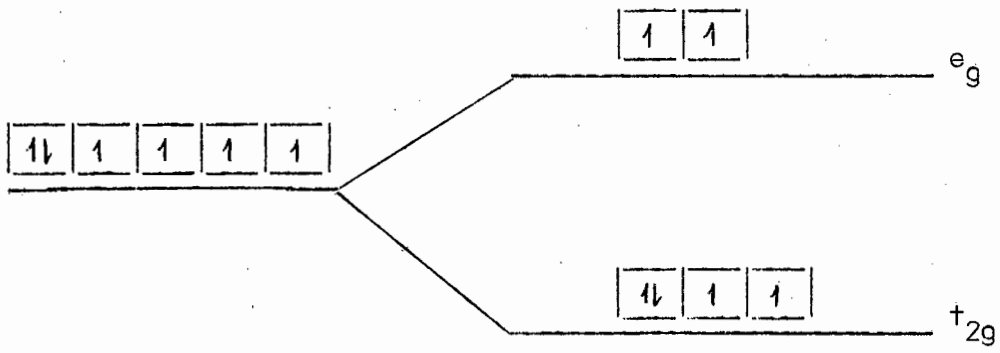

in this case the electrons will distribute themselves among both the e_g and t_{2g} orbitals

(b) The ligand produces a large crystal field: they will distribute themselves among the t_{2g} orbitals.

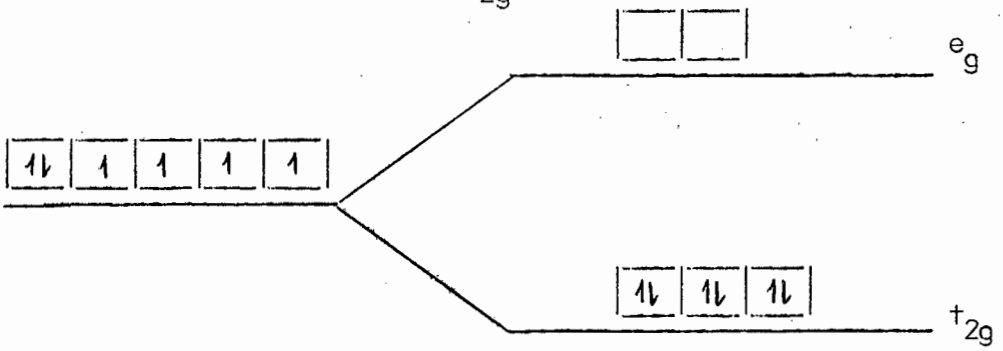

Since the compounds under discussion are diamagnetic, the latter situation prevails, as this shows that there are no unpaired electrons. It is also consistent with the conclusion that CO gives rise to a large crystal field as is evident from its position at the extreme of the spectrochemical series.

8.2 DISCUSSION OF STRUCTURAL RESULTS OF di-μ-diethylphosphido-bis-(tetracarbonylmolybdenum)(compound 1).

The structure of the compound is illustrated in Fig. 16 . The molecule consists of two distorted octahedra, joined by a common edge. The molybdenum atoms, the phosphorus atoms and four of the carbonyl groups are coplanar within experimental error and the two phosphine ligands are trans to each other on this plane.

The bond lengths (Table 10) are similar to those found in the related complexes $\left[(OC)_3(Et_3P)Mo(PMe_2)_2Mo(PEt_3)(CO)_3\right]$[57] and $\left[(OC)_2(C_5H_5)Mo\cdot PMe_2\cdot H\cdot Mo(C_5H_5)(CO)_2\right]$[58]

8.2 (a) Metal-Metal bonds.

Recent literature shows that many elements of the "d" block form compounds with metal-metal bonds. The surest indication of the existence of a metal-metal bond is provided by the molecular structure. In general short distances between the metal atoms are indicative of the existence of the bond but these alone do not constitute conclusive evidence.

Several authors have discussed the factors which influence the formation of M-M bonds.[59-61] In particular Sheldon[62] proposes the following criteria for the identification of M-M bonds.

(1) The compound should be diamagnetic

(2) The structure should conform to one of two types

2(a) A dimer or polymer formed by joining coordination polyhedra at shared edges or faces and in which the metal atoms are displaced towards each other from the poly-

hedron centres.

2(b) A polymer containing octahedral M_6, tetrahedral M_4 or trigonal M_3 clusters of metal atoms with short M-M distances and whose general stereochemistry cannot be accounted for by the typical coordination and oxidation numbers of the metal.

Lewis and Nyholm[63] discuss M-M bonds in transition metal complexes and list the M-M bond distances between metals of the "d" group. In particular they list eight molecules having Mo-Mo bonds varying in bond length from 2.8 to 3.84 Å.

8.2 (b) The molybdenum-molybdenum bond.

The interpretation of the metal-metal bond length depends on the selection of the correct single-bond radius for molybdenum.

Evidence from previous structures shows that the molybdenum radius is dependent on its oxidation state. Cotton and Wing[64] arrived at a value of 1.61 Å for octahedrally coordinated Mo^{o}, and Doedens and Dahl accepted this value as correct for the hepta- or octa-coordinate Mo^{II} complex,

$$\left[(OC)_2(C_5H_5)Mo\cdot PMe_2\cdot H\cdot Mo(C_5H_5)(CO)_2\right]^{58}$$

Bennett and Mason[65] also give the value of 1.60 ± .03 Å in two heptaco-ordinate cyclopentadienyl and ethyl complexes of Mo^{I} and Mo^{II}.

Lawton and Mason[66] report a radius of 1.45 Å in molybdenum acetate, in which the metal is pentaco-coordinate.

Bennett and Mason suggest that the radius changes by 0.05 Å for unit change in formal oxidation number. If the oxidation state of the metal in the compound under discussion is Mo^{I} (Section 8.1) and if the value of 1.61 Å is taken for Mo^{0}, this gives a value of 1.56 Å for Mo^{I}. The calculated M-M bond length would then be 3.12 Å, which is in good agreement with that found in the compound (3.057 Å). Bennett's and Mason's suggestion, however, is based on a 'hard ball' approach which is oversimplified and as such is not universally applicable. The value of 1.56 Å for Mo^{I} cannot therefore be taken as reliable. As discussed in section 8.1, however, it is preferable to regard the metal as being zerovalent in which case the value for the molybdenum radius is 1.61 Å, giving a predicted M-M bond length of 3.22 Å.

This confusing evidence makes it impossible to assign a bonding radius to the molybdenum atom with any certainty.

Therefore the principal bond lengths observed in the related compounds

(a) $\left[(OC)_3(Et_3P)Mo(PMe_2)_2Mo(PEt_3)(CO)_3\right]$

(b) $\left[(OC)_2(C_5H_5)Mo\cdot PMe_2\cdot H\cdot Mo(C_5H_5)(CO)_2\right]$

and (c) that found in the present work are shown in Table 22 These are compared with the values predicted for the molybdenum radii: 1.56 Å, 1.61 Å

TABLE 22

Observed and predicted bond lengths (Å)

The bonding radii used are[67] : P = 1.1 Å

sp - hybridised C = 0.69 Å

	Observed			Predicted	
				Mo^{I}	Mo^{O}
	(a)	(b)	(c)	r=1.56	r=1.61
Mo-Mo	3.090	3.26	3.057	3.12	3.22
Mo-P (bridging)	2.45	2.43	2.50	2.66	2.71
Mo-C	1.96	1.93	1.99	2.25	2.30

The metal-metal distance observed (3.057Å) is somewhat shorter than that predicted for a metal radius of 1.56 Å, which best fits the observed value, but falls within the range 2.1 - 3.3 Å for known Mo-Mo bonds and therefore indicates a strong interaction between the two atoms. The strength of the interaction is shown by the bond angles within the planar ring comprising the two molybdenum and two phosphorus atoms. The angle at molybdenum is increased from 90°, expected for a perfect dioctahedral structure, to 104.6° and the angle at phosphorus is reduced from the normal tetrahedral angle of 109.47° to 75.36°.

This distortion suggests that this metal-metal interaction which is responsible for the compound being diamagnetic takes place directly between the metal atoms by the sharing of electrons in the d_{xy} orbitals.

If the metal-metal bond is included, the molybdenum coordination is pentagonal bipyramidal. The angles between the ligands in the

equatorial plane, however, are 52.0, 52.7, 84.8, 87.0 and 83.5°, all markedly different from 72°, which is the expected value for a regular pentagonal bipyramid. Clearly the coordination of the molybdenum atom may not be regarded as pentagonal bypiramidal, and the arrangement of the ligands does not resemble the arrangement of the ligands of any of the known heptaco-ordination types. Thus the metal-metal interaction causes distortion but is not sufficiently strong to disrupt the essentially octahedral ligand field round the molybdenum atom. (Fig. 24)

8.2(c) Relationship of Mo-C and C-O bond lengths to bond orders.

Cotton and Wing[64] have derived relationships between the lengths and formal bond orders of Mo-C and C-O bonds in octahedral Mo^0 complexes. Their result is shown in Fig. 25. Their curves are comparable to the curve which is known for C-C[68] bonds, being concave upward and approaching the value of zero bond order asymptotically as the bond length goes to infinity.

Applying their analysis to the present compound yields bond orders of 1.78 for the M-C bonds (average) and 2.35 for the C-O bonds (average).

This is a well known effect of back donation of electrons from the metal atom to the metal-carbon bond

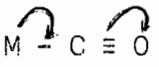

This in turn causes a reduction in the order of the C-O bond. Thus whereas the C-O stretching frequency in carbon monoxide itself is about 2155 cm^{-1}, the corresponding frequencies in terminal metal

Fig. 24 Coplanar atoms in the molecule.

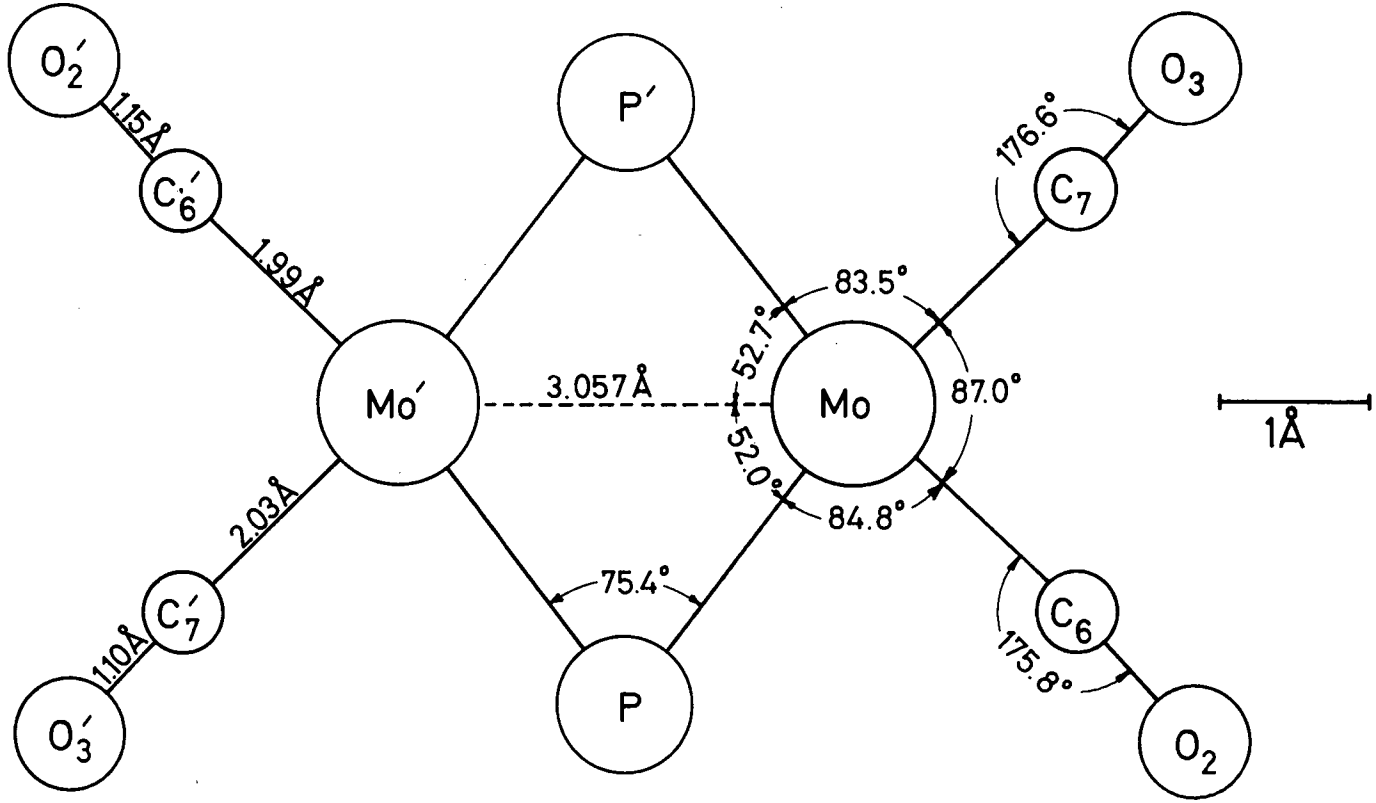

Primed atoms are centro-symmetrically related to unprimed atoms.

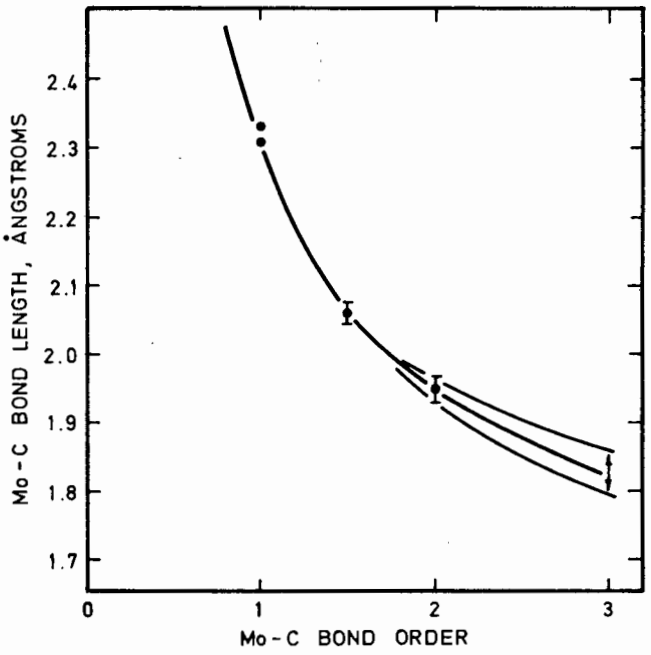
Mo-C BOND LENGTH, ÅNGSTROMS
2.4
2.3
2.2
2.1
2.0
1.9
1.8
1.7
0
1
2
3
Mo-C BOND ORDER

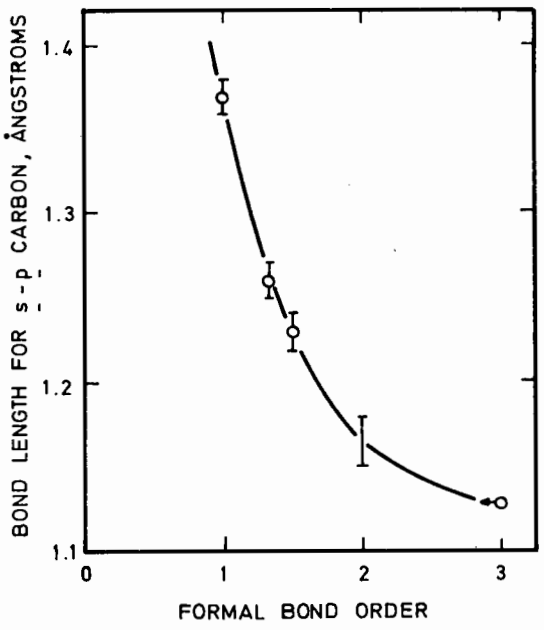
BOND LENGTH FOR s-p CARBON, ÅNGSTROMS
1.4
1.3
1.2
1.1
0
1
2
3
FORMAL BOND ORDER

Fig. 25

carbonyl groups usually lie at lower values, around 2000 cm^{-1}.

It is interesting to note that the orders of the metal-carbon and carbon-oxygen bonds are roughly complementary, and any effect which increases one necessarily decreases the other. This is illustrated[1] by the three species $Ni(CO)_4$, $[Co(CO)_4]^-$ and $[Fe(CO)_4]^{2-}$. These are isoelectronic and isostructural, but with a steadily increasing excess of negative charge. This charge has the effect of increasing the extent of metal-carbon back bonding and thus raise the metal-carbon bond order. At the same time a corresponding decrease in the carbon-oxygen bond order may be expected. The bond orders (N) obtained from spectroscopic data are shown in Table 23.

TABLE 23

	N_{M-C}	N_{C-O}	$\sum N$
$Ni(CO)_4$	1.33	2.64	3.97
$[Co(CO)_4]^-$	1.89	2.14	4.03
$[Fe(CO)_4]^{2-}$	2.16	1.85	4.01

Table 23 indicates the reciprocal nature of the C-O and M-C bond orders, $\sum N$ being approximately four in each case.

For the compound under study $\sum N = 1.78 + 2.35 = 4.13$. This is only an approximate figure however, because, as Cotton and Wing point out, the bond-length vs bond-order curves are inaccurate in the bond-order region 2-3.

8.2(d) The molybdenum-phosphorus bond.

Table 22 shows that the observed Mo - P (bridging) bond in this

compound, as well as in the other two similar compounds listed, is shorter than the predicted bond length by approximately 0.3 Å. This would imply π bonding between the molybdenum and phosphorus atoms. This is explained by the molecular orbital diagram shown in Fig. 26. The left hand side diagram shows the molecular orbitals for octahedrally-coordinated Mo^{o}. The situation indicated is for σ bonding only. For simplicity the orbitals of the coordinated ligands are assumed degenerate. The right hand side diagram describes the situation for σ bonding and metal-ligand π bonding. As before the σ bonding molecular orbitals of the ligands are assumed degenerate. The diagram shows the overlap of unoccupied ligand π bonding orbitals (e.g. the d-orbitals of phosphorus) with the metal atom t_{2g} orbitals .

The right hand side diagram is more realistic because it takes account of π bonding, and both phosphorus and carbon monoxide are known to be strong π bonding ligands. Mais, Owston and Thomson[57] maintain that use of the twelve ligand electrons in σ bond formation and metal-carbon π bonding of the carbonyl groups exhausts the total bonding capacity of the Mo^{o} atom but P also has <u>vacant</u> 3d orbitals which can be involved in Mo-P π bonding as the right hand diagram illustrates. Overlap of these with the non-bonding t_{2g} Mo^{o} atomic orbitals causes their conversion into a set of lower energy bonding πt_{2g} orbitals and a set of higher energy anti-bonding $\pi^{*}t_{2g}$ orbitals. Only the former are occupied and are of lower energy than the non-bonding t_{2g} orbitals, hence stablising the Mo-P bonds and shortening them.

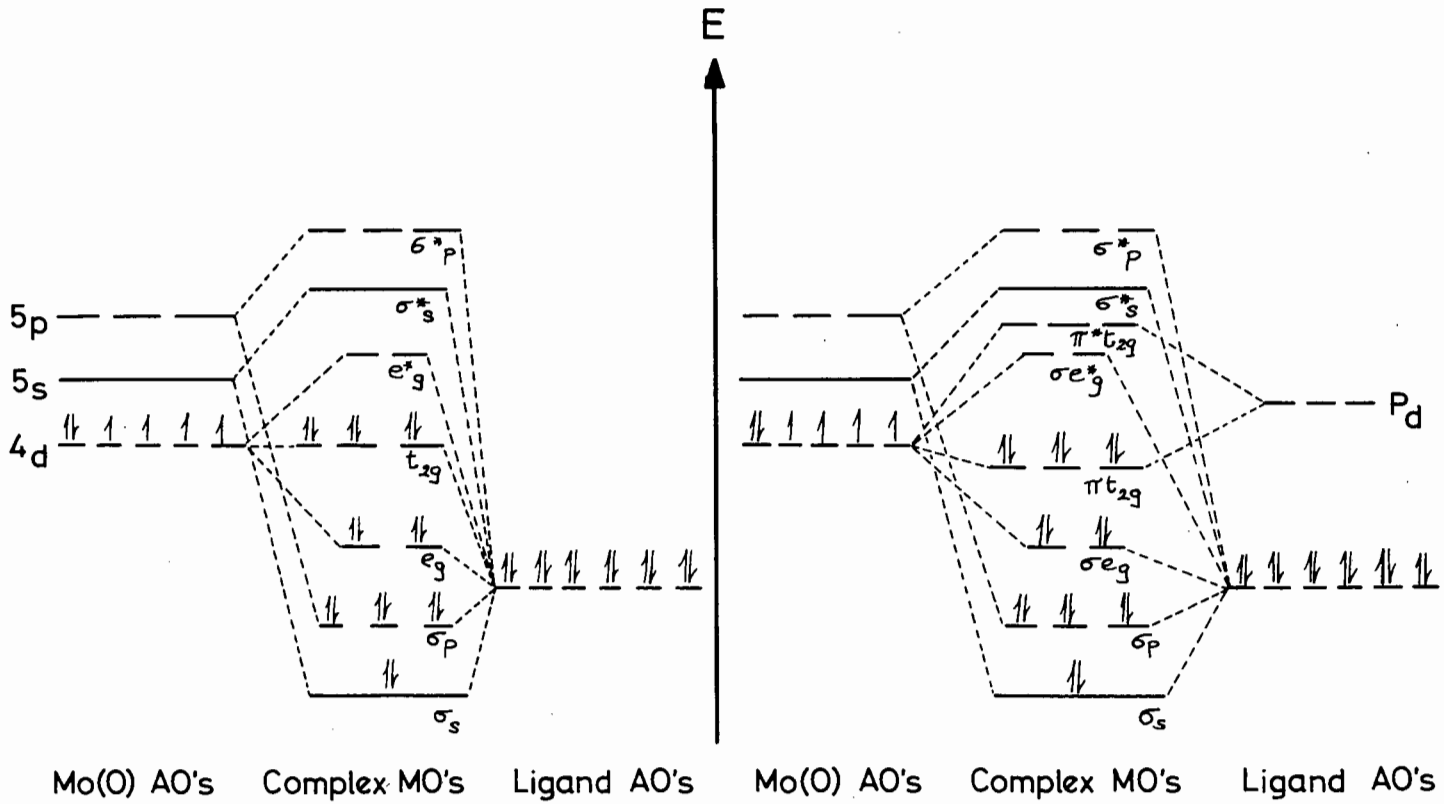
E
5p
5s
4d
σ*p
σ*s
e*g
t2g
eg
σp
σs
Mo(0) AO's
Complex MO's
Ligand AO's
σ*p
σ*s
π*t2g
σe*g
Pd
πt2g
σeg
σp
σs
Mo(0) AO's
Complex MO's
Ligand AO's

Fig. 26

8.3 DISCUSSION OF THE STRUCTURAL RESULTS OF μ-Tetraethyldiphosphine-bis(pentacarbonylmolybdenum).

The structure of the compound is shown in Fig. 23. It consists of two distorted octahedra joined by a diphosphine bridge. The coordination of the phosphorus atom is approximately tetrahedral and the configuration around the phosphorus-phosphorus bond is close to the ethane-like staggered configuration.

The P-P-Mo and Mo-P-C bond-angles (≈ 119° and 118° respectively) are all appreciably larger than the ideal tetrahedral value and the C-P-C and C-P-P bond-angles (≈ 107° and ≈ 95° respectively) are correspondingly smaller, an effect which is commonly observed in phosphine complexes of metals and not yet adequately explained.

The angles round the Mo atoms are all close to 90°, the ideal octahedral value.

8.3 (a) The phosphorus-phosphorus bond.

The P-P bond length found in the compound (2.21 Å) compares favourably with those found in other accurate analyses. (Table 24)

TABLE 24

Phosphorus-phosphorus bond lengths.

Compound	Bond-length (Å)	Ref
P (black)	2.18	69
P_4 gas	2.21 (2)	70
P_2I_4	2.21 (6)	71
P_4S_7	2.35 (1)	72
P_4S_5	2.20 (2)	73
P_4S_3	2.23	74
$P_4I_2S_3$	2.12-2.25	75
P_4Se_3	2.25 (3)	76
$\lvert PSCH_3Ph\rvert_2$	2.21	77
$\left[(OC)_3Ni(PPh_2)_2Ni(CO)_3\right]$	2.277 (4)	67

There are two exceptions to the mean value of ≈ 2.21 Å: P_4S_7, where the bond is seriously strained and atypical and in $\left[(OC)_3Ni(PPh_2)_2Ni(CO)_3\right]$. In the latter compound the bond lengthening is explained by the steric hindrance effects.

In this compound the nearest approach distance of carbon atoms from the ethyl groups attached to the two different phosphorus atoms is 3.36 Å ($C_6 - C_8'$) so there is no possibility of steric hindrance which might cause a lengthening in the P-P bond.

8.3 (b) Relationship of the Mo-C and C-O bond lengths to bond orders.

The Mo-C and C-O bond lengths in $Mo(CO)_6$ are 2.08 Å and 1.15 Å respectively[78]. From the curves relating bond lengths and

bond orders (Section 8.2(c), Fig. 25), the corresponding bond orders are 1.4 and 2.35 respectively.

In the compound under discussion the average Mo-C bond length is 2.06 Å which corresponds to a bond order of 1.8.

Due to the atoms O_4 and O_5 being located in the vicinity of the Fourier ripple peak previously described (Fig. 21) the $C_4 - O_4$ and $C_5 - O_5$ bond lengths are both shorter than normal and are not regarded as typical (Table 19). The other three C-O bond lengths (C_1-O_1 = 1.06 (5), C_2-O_2 = 1.18 (4), C_3-O_3 = 1.09 (3)) are too disparate to take a meaningful average, but they may be regarded as being essentially the same as those in $Mo(CO)_6$. The bonding and bond orders in the two compounds are therefore closely similar.

The principal bond lengths observed in the compound and in $Mo(CO)_6$ are shown in Table 25. These are compared with the values predicted for the Mo radius of 1.61 Å, the latter value being chosen as correct for Mo^0 (Section 8.2(b))

TABLE 25

Observed and predicted bond lengths.

The bonding radii used are[67]: P = 1.1 Å, C = 0.69 Å, Mo = 1.61 Å.

	Observed in $Mo(CO)_6$	in compd.2	Predicted	Difference
Mo - P	-	2.54	2.71	0.17
Mo - C	2.08	2.06	2.30	≈ 0.23 (average)

Cotton[79] has suggested that the replacement of a carbonyl group by a ligand with less double-bonding propensity allows the remaining carbonyl groups to double bond more closely. If the suggestion is correct, and if, as was suggested above the Mo-C and C-O bond orders in the compound are essentially the same as in $Mo(CO)_6$, it follows that the P_2Et_4 ligand in the complex forms double bonds with the Mo atom approximately as readily as a CO group.

This is supported by the data in Table 25, which shows that the observed Mo-P bond length is shorter than the predicted bond length by 0.17 $\mathring{A}$, which could be the result of partial Mo-P π bonding.

The bond shortening of 0.17 $\mathring{A}$, while finite, is not necessarily precise, because, as discussed in Section 8.2(b), there is uncertainty as to the choice of a value for the Mo radius.

The bond shortening in the Mo-C bond can be explained in terms of the well known effect of back donation of electrons from the metal atoms to the Mo-C bond discussed in Section 8.2(c), with the corresponding increase in bond order described above.

9. CONCLUSION

The structures of two compounds, derived from the reaction of tetraethyldiphosphine on molybdenum hexacarbonyl have been elucidated by X-ray diffraction methods.

Compound 1, Di-μ-diethylphosphido-bis-(tetracarbonylmolybdenum) has a planar centrosymmetric molecule corresponding to structure XI, Fig. 4. The environment of each metal atom is approximately octahedral and there is a metal-metal bond 3.057 Å long.

While Thomson[15] suggested that the photochemical substitution of a single CO group by PPh_3 indicated the probable existence of a structurally unique CO group, the present work has shown that the symmetric structure does not imply its existence. Nevertheless it is to be realised that even for the structure elucidated, the two pairs of CO groups (C_6O_2, C_7O_3 in the "horizontal" plane of the molecule and C_5O_1, C_8O_4 in the "perpendicular" plane - see Fig. 16) are in chemically different environments, the former being *trans*- to the PEt_2 bridging phosphorus atoms and the latter being *cis*- to these atoms. Therefore it is not surprising that the reaction leads to the formation of a simple monosubstitution product rather than a mixture of the two theoretically possible geometric isomers. On the other hand the structure elucidated does not explain why further substitution by excess PPh_3 does not occur except possibly for statistical and steric reasons.

Compound 2, μ-Tetraethyldiphosphine-bis-(pentacarbonylmolybdenum) has a molecule consisting of two slightly distorted octahedra joined by

a diphosphine bridge. The diphosphine link between the two molybdenum atoms has a catenary form. There is no interaction between the two Mo atoms.

The bond angles about the P atoms do not conform to those theoretically expected for complete sp^3 hybridisation of phosphorus but have values greater or less than $109^{\circ}28'$. The angles indicate a divergence from the tetrahedral conformation which implies a measure of s and p character in certain of the P-X bonds (X = Mo,C,P) such as has been found for simple molecules, e.g. NH_3, PH_3 etc which may be explained in either of the following ways:

(1) Formally complete sp^3 hybridisation (i.e. a nominal angle $H\text{-}\hat{X}\text{-}H = 109^{\circ}28'$ (X = N,P,As,Sb); the angle being decreased by withdrawal of electron pairs in the X-H bonds by H, thus polarising the electron density in the X-H bonds towards H. This approach is supported by the fact that the bond angle $H\text{-}\hat{X}\text{-}H$ decreases as X is successively N,P,As,Sb; i.e. in order of decreasing electronegativity.

(2) No hybridisation (i.e. a nominal angle $H\text{-}\hat{X}\text{-}H = 90^{\circ}$ (X = N,P,As,Sb); the angle being increased by replusion between the positive hydrogen dipoles, the repulsion decreasing in the order X = N>P>As>Sb, i.e. in the order of decreasing dipole moment.

In both compounds the relationship between the Mo - C and C - O bond lengths and bond orders is discussed, and there is evidence of bond shortening of the Mo - P bonds, which is attributed to Π bonding between the molybdenum and phosphorus atoms.

10. BIBLIOGRAPHY.

1. E.W. Abel, *Quart. Rev.*, 17, 133 (1963) and references therein.
2. P. Chini, *Inorg. Chim. Acta Rev.*, 2, 31 (1968).
3. C.H. Wei and L.F. Dahl, *Inorg. Chem.*, 4, 1 (1965).
4. W. Hieber and J. Gruber, *Z.anorg. allgem. Chem.*, 296, 91 (1958).
5. C.H. Wei and L.F. Dahl, *Inorg. Chem.*, 4, 493 (1965).
6. D.A. Brown, *Inorg. Chim. Acta Rev.*, 1, 35 (1967).
7. R.G. Hayter, *J.Am.Chem. Soc.*, 84, 3046 (1962).
8. J. Chatt and D.A. Thornton, *J.Chem.Soc.*, 1005 (1964).
9. W. Hieber and P. Spacu, *Z. Anorg. Chem.*, 233, 353 (1937).
10. R.F. Lambert, *Chem. and Ind.*, 830 (1961).
11. J. Chatt and F.A. Hart, *J. Chem. Soc.*, 1378 (1960).
12. F. Zingales and F. Canziani, *Gazzetta*, 92, 343 (1962).
13. A. Ferrari, A. Braibanti and G. Bigliardi, *Acta. Cryst.*, 16, 498 (1963).
14. J. Chatt and D.T. Thomson, *J. Chem. Soc.*, 2713 (1964).
15. D.T. Thomson, *J. Organometal Chem.*, 4, 74-82 (1965).
16. R.G. Hayter, *Inorg. Chem.*, 3, 711 (1964).
17. L.F. Dahl and C.H. Wei, *Inorg. Chem.*, 2, 328 (1963).
18. H.L. Nigam, R.S. Nyholm and M.H.B. Stiddard, *J. Chem. Soc.*, 1806 (1960).
19. J. Chatt and H.L. Watson, *J. Chem. Soc.*, 4980 (1961).
20. R. Poilblanc and M. Bigorgne, *Compt. Rend.*, 250, 1064 (1960).
21. J. Chatt and D.T. Thomson, *J. Chem. Soc.*, 2713 (1964).
22. L.F. Dahl, C. Martell and D.L. Wampler, *J. Amer. Soc.*, 83, 1761 (1961).
23. G. Brauer, *Handbook of Preparative Inorganic Chemistry, Vol. 1* p.533 (Academic Press, 1963-5).

24. G.H. Stout and L.H. Jensen, *X-ray Structure Determination*, p.37 (Macmillan, 1968).

25. M.J. Buerger, *Crystal Structure Analysis*, p.27-29, (John Wiley and Sons, 1960).

26. *ibid* p.162.

27. M.J. Buerger, *X-ray Crystallography*, p.233, (John Wiley and Sons, 1942).

28. M.J. Buerger, *Crystal Structure Analysis*, p.175, (John Wiley and Sons, 1960).

29. G.H. Stout and L.H. Jensen, *X-ray Structure Determination*, p.449. (Macmillan, 1968).

30. *Int. Tables for X-ray Crystallography*, 2, 61 (1959).

31. *ibid* 2, 43, (1959)

32. M.J. Buerger, *X-ray Crystallography*, p.97, (John Wiley and Sons,1942).

33. *ibid* p.411

34. *ibid* p.372

35. *ibid* p.373

36. W.A. Wooster, *J. Sci. Instr.*, 41, 130 (1964).

37. A. Bairsto, *ibid*, 25, 215 (1948).

38. C.W. Bunn, *Chemical Crystallography*, p.186, (Oxford, 1961).

39. O. Weisz and W.F. Cole, *J. Sci. Instr.*, 25, 213 (1948).

40. C.W. Bunn, *Chemical Crystallography*, p.321, (Oxford, 1961).

41. E.R. Howells, D.C. Phillips and D. Rogers, *Acta Cryst.*, 3; 210 (1950).

42. M.J. Buerger, *X-ray Crystallography*, p.178, (John Wiley and Sons,1942).

43. W.L. Bond, *Rev. Sci. Instr.*, 22, 344 (1951).

44. *Int. Tables for X-ray Crystallography*, 3, 175-192 (1962).

45. M.J. Buerger, *Crystal Structure Analysis*, p. 87-111 (John Wiley and Sons, 1960).

46. *Int. Tables for X-ray Crystallography*, 1, 101 (1962).

47. M.J. Buerger, *Vector Space*, p.127, (John Wiley and Sons, 1959).

48. *Int. Tables for X-ray Crystallography*, 1, 89 (1962).

49. M.H. Linck, *Ph.D. thesis, University of Cape Town* (as yet unpublished).

50. *Int. Tables for X-ray Crystallography*, 3, 213 (1962).

51. J.D.H. Donnay and W. Nowacki, *Crystal Data, Geological Society of America*, memoir 60, New York (1954).

52. *Int. Tables for X-ray Crystallography*, 1, 7 (1962).

53. C.W. Bunn, *Chemical Crystallography*, p.261 (Oxford, 1961).

54. *Int. Tables for X-ray Crystallography*, 1, 30, (1962).

55. M.J. Buerger, *Vector Space*, p.106 (John Wiley and Sons, 1959).

56. *Int. Tables for X-ray Crystallography*, 1, 150, (1962).

57. P.H. B. Mais, P.G. Owston and D.T. Thomson, *J. Chem.Soc.*, 1735 (1967).

58. R.J. Doedens and L.F. Dahl, *J. Amer. Chem. Soc.*, 87, 2576 (1965).

59. L. Pauling, *The Nature of the Chemical Bond*, p. 436-442 (Cornell, 1960).

60. F.A. Cotton and G. Wilkinson, *Advanced Inorganic Chemistry*, p.652-658 (John Wiley and Sons, 1966).

61. J.P. Fackler Jr. and D. Coucouvanis, *Inorg. Chem.*, 7, 181 (1968).

62. J.C. Sheldon, *Aust. J. Chem.*, 17, 1191 (1964).

63. J. Lewis and R.S. Nyholm, *Sci. Progr.*, 52, 557 (1964).

64. F.A. Cotton and R.M. Wing, *Inorg. Chem.*, 4, 315 (1965).

65. M.J. Bennett and R. Mason, *Nature*, 205, 760 (1965).

66. D. Lawton and R. Mason, *J. Amer. Chem. Soc.*, 87, 921 (1965).

67. R.H.B. Mais, P.G. Owston, D.T. Thomson and Eliza M. Wood, *J.Chem.Soc.*, 1744 (1967).

68. L. Pauling, *The Nature of the Chemical Bond*, p. 236, (Cornell, 1960).

69. R. Hultgren, N.S. Gingrich and B.E. Warren, *J. Chem. Phys.*, 3, 351 (1935).

70. L.R. Maxwell, S.B. Hendricks and V.M. Mosley, *J. Phys. Chem.*, 3, 699 (1935).

71. Y.C. Leung and J. Waser, *J. Phys. Chem.*, 60, 539 (1956).

72. A. Vos and E.H. Wiebenga, *Acta Cryst.*, 9, 92 (1956).

73. S. van Houten and E.H. Wiebenga, *Acta Cryst.*, 10, 156, (1957).

74. Y.C. Leung, J. Waser, S. van Houten, A. Vos, G.A. Wiegers and E.H. Wiebenga, *Acta Cryst.*, 10, 574 (1957).

75. D.A. Wright and B.R. Penfold, *Acta Cryst.*, 12, 455 (1945).

76. E. Keuler and A. Vos, *Acta Cryst.*, 12, 323 (1959).

77. P.J. Wheatley, *J. Chem. Soc.*, 523 (1960).

78. L.O. Brockway, R.V.G. Ewens and M.W. Lister, *Trans Faraday Soc.*, 34, 1350 (1938).

79. F.A. Cotton, *Inorg. Chem.*, 3, 702, (1964).

APPENDIX I

h	k	ℓ	F_o	F_c	h	k	ℓ	F_o	F_c	h	k	ℓ	F_o	F_c
0	0	-14	47.9	-47.3	6	0	16	101.3	88.4	1	1	-2	144.2	146.5
0	0	-2	358.8	439.9	6	0	20	63.6	-48.4	1	1	-4	92.6	94.4
0	0	-4	82.6	79.2	6	0	-2	37.1	50.9	1	1	5	123.1	-114.2
0	0	-6	90.8	72.5	6	0	-4	52.5	-39.4	1	1	-5	156.7	-133.5
0	0	-8	84.0	82.4	6	0	-10	95.4	-78.9	1	1	-6	127.4	122.8
0	0	-10	97.1	80.7	8	0	0	53.9	73.9	1	1	-7	35.8	35.0
0	0	-12	31.8	37.5	8	0	-2	172.6	165.2	1	1	-8	38.4	41.2
0	0	-16	97.6	-112.5	8	0	4	111.8	110.3	1	1	9	177.0	-171.0
0	0	-18	111.8	-103.6	8	0	-4	198.4	209.2	1	1	-9	37.9	32.4
0	0	-20	94.2	-82.5	8	0	-6	168.0	183.0	1	1	-11	48.8	43.2
2	0	0	144.5	-99.0	8	0	-8	136.8	119.7	1	1	-12	39.4	31.3
2	0	2	120.3	-125.4	8	0	10	64.1	-68.5	1	1	-14	46.8	39.9
2	0	-2	23.2	-10.9	8	0	-10	93.9	80.6	1	1	-15	93.1	105.4
2	0	4	80.6	-64.6	8	0	12	135.7	-139.7	1	1	-17	101.7	119.3
2	0	-4	87.7	91.1	8	0	14	130.0	-146.0	1	1	-19	88.5	103.4
2	0	-6	235.0	250.7	8	0	16	122.3	-126.5	3	1	1	126.9	-125.3
2	0	8	264.6	-263.5	8	0	18	87.1	-88.7	3	1	-1	67.6	-74.1
2	0	-8	281.3	301.5	8	0	20	57.3	-69.8	3	1	2	83.1	-74.4
2	0	10	314.0	-322.0	10	0	0	101.3	-89.8	3	1	-2	90.8	-93.8
2	0	-10	139.4	137.9	10	0	-2	137.9	-114.2	3	1	-3	121.6	-124.9
2	0	12	233.7	151.4	10	0	4	183.9	-180.6	3	1	4	168.4	-137.1
2	0	14	142.5	-138.5	10	0	-4	96.5	-93.1	3	1	-5	173.5	-183.6
2	0	-14	89.1	110.2	10	0	6	187.3	-194.8	3	1	6	92.8	-94.5
2	0	16	68.7	-70.3	10	0	-6	49.1	-61.5	3	1	-6	23.4	-32.4
2	0	-18	101.9	92.7	10	0	8	161.2	-160.7	3	1	-7	256.1	-275.4
4	0	0	177.1	-174.9	10	0	10	61.3	-61.2	3	1	9	168.4	155.1
4	0	2	523.2	-501.8	10	0	-12	63.0	65.6	3	1	-9	231.0	-251.6
4	0	-2	43.7	36.6	12	0	0	106.1	-79.5	3	1	10	69.9	-58.4
4	0	4	374.2	-331.3	12	0	-2	83.7	-81.8	3	1	-10	53.6	50.1
4	0	-4	174.6	-161.8	12	0	-4	87.7	-82.6	3	1	11	204.7	202.4
4	0	-6	182.5	-177.3	12	0	6	109.8	106.4	3	1	-11	144.2	-151.6
4	0	-8	185.9	-188.6	12	0	-6	77.2	-67.8	3	1	13	137.6	146.9
4	0	10	116.6	106.5	12	0	-8	71.8	-92.6	3	1	-13	99.7	-98.9
4	0	-10	108.4	-110.4	12	0	10	97.3	91.5	3	1	-14	53.6	33.1
4	0	12	119.8	86.5	12	0	-10	82.0	-108.4	3	1	15	103.7	123.6
4	0	16	98.2	90.2	12	0	12	87.4	84.9	3	1	-15	37.9	-43.0
4	0	18	106.1	107.6	12	0	14	115.5	107.3	3	1	17	74.0	85.0
4	0	20	105.9	116.5	12	0	16	93.4	111.4	3	1	-17	38.9	-51.4
6	0	0	101.9	111.9	14	0	0	110.4	141.5	3	1	19	68.6	80.3
6	0	2	299.8	270.8	14	0	2	103.3	117.5	3	1	-19	34.0	-31.4
6	0	4	345.2	319.9	14	0	-2	111.0	119.9	3	1	21	70.4	77.2
6	0	6	203.8	189.9	14	0	4	107.0	82.1	5	1	0	16.0	18.1
6	0	8	113.0	89.7	14	0	-4	72.1	66.7	5	1	1	261.5	280.6
6	0	10	106.4	114.6	14	0	6	105.9	80.9	5	1	-1	166.6	171.0
6	0	12	192.7	197.9	14	0	8	77.7	79.2	5	1	-2	19.0	-29.9
6	0	-12	126.3	-122.5	14	0	10	77.7	69.1	5	1	3	374.7	376.6
6	0	14	137.7	135.1	16	0	8	87.4	-96.8	5	1	-3	131.7	136.2
6	0	-14	100.5	-109.1	16	0	10	89.1	-112.2	5	1	-4	56.9	-57.5

h	k	ℓ	F_o	F_c	h	k	ℓ	F_o	F_c	h	k	ℓ	F_o	F_c
5	1	5	229.9	227.0	9	1	-8	53.6	60.6	9	1	14	24.6	-23.6
5	1	-5	110.4	117.3	9	1	9	53.1	-61.8	9	1	11	44.2	29.0
5	1	6	83.1	96.0	9	1	10	77.0	-84.0	9	1	2	45.2	-58.8
5	1	-6	38.6	-29.3	9	1	13	87.7	75.9	9	1	0	19.0	-32.9
5	1	7	148.0	136.2	9	1	15	98.4	89.6	7	1	16	48.8	-45.7
5	1	-7	71.2	74.7	9	1	19	66.6	69.9	7	1	-13	104.3	97.4
5	1	8	98.4	87.3	11	1	2	69.7	-52.7	7	1	-9	106.0	104.6
5	1	-8	61.3	-48.8	1	1	3	246.2	-220.7	7	1	-6	34.0	31.4
5	1	9	47.8	52.0	11	1	3	85.2	80.0	7	1	-5	188.5	165.5
5	1	-9	55.9	50.2	11	1	5	124.6	138.6	7	1	4	74.0	53.7
5	1	-10	82.6	-76.9	11	1	7	171.9	175.0	5	1	21	74.0	-81.8
5	1	11	37.9	23.3	11	1	-7	59.2	-45.5	5	1	-15	109.6	-98.4
5	1	-11	60.5	-50.4	11	1	8	37.1	-27.6	5	1	13	47.0	36.1
5	1	14	42.2	44.8	11	1	9	159.0	143.2	5	1	12	16.0	17.5
5	1	16	59.2	57.6	11	1	-9	86.7	-91.0	5	1	10	21.6	16.4
5	1	-17	67.67	-77.1	11	1	11	91.0	101.5	5	1	2	60.5	-53.7
5	1	18	59.5	67.6	11	1	-11	80.3	-91.4	3	1	8	90.0	-78.6
5	1	19	92.8	-79.6	11	1	13	91.5	83.0	3	1	7	106.3	78.9
5	1	20	37.6	30.8	11	1	15	67.6	84.3	3	1	5	87.5	67.7
7	1	0	103.0	105.8	11	1	17	66.1	69.1	3	1	-4	75.8	-60.0
7	1	-1	49.6	48.2	13	1	1	91.8	101.0	3	1	3	40.1	45.1
7	1	2	70.9	52.1	13	1	2	43.2	49.0	1	1	-16	33.5	38.1
7	1	-2	71.9	65.4	13	1	3	73.2	56.6	1	1	-13	89.5	80.1
7	1	3	140.9	-116.4	13	1	-3	77.0	97.8	1	1	-10	21.3	21.1
7	1	-3	101.5	112.4	13	1	4	79.3	70.5	1	1	-3	49.3	-59.6
7	1	5	156.9	-138.2	13	1	-5	70.2	74.5	1	1	-1	312.9	-288.5
7	1	6	113.2	97.1	13	1	6	39.4	41.2	13	1	-1	127.2	118.8
7	1	7	181.3	-157.7	13	1	-7	61.8	51.0	11	1	12	23.6	32.5
7	1	-7	130.7	128.1	13	1	-9	47.0	54.6	11	1	-6	31.2	-37.9
7	1	9	96.9	-94.0	13	1	12	58.5	40.7	11	1	6	23.6	-35.7
7	1	11	150.1	-156.1	13	1	15	77.8	-85.6	11	1	4	20.3	-32.0
7	1	-11	101.2	99.7	15	1	1	66.4	-75.7	9	1	12	48.3	-39.1
7	1	13	140.9	-164.1	15	1	-1	55.2	-67.1	0	2	0	229.3	-207.0
7	1	15	116.0	-140.1	15	1	-2	54.6	39.0	0	2	1	69.3	-73.6
7	1	-15	79.8	87.7	15	1	3	64.1	-65.4	0	2	2	218.7	-237.1
7	1	17	79.1	-91.2	15	1	-3	49.3	-42.9	0	2	3	66.9	-83.9
7	1	18	61.0	-41.9	15	1	-4	59.2	42.6	0	2	4	329.8	-340.0
7	1	1	18.0	-24.6	15	1	5	77.8	-69.9	0	2	5	193.1	-162.3
9	1	1	117.2	-111.3	15	1	9	84.2	-98.8	0	2	8	74.1	-81.3
9	1	-1	154.8	-171.4	15	1	11	78.8	-90.8	0	2	9	40.7	-34.0
9	1	3	161.2	-160.0	11	1	-2	30.7	-24.2	0	2	10	54.2	-54.6
9	1	-3	157.9	162.2	15	1	13	35.1	-47.9	0	2	11	112.7	-116.2
9	1	5	161.8	-164.7	15	1	7	101.0	-95.3	0	2	12	33.8	23.9
9	1	-5	140.1	-159.7	13	1	14	23.9	30.3	0	2	13	133.6	-126.4
9	1	-6	60.8	60.7	13	1	13	42.4	-45.0	0	2	14	51.0	45.9
9	1	7	130.5	-112.5	11	1	-8	31.5	-36.6	0	2	15	103.3	-110.3
9	1	-7	98.7	-91.3	11	1	-4	31.8	-41.5	0	2	16	76.7	65.4
9	1	8	61.5	-66.9	9	1	17	61.3	75.8	0	2	17	50.1	-64.0

h	k	ℓ	F_o	F_c	h	k	ℓ	F_o	F_c	h	k	ℓ	F_o	F_c
0	2	18	84.4	79.0	4	2	15	74.1	53.4	8	2	-10	78.2	-74.8
0	2	20	62.1	67.5	4	2	-15	75.5	54.7	8	2	11	102.1	-100.2
2	2	0	28.3	25.7	4	2	16	78.4	-88.4	8	2	12	80.8	79.1
2	2	1	58.7	-47.6	4	2	17	39.8	57.6	8	2	-12	58.5	-46.6
2	2	-1	170.3	-191.5	4	2	18	63.3	-75.7	8	2	14	87.0	94.1
2	2	-2	167.2	-172.5	4	2	19	52.5	44.4	8	2	-15	54.4	44.9
2	2	3	172.9	-157.0	4	2	20	69.8	-84.7	8	2	16	86.1	99.7
2	2	-3	230.5	-266.8	6	2	0	49.6	-30.9	8	2	18	62.3	76.8
2	2	4	208.9	198.8	6	2	1	142.0	146.3	8	2	20	61.1	56.8
2	2	-4	191.9	-216.0	6	2	-1	170.0	184.0	10	2	0	84.9	82.8
2	2	-5	162.8	-166.2	6	2	2	136.5	-148.4	10	2	-1	31.9	-24.0
2	2	6	226.7	220.5	6	2	3	53.2	52.2	10	2	2	86.6	84.1
2	2	-6	91.6	-91.1	6	2	-3	123.7	128.0	10	2	-2	99.5	88.6
2	2	7	99.7	-81.8	6	2	4	154.7	-156.5	10	2	3	57.3	-51.1
2	2	-7	121.6	-116.0	6	2	-4	40.3	-32.4	10	2	4	102.4	121.9
2	2	8	148.4	154.9	6	2	-5	59.7	60.2	10	2	-4	59.2	57.2
2	2	-10	125.4	-127.8	6	2	6	184.7	-170.1	10	2	5	22.0	-22.4
2	2	12	150.4	160.5	6	2	-7	71.9	63.1	10	2	-5	88.5	-84.5
2	2	-12	100.0	-102.7	6	2	8	188.8	-190.3	10	2	6	114.4	109.1
2	2	13	102.6	94.0	6	2	-8	50.8	28.4	10	2	8	104.1	96.4
2	2	14	110.3	97.8	6	2	10	119.2	-116.3	10	2	9	98.3	97.4
2	2	-14	85.4	-77.9	6	2	-10	55.8	37.7	10	2	-9	89.9	-84.7
2	2	15	89.0	81.9	6	2	-11	68.8	83.5	10	2	-10	56.6	-36.7
2	2	16	69.8	55.7	6	2	12	124.2	-106.5	10	2	11	120.9	110.1
2	2	-16	93.0	-84.8	6	2	-12	87.8	79.5	10	2	-11	47.9	-55.2
2	2	17	58.7	54.4	6	2	13	69.0	-43.1	10	2	12	41.0	39.5
2	2	18	40.0	34.1	6	2	-13	65.4	56.2	10	2	-12	59.9	-55.6
2	2	-18	83.0	-68.7	6	2	14	70.7	-80.2	10	2	13	82.7	67.4
2	2	-19	68.8	50.0	6	2	-14	95.9	91.8	10	2	17	50.6	50.2
2	2	10	149.4	144.8	6	2	15	78.6	-80.3	10	2	19	64.2	62.0
4	2	0	176.0	193.5	6	2	16	44.8	-52.3	12	2	0	53.9	43.5
4	2	2	43.9	37.9	6	2	-16	66.4	84.5	12	2	1	94.7	109.3
4	2	-2	183.5	194.7	6	2	17	90.2	-104.0	12	2	-1	75.3	44.5
4	2	4	89.2	72.8	6	2	-17	47.0	-37.3	12	2	-2	68.6	54.5
4	2	-4	113.2	137.2	8	2	0	119.9	-123.8	12	2	3	124.2	129.1
4	2	5	199.8	202.4	8	2	1	175.3	-159.0	12	2	-4	60.9	69.4
4	2	6	130.5	121.4	8	2	-1	113.9	-126.9	12	2	5	94.7	85.4
4	2	-6	113.4	115.6	8	2	2	65.2	-67.0	12	2	6	85.4	-74.4
4	2	7	225.0	213.5	8	2	-2	101.9	-110.7	12	2	-6	87.0	68.1
4	2	8	69.0	59.6	8	2	-3	65.0	-69.9	12	2	7	53.0	46.7
4	2	-8	137.4	126.4	8	2	-4	132.1	-139.0	12	2	8	91.6	-97.7
4	2	9	152.3	137.3	8	2	5	61.1	-68.0	12	2	-8	64.7	71.5
4	2	-9	145.6	-150.1	8	2	6	65.4	46.4	12	2	10	102.6	-83.7
4	2	11	60.9	56.8	8	2	-6	133.6	-133.5	12	2	-10	57.5	63.4
4	2	-11	136.0	-142.0	8	2	7	109.3	-114.8	12	2	12	86.3	-67.9
4	2	12	43.9	-53.0	8	2	-8	90.9	-97.0	12	2	14	85.1	-81.9
4	2	13	69.5	55.3	8	2	9	136.2	-140.5	12	2	16	73.8	-81.3
4	2	14	97.1	-87.9	8	2	-9	58.0	53.6	14	2	0	91.1	-89.1

h	k	ℓ	F_o	F_c	h	k	ℓ	F_o	F_c	h	k	ℓ	F_o	F_c
14	2	2	76.5	-90.8	8	2	-14	27.3	-31.0	3	3	-4	149.1	135.4
14	2	-2	85.1	-81.0	8	2	13	26.8	-44.3	3	3	5	60.0	-51.0
14	2	-3	67.6	62.8	8	2	-7	100.9	82.3	3	3	-5	135.8	134.8
14	2	4	96.1	-77.5	8	2	3	38.8	-51.8	3	3	6	311.0	303.4
14	2	-4	64.5	-66.3	6	2	18	4.7	-4.7	3	3	-6	85.8	79.6
14	2	-5	62.8	65.1	6	2	-9	82.2	75.7	3	3	7	126.5	-121.9
14	2	6	86.8	-72.5	6	2	9	35.0	-56.4	3	3	-7	103.6	97.1
14	2	-6	50.3	-36.2	6	2	7	11.7	-21.0	3	3	8	207.5	195.3
14	2	-7	41.9	41.2	6	2	5	22.5	42.6	3	3	-8	45.9	-44.4
14	2	8	60.2	-57.4	6	6	-2	20.8	-20.2	3	3	-9	101.8	98.3
14	2	13	80.1	-91.5	4	2	-17	27.1	-30.4	3	3	10	96.4	91.5
14	2	15	64.2	-65.6	4	2	-7	17.2	-24.6	3	3	-10	107.9	-119.7
16	2	-1	35.9	-38.4	4	2	1	16.7	21.1	3	3	-12	56.6	-58.5
16	2	3	61.4	-42.8	1	3	0	43.8	-36.1	3	3	13	72.3	-62.8
16	2	5	58.7	62.7	1	3	-1	141.9	128.7	3	3	-13	80.0	81.2
16	2	6	68.3	49.8	1	3	2	60.8	-53.3	3	3	-14	88.7	-55.0
16	2	7	48.4	-48.8	1	3	-2	299.8	-340.5	3	3	15	76.8	-71.1
16	2	8	52.7	64.0	1	3	-3	83.1	77.3	3	3	-15	61.9	54.5
16	2	9	32.6	-29.6	1	3	4	80.5	-73.9	3	3	-16	56.0	-53.5
16	2	10	63.0	78.2	1	3	-4	294.7	-316.4	3	3	17	65.3	-64.0
4	2	-13	94.0	-86.4	1	3	5	171.7	145.0	3	3	-18	73.6	-71.7
4	2	-10	42.9	54.1	1	3	-5	37.7	28.9	3	3	19	76.5	-52.7
4	2	10	21.8	-35.6	1	3	6	42.2	36.7	5	3	0	149.6	142.2
4	2	3	86.8	54.1	1	3	-6	206.2	-222.7	5	3	1	153.3	-141.2
4	2	-1	26.8	35.9	1	3	7	114.8	104.1	5	3	-1	158.1	-165.0
2	2	20	16.0	23.8	1	3	-8	102.8	-95.0	5	3	3	90.9	-76.6
2	2	-15	25.9	-24.1	1	3	9	72.8	84.1	5	3	-3	99.4	-94.5
2	3	9	35.7	-56.2	1	3	-9	45.1	39.3	5	3	4	78.9	-76.1
2	2	5	148.0	-112.6	1	3	10	80.5	81.6	5	3	-4	32.1	42.6
2	2	2	26.1	34.0	1	3	-10	133.1	-115.6	5	3	5	71.2	-72.3
0	2	7	75.0	-55.4	1	3	11	49.9	41.6	5	3	-5	66.7	-78.8
0	2	6	185.4	-149.1	1	3	-11	46.2	-38.5	5	3	6	132.1	-117.9
16	2	1	35.0	-31.9	1	3	12	145.1	147.8	5	3	-6	85.5	89.8
14	2	11	73.8	-66.8	1	3	-13	63.5	-59.2	5	3	8	214.2	-196.8
14	2	10	28.5	-32.9	1	3	14	126.7	139.6	5	3	-8	125.7	134.8
14	2	5	20.1	-34.1	1	3	-14	82.1	-86.3	5	3	9	72.5	-68.6
14	2	3	36.7	-48.2	1	3	-15	68.3	-53.4	5	3	10	150.7	-135.3
12	2	-9	24.7	30.6	1	3	16	110.5	108.5	5	3	-10	144.8	161.5
12	2	9	34.5	40.0	1	3	-16	83.9	-59.5	5	3	12	82.4	-84.4
12	2	-7	17.7	27.5	1	3	-17	55.8	-53.1	5	3	-12	127.0	127.1
12	2	4	9.5	-26.6	1	3	18	91.9	82.5	5	3	-14	98.0	87.7
12	2	-3	18.4	15.5	1	3	-19	55.2	-43.0	5	3	-17	59.8	46.4
10	2	15	31.9	43.9	1	3	20	55.0	51.6	5	3	18	111.9	-103.1
10	2	10	75.3	68.4	3	3	0	108.4	115.0	7	3	0	240.0	-262.2
10	2	-7	127.8	-117.0	3	3	1	48.6	-54.6	7	3	-1	60.0	-69.2
10	2	-6	31.9	50.0	3	3	-2	244.8	252.2	7	3	2	198.8	-202.0
10	2	-3	41.7	-48.1	3	3	-3	181.5	180.4	7	3	-2	199.0	-199.2
10	2	1	55.6	-44.8	3	3	4	179.9	171.8	7	3	-3	35.3	-49.5

h	k	ℓ	F_o	F_c	h	k	ℓ	F_o	F_c	h	k	ℓ	F_o	F_c
7	3	4	38.2	-56.2	11	3	15	53.6	-53.5	2	4	9	60.5	39.1
7	3	-4	102.0	-121.9	11	3	16	60.0	-46.3	2	4	-9	65.2	46.3
7	3	5	49.9	48.9	13	3	0	65.9	-66.0	2	4	-10	53.1	36.3
7	3	-5	39.3	-38.6	13	3	2	111.6	-116.3	2	4	11	54.9	-32.5
7	3	6	83.4	-79.1	13	3	4	106.8	-105.0	2	4	-11	72.8	42.1
7	3	7	123.0	100.6	13	3	-5	63.2	-55.6	2	4	-12	81.6	61.5
7	3	8	83.1	-89.0	13	3	6	79.4	-71.9	2	4	13	63.4	-72.0
7	3	9	115.0	114.1	13	3	8	65.1	-70.6	2	4	-14	61.0	43.7
7	3	-9	77.0	-77.0	13	3	10	90.1	-79.2	2	4	15	70.3	-82.9
7	3	10	103.6	-102.2	13	3	12	73.3	-100.0	2	4	16	76.2	-46.2
7	3	-10	53.6	-41.5	13	3	14	78.4	-88.4	2	4	-17	53.9	-43.6
7	3	11	99.9	97.9	15	3	0	66.1	-48.6	2	4	19	68.6	-80.4
7	3	-11	75.4	-67.1	15	3	2	51.0	-30.7	4	4	0	66.1	-49.4
7	3	15	45.9	41.1	15	3	-2	69.1	-69.6	4	4	1	84.0	-97.2
7	3	16	68.3	62.2	15	3	3	73.3	46.7	4	4	2	31.1	-23.8
7	3	18	85.3	86.9	15	3	-4	66.4	-86.5	4	4	-2	94.1	-86.0
7	3	20	65.1	69.6	15	3	5	72.0	55.4	4	4	3	150.7	-128.5
9	3	0	81.3	72.2	15	3	12	87.7	78.7	4	4	4	33.8	-19.8
9	3	1	119.8	123.6	0	4	1	84.3	78.3	4	4	5	189.9	-184.9
9	3	-1	100.2	100.8	0	4	2	100.2	86.4	4	4	-6	55.6	44.0
9	3	3	108.1	105.4	0	4	3	67.4	56.5	4	4	7	222.5	-236.0
9	3	-4	46.7	-41.1	0	4	4	118.1	104.3	4	4	-7	94.1	83.3
9	3	-5	52.6	61.1	0	4	5	158.6	175.5	4	4	-8	48.7	37.0
9	3	6	76.5	73.7	0	4	6	87.0	82.7	4	4	9	243.4	-255.9
9	3	-6	112.7	-116.8	0	4	7	172.0	191.8	4	4	-9	109.0	118.3
9	3	-7	66.7	44.2	0	4	8	40.2	25.3	4	4	10	69.6	-42.6
9	3	8	132.1	130.2	0	4	9	137.5	138.0	4	4	11	143.4	-142.3
9	3	-9	50.2	32.9	0	4	10	52.4	-33.4	4	4	13	68.3	-88.3
9	3	10	186.0	188.2	0	4	11	112.5	123.6	4	4	-13	136.7	131.7
9	3	-10	99.4	-91.6	0	4	12	47.6	-20.8	4	4	14	52.2	41.8
9	3	12	137.4	141.2	0	4	13	98.0	121.1	4	4	-14	44.8	-39.4
9	3	-12	76.8	-65.7	0	4	15	132.1	127.1	4	4	15	74.5	-68.0
9	3	14	80.5	79.3	0	4	17	74.2	90.1	4	4	-15	109.3	113.8
9	3	-14	61.9	-47.7	0	4	19	41.4	39.3	4	4	16	79.4	44.0
11	3	0	86.6	107.6	2	4	0	70.3	78.8	4	4	17	72.0	-55.5
11	3	2	142.4	147.5	2	4	1	95.8	111.0	4	4	-17	76.7	71.8
11	3	-2	72.3	84.2	2	4	-1	223.5	231.4	4	4	19	54.4	-38.4
11	3	4	122.5	112.6	2	4	2	43.1	38.9	6	4	0	88.0	79.2
11	3	-4	63.2	64.4	2	4	3	139.7	143.8	6	4	1	190.4	-184.2
11	3	5	36.1	-52.4	2	4	-3	256.1	283.9	6	4	-1	188.0	-194.2
11	3	6	48.1	47.5	2	4	4	52.4	-45.4	6	4	-2	59.5	61.9
11	3	-6	86.9	81.3	2	4	5	142.1	135.7	6	4	3	77.9	-77.5
11	3	-7	51.5	39.3	2	4	-5	222.1	244.8	6	4	-3	204.6	-213.6
11	3	-8	85.5	96.5	2	4	6	83.3	-72.1	6	4	4	53.4	-48.3
11	3	9	82.1	-69.8	2	4	-6	36.7	33.9	6	4	-5	161.0	-167.4
11	3	10	51.5	-45.2	2	4	7	131.1	130.2	6	4	6	25.4	29.1
11	3	11	94.0	-82.0	2	4	-7	165.4	188.5	6	4	8	82.6	68.3
11	3	13	79.2	-74.5	2	4	8	59.8	-58.7	6	4	9	68.3	48.3

h	k	ℓ	F_o	F_c	h	k	ℓ	F_o	F_c	h	k	ℓ	F_o	F_c
6	4	-9	99.0	-96.3	14	4	4	62.0	53.6	5	5	4	82.6	73.5
6	4	10	90.4	68.3	14	4	7	72.5	56.3	5	5	-4	178.6	-186.0
6	4	11	66.4	50.2	14	4	9	69.6	75.7	5	5	6	81.6	73.8
6	4	-11	108.8	-93.9	14	4	11	71.5	91.5	5	5	8	133.7	111.1
6	4	13	106.8	91.7	14	4	13	82.3	105.8	5	5	-8	82.1	-97.8
6	4	15	83.8	91.0	16	4	7	55.6	54.8	5	5	-9	78.3	-55.2
6	4	17	111.7	113.1	1	5	-1	98.2	114.5	5	5	10	138.8	160.1
6	4	19	100.2	103.5	1	5	-2	166.9	185.1	5	5	-10	113.3	-118.1
6	4	0	60.3	48.4	1	5	-4	165.6	158.5	5	5	-12	99.7	-102.1
8	4	1	178.4	167.0	1	5	-5	88.8	-78.6	5	5	13	46.1	-36.1
8	4	-1	129.6	117.4	1	5	-6	292.7	309.0	5	5	14	113.5	125.9
8	4	3	142.9	133.3	1	5	-7	95.7	-85.1	5	5	-14	86.0	-87.9
8	4	4	44.6	33.0	1	5	-8	192.1	198.9	5	5	-15	48.2	37.6
8	4	5	158.6	154.6	1	5	9	69.6	79.3	5	5	16	104.6	96.6
8	4	7	137.0	122.7	1	5	11	71.7	73.8	5	5	18	100.8	92.7
8	4	8	73.5	-54.9	1	5	-11	28.4	23.2	7	5	0	145.9	154.8
8	4	9	168.6	159.8	1	5	12	107.1	-89.4	7	5	2	161.0	155.0
8	4	-9	16.4	-40.9	1	5	-12	95.9	91.1	7	5	-2	152.3	162.3
8	4	10	83.5	-40.6	1	5	14	115.3	-111.0	7	5	3	81.9	61.9
8	4	11	161.0	152.9	1	5	-14	75.7	62.9	7	5	-3	72.4	-62.3
8	4	-11	66.1	-62.8	1	5	16	114.5	-124.5	7	5	4	162.0	165.8
8	4	13	83.8	74.9	1	5	17	63.5	-34.0	7	5	-4	133.2	140.3
8	4	-13	63.9	-69.5	1	5	-17	50.0	-43.7	7	5	-5	52.0	-42.5
8	4	-15	70.3	-70.6	3	5	0	130.1	-131.5	7	5	6	142.4	160.8
10	4	0	72.0	-56.1	3	5	-1	50.2	-32.0	7	5	-6	102.0	96.2
10	4	1	79.1	67.7	3	5	2	241.1	-251.0	7	5	7	58.6	-31.0
10	4	-1	88.9	89.0	3	5	-2	111.7	-124.6	7	5	8	89.3	78.1
10	4	2	98.5	-82.6	3	5	3	82.4	76.7	7	5	-8	70.9	68.5
10	4	-3	114.7	116.6	3	5	4	194.4	-188.5	7	5	10	79.3	67.7
10	4	-5	100.0	100.3	3	5	-4	88.0	-91.5	7	5	13	78.0	54.9
10	4	7	79.9	-52.8	3	5	5	85.4	67.6	7	5	14	63.0	-39.1
10	4	9	114.7	-104.6	3	5	-5	51.8	52.8	7	5	-14	63.2	42.4
10	4	-9	93.8	106.6	3	5	6	171.2	-157.3	7	5	15	50.7	43.3
10	4	11	121.5	-121.0	3	5	-7	71.2	78.7	7	5	-15	43.6	-33.5
10	4	-11	79.1	78.8	3	5	8	195.4	-185.8	7	5	18	73.2	-63.8
10	4	13	115.2	-117.1	3	5	9	70.4	-66.4	9	5	2	64.8	-57.4
10	4	15	79.9	-95.4	3	5	-9	60.7	35.5	9	5	-2	71.7	64.9
10	4	17	73.0	-83.1	3	5	10	136.2	-126.6	9	5	-3	63.0	48.4
12	4	1	122.3	-127.6	3	5	11	77.3	-58.9	9	5	4	109.7	-106.6
12	4	3	134.3	-134.6	3	5	12	45.6	-29.7	9	5	-4	76.3	54.8
12	4	-3	84.0	-65.6	3	5	-12	58.1	52.6	9	5	-5	53.0	61.9
12	4	5	123.3	-124.2	3	5	14	58.1	-21.8	9	5	6	122.7	-124.1
12	4	7	103.6	-91.5	3	5	-14	109.9	103.7	9	5	8	116.8	-113.1
12	4	9	68.1	-58.0	5	5	1	45.4	-44.5	9	5	-8	78.3	79.2
12	4	10	47.3	48.9	5	5	-1	59.7	53.2	9	5	10	128.1	-120.6
12	4	11	71.0	-43.6	5	5	-2	91.1	-87.1	9	5	12	109.9	-114.2
12	4	12	62.7	57.8	5	5	3	85.2	-85.5	9	5	13	43.1	-20.3
12	4	13	48.7	-41.9	5	5	-3	70.4	64.0	9	5	14	87.7	-106.0

h	k	ℓ	F_o	F_c	h	k	ℓ	F_o	F_c	h	k	ℓ	F_o	F_c
9	5	16	82.1	-76.6	2	6	-3	151.6	-141.3	6	6	-4	50.2	-48.0
9	5	18	60.9	-50.9	2	6	5	111.7	-91.3	6	6	5	74.2	70.7
11	5	2	89.0	-96.8	2	6	-5	128.2	-127.2	6	6	-5	126.7	148.7
11	5	-2	116.8	-128.9	2	6	-5	128.2	-127.2	6	6	6	83.1	70.2
11	5	0	100.2	-110.1	2	6	-6	73.9	70.8	6	6	7	41.2	36.7
11	5	4	78.6	-60.8	2	6	-7	105.1	-116.9	6	6	-7	114.9	128.8
11	5	5	62.7	-50.1	2	6	8	91.5	-78.0	6	6	8	47.0	37.9
11	5	6	80.8	-49.6	2	6	-8	107.1	94.1	6	6	9	44.1	-31.0
11	5	-6	68.9	-88.0	2	6	9	49.6	28.0	6	6	-9	108.8	89.0
11	5	7	57.6	-53.3	2	6	-9	90.1	-79.2	6	6	10	58.6	34.1
11	5	-8	81.9	-66.2	2	6	10	114.9	-116.5	6	6	-10	56.6	-34.8
11	5	12	48.9	42.2	2	6	-10	52.2	45.2	6	6	11	76.8	-83.9
11	5	12	48.9	42.2	2	6	11	45.9	38.7	6	6	-11	58.9	45.5
11	5	14	61.5	66.7	2	6	-11	80.5	-77.9	6	6	12	95.8	82.3
11	5	16	58.4	83.0	2	6	12	84.9	-82.7	6	6	-12	74.2	-56.2
13	5	0	50.5	47.2	2	6	12	84.9	-82.7	6	6	13	100.4	-113.9
13	5	1	36.4	-42.6	2	6	-12	36.6	44.4	6	6	14	62.3	54.0
13	5	-1	55.3	-49.5	2	6	-14	44.7	36.5	6	6	15	64.6	-78.8
13	5	2	90.8	70.0	2	6	15	53.4	39.4	6	6	17	62.9	-65.3
13	5	4	93.6	98.6	2	6	-16	47.3	44.3	8	6	0	64.9	72.7
13	5	6	102.5	117.1	4	6	0	69.0	-72.1	8	6	1	103.9	-110.7
13	5	8	101.8	119.2	4	6	1	111.7	114.1	8	6	-1	68.4	-65.7
13	5	10	77.3	97.2	4	6	-1	61.2	65.7	8	6	-2	83.7	79.3
13	5	12	79.3	79.1	4	6	2	102.5	-106.5	8	6	3	130.2	-132.0
13	5	14	56.1	56.6	4	6	3	177.8	161.1	8	6	5	160.8	-179.6
15	5	2	58.6	49.7	4	6	-3	42.4	25.6	8	6	-6	66.1	73.6
15	5	8	26.5	-24.0	4	6	4	103.9	-85.6	8	6	7	144.9	-143.0
15	5	9	39.0	34.8	4	6	-4	82.5	-82.2	8	6	-8	44.1	41.0
0	6	0	194.6	155.8	4	6	5	159.4	147.0	8	6	10	53.1	-33.2
0	6	2	81.7	71.9	4	6	-5	89.5	-82.1	8	6	11	47.6	-51.8
0	6	4	48.5	39.8	4	6	-6	75.3	-72.6	8	6	14	81.1	-70.3
0	6	5	50.5	-44.2	4	6	7	102.5	98.6	8	6	15	36.3	-35.6
0	6	6	37.5	36.8	4	6	-8	99.9	-104.4	8	6	16	64.6	-56.9
0	6	7	117.8	-124.2	4	6	9	127.6	127.8	10	6	0	34.6	-13.6
0	6	8	34.3	14.8	4	6	-9	85.7	-91.2	10	6	-1	81.7	-88.9
0	6	10	53.7	48.4	4	6	-10	62.9	-58.8	10	6	2	64.3	-47.9
0	6	11	128.2	-136.7	4	6	11	127.3	133.0	10	6	-3	97.8	-114.3
0	6	13	114.0	-95.8	4	6	-11	95.2	-82.1	10	6	4	73.9	-81.9
0	6	15	68.1	-68.3	4	6	13	120.4	123.2	10	6	-4	57.1	-43.7
0	6	16	47.9	-39.2	4	6	-13	89.8	-90.4	10	6	-5	92.6	-91.3
2	6	0	83.4	-89.2	4	6	15	88.9	84.8	10	6	6	86.9	-77.4
2	6	1	205.9	-208.2	4	6	17	23.9	30.1	10	6	-6	59.7	-31.2
2	6	-1	163.4	-180.3	6	6	0	91.5	66.2	10	6	-7	62.6	-79.9
2	6	-1	163.4	-180.3	6	6	1	95.2	90.4	10	6	8	87.7	-75.8
2	6	-1	151.3	-180.3	6	6	-1	110.3	92.2	10	6	-9	84.0	-65.5
2	6	2	36.6	-29.8	6	6	2	103.9	115.0	10	6	-10	54.5	38.7
2	6	-2	68.4	-68.6	6	6	-3	123.0	142.0	10	6	11	73.9	63.3
2	6	3	179.9	-173.0	6	6	4	99.0	90.8	10	6	-11	61.2	-68.5

h	k	ℓ	F_o	F_c
10	6	13	84.3	97.3
12	6	0	60.9	51.4
12	6	-1	82.0	84.7
12	6	2	50.8	42.5
12	6	3	83.4	74.8
12	6	-3	58.0	76.2
12	6	-5	47.0	41.4
12	6	6	47.3	34.7
12	6	7	86.3	97.0
12	6	9	74.5	89.8
12	6	11	58.6	49.0
12	6	14	38.4	38.9
14	6	0	50.2	49.7
14	6	2	39.5	36.5
14	6	-2	44.7	51.5
14	6	7	61.7	-75.2
14	6	9	75.6	-82.2
14	6	11	43.0	-67.6

R = 11.0%

h	k	ℓ	F_o	F_c	h	k	ℓ	F_o	F_c	h	k	ℓ	F_o	F_c
0	2	0	115.5	-157.4	0	8	5	121.9	121.8	0	16	10	23.2	20.0
0	2	1	225.6	-275.8	0	8	8	111.7	-91.6	0	18	0	60.2	60.1
0	2	3	163.1	-180.6	0	8	9	131.6	-118.4	0	18	2	26.5	-23.9
0	2	4	201.3	178.9	0	8	11	105.6	-86.6	0	18	4	71.6	-81.5
0	2	5	288.7	266.8	0	8	12	67.4	59.1	0	0	4	259.6	-252.2
0	2	6	84.0	-69.8	0	8	13	79.9	74.3	0	0	6	76.0	69.5
0	2	7	36.2	42.1	0	8	16	39.8	-40.3	0	0	8	242.2	248.7
0	2	8	167.0	-154.5	0	8	17	42.8	-54.2	0	0	10	115.3	-112.3
0	2	9	218.1	-219.5	0	10	0	128.0	-139.4	0	0	12	152.9	-161.0
0	2	10	58.0	42.1	0	10	1	127.4	129.8	0	0	14	40.6	40.6
0	2	11	91.5	-92.5	0	10	2	28.2	-17.2	0	0	18	72.7	-85.0
0	2	12	60.2	70.4	0	10	3	88.2	75.7	0	0	2	32.0	26.3
0	2	13	86.2	102.9	0	10	5	186.1	-185.6	0	0	16	60.8	57.6
0	2	14	43.6	-41.8	0	10	6	28.7	-23.7	0	18	6	1.9	2.4
0	2	16	54.2	-58.0	0	10	7	113.6	-100.4	0	18	5	42.0	29.9
0	2	17	61.3	-66.2	0	10	8	43.6	-45.8	0	14	2	16.0	-26.4
0	4	0	43.1	-43.7	0	10	9	82.9	89.2	0	12	11	14.9	-21.3
0	4	1	241.9	230.0	0	10	11	46.4	31.0	0	12	5	11.1	-7.3
0	4	2	107.2	107.3	0	10	12	44.2	36.1	0	10	15	27.6	-27.1
0	4	3	384.6	386.9	0	10	13	93.1	-99.1	0	10	4	53.6	41.0
0	4	4	195.5	176.3	0	12	0	107.8	116.3	0	8	14	29.5	-25.1
0	4	5	321.6	-300.8	0	12	1	52.8	-46.8	0	8	10	52.5	41.2
0	4	6	48.6	45.7	0	12	2	57.7	-52.0	0	6	3	25.1	-30.2
0	4	7	142.4	-130.1	0	12	3	48.9	-45.1	0	6	1	25.9	-44.1
0	4	8	115.5	-111.1	0	12	4	141.3	-147.4	0	2	2	73.8	83.8
0	4	9	146.0	129.5	0	12	8	128.8	122.1	1	1	2	229.7	-272.8
0	4	10	58.9	51.4	0	12	10	35.1	-38.3	1	1	4	64.0	63.1
0	4	13	141.0	-140.4	0	12	12	47.0	-56.0	1	1	5	105.1	-96.5
0	4	14	41.2	-39.9	0	12	14	37.8	44.3	1	1	6	214.0	195.5
0	4	16	52.2	-55.2	0	14	0	118.0	-123.5	1	1	7	118.3	108.6
0	4	17	69.4	71.5	0	14	1	60.8	-59.8	1	1	8	49.7	-48.8
0	6	0	258.2	275.0	0	14	3	74.1	-66.5	1	1	9	42.7	38.1
0	6	2	55.0	-55.9	0	14	4	44.2	47.4	1	1	10	160.8	-161.1
0	6	4	272.6	-274.9	0	14	5	71.3	70.8	1	1	11	83.5	-83.3
0	6	6	90.7	78.2	0	14	6	41.7	-37.0	1	1	12	28.3	33.0
0	6	7	89.3	-75.4	0	14	7	52.2	45.4	1	1	14	77.2	81.9
0	6	8	243.0	221.5	0	14	8	77.4	-74.7	1	1	16	47.0	-47.9
0	6	9	97.8	-79.0	0	14	9	52.8	-58.4	1	1	18	45.9	-49.9
0	6	10	86.8	-83.4	0	14	12	51.4	60.3	1	1	19	45.1	-48.2
0	6	11	75.7	-58.9	0	14	13	36.7	46.3	1	2	1	56.7	-62.5
0	6	12	126.6	-128.4	0	16	0	54.7	-47.6	1	2	2	32.7	28.4
0	6	14	38.7	39.9	0	16	1	54.4	60.6	1	3	1	75.1	-91.5
0	6	16	61.6	68.3	0	16	3	61.3	63.3	1	3	2	51.0	47.8
0	6	18	38.4	-38.1	0	16	5	64.9	-64.9	1	3	3	287.3	320.3
0	8	0	252.7	-266.6	0	16	6	25.1	-21.2	1	3	4	52.1	-55.1
0	8	1	135.5	-140.5	0	16	7	25.7	-28.7	1	3	5	165.6	166.0
0	8	3	157.9	-150.7	0	16	8	28.4	-24.9	1	3	7	214.0	-169.9
0	8	4	155.6	150.1	0	16	9	53.6	64.7	1	3	9	101.0	-94.9

h	k	ℓ	F_o	F_c	h	k	ℓ	F_o	F_c	h	k	ℓ	F_o	F_c
1	3	11	124.3	120.3	1	9	15	55.9	-64.7	2	1	4	17.2	21.8
1	3	15	110.8	-113.2	1	10	3	44.5	-43.8	2	1	5	44.6	-40.1
1	3	17	40.0	-34.4	1	10	4	24.8	16.4	2	1	7	43.8	-36.6
1	4	3	125.9	-118.1	1	11	1	30.8	33.7	2	1	8	69.6	-71.8
1	4	4	27.0	-17.8	1	11	2	108.6	110.2	2	1	9	74.3	-68.1
1	4	5	42.9	-35.9	1	11	3	123.7	-115.7	2	1	11	42.2	-45.8
1	4	7	55.1	54.7	1	11	4	30.5	-31.6	2	1	12	52.6	54.6
1	4	8	25.6	-23.5	1	11	5	57.2	-47.9	2	2	9	93.6	-93.2
1	5	1	78.3	75.3	1	11	6	118.1	-107.8	2	2	11	58.9	-58.5
1	5	2	222.7	222.9	1	11	7	41.8	47.2	2	2	12	48.2	46.1
1	5	3	98.3	-86.2	1	11	9	46.7	45.9	2	2	13	68.0	71.5
1	5	4	85.4	-68.2	1	11	10	68.9	69.8	2	2	14	29.7	-30.2
1	5	5	94.0	-87.7	1	11	11	53.5	-44.7	2	2	16	39.9	-41.6
1	5	6	239.7	-221.4	1	11	12	44.0	-36.0	2	2	17	47.9	-53.6
1	5	7	124.8	111.1	1	11	14	48.6	-51.4	2	3	0	39.6	-47.6
1	0	2	105.9	-98.9	1	11	15	42.7	52.3	2	3	2	16.1	18.0
1	5	9	52.1	46.2	1	13	2	124.5	-131.0	2	3	3	49.8	54.2
1	5	10	60.2	55.1	1	13	3	60.0	-61.3	2	3	4	17.2	-20.8
1	5	11	71.0	-69.9	1	13	5	39.1	-37.1	2	3	5	86.0	-91.7
1	5	12	77.8	-74.3	1	13	6	82.4	83.0	2	3	7	77.9	-82.9
1	5	13	32.9	-30.9	1	13	8	28.9	-31.4	2	3	9	33.3	32.0
1	5	14	91.8	-91.8	1	13	10	78.3	-82.0	2	3	13	62.8	-60.9
1	5	15	42.7	38.6	1	15	1	82.9	-89.6	2	3	17	33.3	30.4
1	5	16	30.0	33.8	1	15	3	38.6	44.3	2	4	1	61.5	-69.6
1	6	1	29.4	-33.4	1	15	7	82.9	-83.4	2	4	2	81.1	82.9
1	7	1	82.1	83.8	1	15	11	57.2	69.1	2	4	3	99.8	115.0
1	7	2	187.5	-178.7	1	17	1	31.3	23.4	2	4	4	112.1	110.7
1	7	3	81.6	-79.1	1	17	2	55.1	59.5	2	4	5	122.3	-126.4
1	7	4	36.2	-17.4	1	17	3	46.7	-50.9	2	4	7	71.4	-66.7
1	7	6	186.2	168.5	1	17	5	42.7	-46.8	2	4	8	92.0	-88.1
1	7	7	76.7	66.5	1	17	6	31.3	-38.4	2	4	9	74.0	69.4
1	7	8	97.0	-81.1	1	17	8	21.0	24.6	2	4	10	33.9	39.7
1	7	10	137.5	-144.2	1	17	7	36.7	30.9	2	4	11	44.3	44.9
1	7	11	62.7	-58.3	1	8	3	11.8	-23.3	2	4	13	81.6	-80.8
1	7	14	69.7	65.8	1	8	2	28.1	38.7	2	4	14	30.2	-24.7
1	7	15	28.9	35.7	1	6	7	12.1	-13.7	2	4	16	32.6	-38.5
1	7	16	26.7	-30.2	1	6	2	65.6	-53.5	2	5	2	49.2	-49.6
1	8	6	47.5	-36.9	1	5	18	43.7	42.9	2	5	3	44.0	-51.6
1	9	1	166.4	-172.7	1	4	2	21.3	-23.2	2	5	4	117.8	-118.9
1	9	3	118.1	111.8	1	3	10	28.3	-26.8	2	5	8	58.6	52.5
1	9	4	43.7	-50.8	1	3	8	51.8	-61.7	2	5	9	46.9	-48.2
1	9	5	100.5	89.2	1	2	6	31.0	-33.4	2	5	11	29.4	-38.8
1	9	6	79.4	-66.7	1	2	5	30.8	21.0	2	5	14	30.7	36.6
1	9	7	116.4	-120.8	1	2	4	15.9	-28.9	2	6	0	151.0	150.8
1	9	8	64.0	-55.4	1	1	3	9.7	-10.9	2	6	3	46.6	-52.6
1	9	9	59.7	-57.3	1	1	1	183.7	207.3	2	6	4	128.8	-137.1
1	9	11	103.5	104.1	2	0	4	80.8	86.9	2	6	5	54.2	-42.8
1	9	14	36.4	-28.9	2	1	3	48.2	-53.6	2	6	7	29.7	-32.8

h	k	ℓ	F_o	F_c	h	k	ℓ	F_o	F_c	h	k	ℓ	F_o	F_c
2	6	8	123.6	114.5	2	11	5	43.2	41.7	2	15	11	27.1	25.6
2	6	9	23.9	-32.8	2	11	7	47.9	47.2	2	14	13	34.6	35.1
2	6	10	40.9	-44.6	2	11	8	38.0	40.8	2	12	11	16.1	-24.2
2	6	11	46.4	-33.9	2	11	13	35.9	27.9	2	11	0	16.9	25.4
2	6	12	83.9	-78.4	2	11	14	21.9	20.5	2	10	4	13.8	18.3
2	6	14	34.6	28.7	2	12	0	99.8	91.1	2	9	5	31.0	-43.4
2	6	16	55.5	55.5	2	12	2	41.2	-36.8	2	8	17	40.1	-41.2
2	7	0	136.1	-138.1	2	12	4	104.0	-103.7	2	5	16	42.7	43.2
2	7	2	46.6	-43.2	2	12	8	102.7	96.7	2	4	17	23.2	41.5
2	7	4	34.9	37.5	2	12	10	27.3	-28.8	2	1	2	16.9	-24.7
2	7	5	50.0	48.4	2	12	12	34.1	-43.0	2	1	1	65.2	-79.8
2	7	6	40.4	-24.7	2	12	14	24.2	30.0	3	2	1	96.9	-107.7
2	7	8	58.6	-52.0	2	13	0	62.8	-59.3	3	3	1	94.9	-96.5
2	7	12	58.9	58.0	2	13	4	45.1	36.8	3	5	1	49.6	42.0
2	8	0	92.5	-70.0	2	13	5	32.3	35.6	3	6	1	61.2	-52.7
2	8	1	99.1	-89.6	2	13	7	37.0	34.0	3	7	1	65.8	64.9
2	8	3	98.0	-92.2	2	13	8	38.8	-41.6	3	8	1	141.1	-148.9
2	8	4	49.2	40.6	2	13	12	24.5	29.3	3	9	1	60.9	-63.0
2	8	5	112.9	106.4	2	14	0	74.0	-82.5	3	10	1	33.4	21.0
2	0	8	152.3	148.6	2	14	1	32.3	-35.0	3	11	1	53.5	50.5
2	8	8	74.0	-64.8	2	14	2	25.5	-22.0	3	12	1	21.6	-24.7
2	8	9	81.3	-74.6	2	14	3	32.0	-39.6	3	14	1	40.3	-35.8
2	8	11	72.5	-63.7	2	14	5	60.7	55.3	3	15	1	48.0	-49.3
2	8	12	55.5	51.4	2	14	7	26.8	30.4	3	16	1	48.8	49.3
2	8	13	62.8	59.0	2	14	8	55.2	-46.5	3	1	2	166.0	-168.7
2	8	16	37.2	-32.7	2	14	9	49.0	-46.7	3	2	2	82.6	80.5
2	9	0	49.8	-49.3	2	14	12	33.9	39.2	3	4	2	105.6	85.0
2	9	1	67.0	60.6	2	15	9	41.4	47.5	3	5	2	76.3	77.5
2	9	2	38.3	-42.3	2	16	0	18.5	-38.6	3	6	2	132.8	-129.5
2	9	3	57.9	49.7	2	16	1	43.0	45.6	3	7	2	114.4	-108.9
2	9	4	34.9	-28.4	2	16	3	52.6	49.2	3	8	2	49.9	52.5
2	9	9	56.5	54.7	2	16	5	52.4	-52.2	3	9	2	18.1	23.0
2	9	11	43.5	31.1	2	16	9	38.3	47.3	3	10	2	53.8	47.1
2	10	0	82.4	-79.3	2	17	0	32.6	39.9	3	11	2	80.1	76.8
2	10	1	74.3	75.4	2	17	5	29.9	30.7	3	12	2	87.3	-86.2
2	10	3	61.2	64.5	2	17	7	25.2	25.2	3	13	2	54.9	-62.9
2	10	5	104.0	-87.8	2	18	0	40.1	44.0	3	14	2	48.8	48.5
2	10	6	39.6	-30.3	2	18	4	51.1	-56.6	3	16	2	20.5	26.0
2	10	7	69.1	-65.6	2	2	1	102.7	-118.0	3	17	2	26.0	31.7
2	10	8	43.2	-33.7	2	2	2	26.0	-31.1	3	18	2	33.4	-34.7
2	10	9	42.5	43.8	2	2	3	148.9	-161.2	3	2	3	106.7	94.3
2	10	11	25.5	25.8	2	2	4	65.9	66.2	3	3	3	152.9	152.3
2	10	12	33.9	28.8	2	2	5	60.5	56.7	3	4	3	160.3	-153.1
2	10	13	68.5	-67.4	2	2	7	29.4	29.4	3	0	4	79.6	-73.5
2	11	1	25.8	-24.6	2	2	8	67.5	-73.5	3	5	3	84.8	-78.3
2	11	2	38.8	-31.9	2	2	6	22.9	23.7	3	8	3	33.2	27.1
2	11	4	58.6	-60.4	2	2	0	146.8	-144.1	3	9	3	73.0	70.3

h	k	ℓ	F_o	F_c	h	k	ℓ	F_o	F_c	h	k	ℓ	F_o	F_c
3	10	3	105.1	-102.4	3	15	7	40.3	-40.5	3	6	14	55.4	53.2
3	11	3	65.0	-61.6	3	16	7	34.5	40.2	3	7	14	47.7	44.6
3	14	3	34.5	40.7	3	17	7	25.5	30.3	3	12	14	31.0	43.9
3	15	3	45.5	34.5	3	2	8	50.2	-40.3	3	3	15	58.7	-61.7
3	16	3	30.7	-26.7	3	6	8	45.0	-32.9	3	4	15	65.6	70.3
3	17	3	26.3	-25.2	3	7	8	30.1	-19.1	3	5	15	30.4	30.4
3	2	4	79.8	-94.2	3	10	8	50.2	47.7	3	6	15	30.7	19.2
3	3	4	79.0	-78.3	3	14	8	29.6	35.5	3	7	15	32.3	25.4
3	4	4	44.7	-45.8	3	16	8	27.4	25.1	3	9	15	35.1	-41.0
3	5	4	54.3	-59.8	3	1	9	23.6	27.1	3	10	15	40.0	49.7
3	6	4	27.1	26.8	3	2	9	59.8	-51.8	3	11	15	23.6	30.6
3	12	4	34.0	31.5	3	3	9	48.5	-49.7	3	8	14	35.1	-27.4
3	14	4	22.5	22.4	3	4	9	48.3	44.8	3	11	14	30.1	-24.0
3	18	4	12.0	16.0	3	5	9	22.2	25.7	3	1	14	51.0	48.3
3	2	5	66.7	68.1	3	9	9	47.2	-41.9	3	15	11	37.3	36.0
3	3	5	89.2	94.2	3	10	9	35.4	38.6	3	11	12	13.4	-15.5
3	4	5	108.7	-97.9	3	1	10	77.4	-81.7	3	11	11	29.6	-27.5
3	5	5	67.8	-72.8	3	3	10	15.6	21.2	3	6	11	23.0	19.1
3	7	5	22.7	16.0	3	5	10	68.6	66.6	3	16	10	28.5	25.5
3	8	5	34.0	28.8	3	6	10	80.4	-85.6	3	1	8	8.7	-14.8
3	9	5	37.6	33.0	3	7	10	46.9	-58.2	3	6	7	44.1	-31.6
3	10	5	63.9	-61.3	3	8	10	37.3	40.5	3	17	5	19.2	-20.1
3	11	5	20.8	-29.4	3	10	10	56.0	48.3	3	15	5	40.3	37.7
3	16	5	20.3	-25.1	3	11	10	46.1	41.0	3	14	5	23.8	22.5
3	1	6	101.8	112.3	3	13	10	55.7	-59.7	3	7	4	12.3	-14.9
3	2	6	115.5	-124.2	3	14	10	43.9	54.7	3	18	3	24.1	18.5
3	0	2	150.4	-168.3	3	1	11	52.9	-60.4	3	7	3	12.9	-28.3
3	4	6	110.0	-98.9	3	2	11	86.4	81.4	3	6	3	36.7	-48.6
3	5	6	116.6	-111.5	3	3	11	65.3	68.9	3	3	2	3.8	15.6
3	6	6	133.1	121.8	3	4	11	41.7	-43.9	3	4	1	18.9	18.3
3	7	6	117.4	120.4	3	5	11	36.2	-36.7	4	2	0	187.1	-183.2
3	8	6	69.4	-56.4	3	7	11	23.3	-19.3	4	4	0	55.2	-51.6
3	9	6	34.3	-35.9	3	8	11	74.9	73.4	4	5	0	61.4	61.1
3	11	6	46.9	-45.6	3	9	11	74.9	71.4	4	6	0	127.5	127.3
3	12	6	93.8	91.2	3	10	11	42.5	-39.6	4	7	0	203.0	-215.9
3	13	6	61.2	57.7	3	14	11	27.7	33.6	4	8	0	62.2	-73.0
3	17	6	29.1	-26.2	3	1	12	21.6	23.1	4	9	0	22.1	-12.4
3	1	7	101.8	94.8	3	2	12	34.8	-34.9	4	11	0	80.2	72.5
3	2	7	121.3	-121.5	3	4	12	44.4	-43.8	4	12	0	80.5	84.9
3	0	10	130.9	-137.0	3	5	12	30.7	-28.7	4	13	0	95.9	-98.1
3	3	7	83.1	-85.3	3	12	12	36.7	35.3	4	14	0	44.5	-41.6
3	4	7	53.2	48.1	3	2	13	20.8	27.8	4	17	0	55.2	56.1
3	5	7	65.6	67.6	3	6	13	27.1	21.5	4	15	1	50.1	58.9
3	8	7	99.6	-90.2	3	8	13	29.3	32.1	4	11	1	43.6	-43.7
3	9	7	82.9	-85.9	3	9	13	26.0	30.3	4	10	1	65.8	71.1
3	10	7	46.6	52.2	3	2	14	39.5	-48.6	4	9	1	112.1	114.4
3	13	7	21.4	15.8	3	4	14	29.6	-39.7	4	8	1	36.6	-46.9
3	14	7	32.3	-38.1	3	5	14	57.3	-59.9	4	7	1	31.8	-30.4

h	k	ℓ	F_o	F_c
4	6	1	23.6	-20.2
4	5	1	94.4	-91.5
4	4	1	53.4	51.7
4	3	1	142.8	139.9
4	2	1	95.0	-93.0
4	1	1	141.6	-151.1
4	2	2	49.5	-42.7
4	5	2	58.1	-65.6
4	6	2	25.3	-26.1
4	7	2	34.8	-24.7
4	8	2	25.6	28.9
4	9	2	36.8	-40.6
4	10	2	20.6	28.2
4	11	2	39.5	-29.1
4	16	2	13.8	14.0
4	17	3	23.3	-17.4
4	16	3	23.9	30.3
4	15	3	59.3	59.1
4	11	3	31.5	-23.8
4	10	3	69.3	65.8
4	9	3	96.5	90.8
4	8	3	37.4	-45.5
4	7	3	49.5	-49.5
4	5	3	134.6	-120.3
4	4	3	134.9	133.2
4	3	3	125.1	133.2
4	2	3	103.6	-108.6
4	1	3	88.2	-76.5
4	0	4	95.0	-94.4
4	1	4	126.0	135.1
4	3	4	44.5	-45.1
4	4	4	52.5	38.3
4	5	4	226.4	-213.2
4	6	4	126.3	-123.5
4	7	4	104.2	107.4
4	8	4	64.9	59.5
4	9	4	43.3	-49.7
4	11	4	96.8	-95.7
4	13	4	61.9	71.4
4	14	4	47.2	48.0
4	17	4	33.9	-33.0
4	16	5	33.0	-35.3
4	15	5	40.1	-37.3
4	13	5	63.7	52.8
4	11	5	64.9	69.2
4	10	5	57.2	-55.4
4	9	5	83.2	-94.9
4	8	5	81.7	79.9
4	7	5	52.8	57.5
4	5	5	61.4	64.2
4	3	5	207.8	-193.8
4	2	5	109.2	103.3
4	0	6	37.4	42.8
4	1	6	59.0	-54.3
4	7	6	54.3	-52.8
4	9	6	36.8	-29.6
4	13	7	39.2	43.6
4	11	7	63.7	61.7
4	9	7	45.4	-36.1
4	8	7	32.1	26.4
4	7	7	41.0	27.4
4	3	7	134.6	-111.2
4	0	8	116.6	127.0
4	2	7	46.0	38.2
4	1	8	140.2	-136.5
4	2	8	53.1	-49.6
4	4	8	42.2	-49.0
4	5	8	116.0	116.0
4	6	8	87.3	88.2
4	7	8	102.4	-101.0
4	8	8	70.5	-60.3
4	11	8	73.2	68.6
4	12	8	60.8	55.9
4	13	8	70.8	-73.3
4	15	9	60.8	67.5
4	14	9	30.9	-30.4
4	10	9	45.7	51.7
4	9	9	90.0	94.6
4	7	9	27.4	-31.8
4	5	9	82.6	-81.2
4	4	9	103.6	111.1
4	3	9	92.6	102.7
4	2	9	57.2	-48.0
4	1	9	108.0	-112.0
4	1	10	54.3	50.4
4	4	10	34.2	31.1
4	6	10	34.8	-34.5
4	13	11	16.2	18.3
4	10	11	33.9	30.6
4	9	11	51.9	51.1
4	5	11	40.1	-41.5
4	4	11	34.8	43.8
4	1	11	46.0	-62.3
4	1	12	83.5	92.3
4	2	12	43.6	34.6
4	5	12	44.2	-51.7
4	6	12	35.7	-38.7
4	7	12	81.7	93.2
4	8	12	41.0	39.3
4	9	13	52.5	-60.3
4	8	13	48.1	48.1
4	7	13	38.6	37.8
4	5	13	26.5	38.5
4	4	13	47.8	-53.4
4	3	13	85.3	-103.3
4	2	13	37.4	50.4
4	5	13	54.3	38.5
4	11	14	27.1	33.4
4	8	16	23.0	-24.3
4	6	16	31.8	36.3
4	5	16	59.3	62.8
4	5	17	36.6	-28.2
4	4	17	35.4	25.8
4	3	17	63.7	54.9
4	1	16	53.1	-43.9
4	7	16	31.8	-28.6
4	10	13	44.5	-36.4
4	11	13	54.3	42.3
4	13	12	58.4	49.0
4	11	12	36.0	-36.2
4	7	10	44.8	36.9
4	5	10	47.2	-36.9
4	8	6	16.2	19.9
4	1	5	46.0	36.3
4	14	5	45.4	40.2
4	12	4	54.6	-41.5
4	0	2	114.8	-112.2
4	6	3	18.0	-26.5
4	16	1	30.7	26.2
4	18	0	38.3	33.8
4	3	0	46.0	-31.1
4	1	0	337.7	-344.9

R = 9.1%